DESCRIBING NEW SPECIES OF *CRYPTOSPORIUM* IN FISH

by

Samuel John Bolland

Bachelor of Science, Bachelor of Engineering

This thesis is presented for the degree of Bachelor of Science Honours in

Molecular Biology

College of Science, Health, Engineering and Education

Murdoch University, 2019

Author's Declaration

I declare that this is my own account of my research and contains as its main content work which has not been previously submitted for a degree at any tertiary educational institution.

Samuel John Bolland

Abstract

The protozoan parasite *Cryptosporidium* (class Gregarinomorphea, subclass Cryptogregaria) causes a range of symptoms in humans and clinical signs in animals from asymptomatic to severe diarrhoea and death. However, relatively little information is available regarding the taxonomy, zoonotic potential and host relationships of *Cryptosporidium* in fish. Previous studies have indicated that extensive genetic diversity exists with piscine *Cryptosporidium* species and genotypes. The present study screened fish from two sources in Perth, Western Australia; Water Garden Life Fish Farm (*n*=233) and Vebas Aquarium (*n*=234) for *Cryptosporidium*. Intestinal and gastric tissue was dissected out and screened by PCR and Sanger sequencing using *Cryptosporidium* specific primers that amplify DNA at the 18S and actin loci. Samples that were positive by PCR were also screened by histology. The overall prevalence of *Cryptosporidium* was 4.3% (20/467, 95% CI: 2.6-6.5). Phylogenetic analyses of 18S sequences identified *C. huwi* (*n*=11), piscine genotype 2 (*n*=3), piscine genotype 4 (*n*=1) and piscine genotype 7 (*n*=5). In addition, ten novel sequences most genetically similar to species from the genus *Goussia* and a sequence from the non-parasitic alveolate *Colpodella* were identified. Sequences amplified at the actin locus were *C. huwi* (*n*=7), piscine genotype 2 (*n*=1), piscine genotype 7 (*n*=1) and one novel *Cryptosporidium* sequence. Piscine genotype 2 was most closely related to piscine genotype 4 (4.1% genetic distance) and exhibited 11.1-11.9%, 15.3% and 22.3% genetic distances from *C. molnari, C. huwi* and *C. scophthtalmi*, respectively. At the actin locus, piscine genotype 2 was again most closely related to piscine genotype 4 (7.2% genetic distance) and exhibited genetic distances ranging from 18.1% (*C. molnari*) to 20% (*C. huwi*) and 26.1% for *C. scophthalmi*, respectively, and 20.7%- 32% genetic distance from all other species.

Phylogenetic analysis of concatenated 18S and actin sequences showed that piscine genotype 2 exhibited 14% (*C. molnari*) to 24.6% (*C. canis*) genetic distance from all other *Cryptosporidium* spp. Using concatenated sequences, piscine genotype 7 was most closely related to *C. huwi* at a genetic distance of 7.5% and exhibited 13.4% (*C. molnari*) to 23.1% (*C. scophthalmi*) genetic distances from other piscine *Cryptosporidium* species, with 17.9% (*C. testudinis*) to 22.6% (*C. canis*) genetic distance from all non-piscine *Cryptosporidium* species. Piscine genotype 2 exhibited 14.6% genetic distance from piscine genotype 7. These genetic distances at two separate loci confirm the genetic distinctness of piscine genotype 2 and piscine genotype 7 and indicate that they are likely novel species. Additionally, 10/467 (2.1%, 95% CI; 1.0-3.9) samples that were positive at the 18S locus, produced sequences most genetically similar to species from the genus *Goussia*, subclass Conoidasida, nine were novel sequences and were compared at the 18S locus to established species of *Goussia* and genetic distances between 1.9% and 14.8% were identified, adding to the diversity of this genus. Furthermore, *Schyzocotyle acheilognathi*, the invasive Asian fish tapeworm, was identified (*n*=2) by morphology infecting goldfish from a local fish farm. This is only the second report of *S. acheilognathi* in Western Australia as it was first discovered in 2018 by a Murdoch researcher in feral goldfish from a Lake in Joondalup. Analysis at additional loci or whole genome sequencing will shed more light on the evolutionary relationships between *Cryptosporidium* species, while next generation sequencing would elucidate the prevalence of mixed infections of *Cryptosporidium* in fish. The genetic data produced by the present study describes two piscine genotypes of *Cryptosporidium* (that are likely valid species) in detail and provides new genetic data on the diversity of *Goussia* spp.

Keywords: *Cryptosporidium*, 18S, actin, *Schyzocotyle acheilognathi*, *Goussia*

Acknowledgements

First and foremost I would like to sincerely thank my supervisors Professor Una Ryan (Primary) for her expert guidance, motivational leadership and for inspiring me further into science and Dr Alireza Zahedi (Co-supervisor) for his generosity of time, attention and knowledge, it would be impossible to repay the support and training I received from you both and I will do my best to pay it forward in the future. I would also like to thank my amazing co-supervisor Dr Charlotte Oskam and also Cindy Palermo for patiently walking me through many laboratory procedures and the entire Vector and Waterborne Pathogens Group, Kamil Ali, Siobhon Egan, Professor Peter Irwin, Dr Amanda Barbosa, Megan Evans, Dr Jill Austen, Telleasha Greay, Dr. Kimberly Loh and the other honours students for helping me out on countless occasions regardless of how busy you were. I could not imagine finding another research group so passionate, full of intelligence and welcoming, Dr Jill your tips and wise words were priceless.

Thanks to my incredible wife Sheryl for being the best support imaginable and making me laugh on a daily basis. Thanks to my cat Barry Good-Bear for keeping me company while writing my thesis. Finally, thank you to my friends and family for believing in me and supporting me to pursue my goal to become a researcher in the biomedical sciences.

Table of Contents

List of Figures

List of Tables

Glossary of Terms

Symbol/Abbreviation	Meaning
AGRF	Australian Genome Research Facility
ART	Antiretroviral therapy
BLAST	Basic local alignment search tool
bp	Base pairs
CI	Confidence interval
DAPI	4', 6-diamindino-2-phenylindole
DFA Assay	Direct fluorescent antibody assay
DNA	Deoxyribonucleic acid
DNTP	Deoxyribonucleotide triphosphate
EDTA	Ethylenediaminetetraacetic acid
FDA	Foods and Drugs Association (US regulatory department)
EXB	Extraction reagent blank control
gp	Glycoprotein
HAART	Highly active antiretroviral therapy
H&E	Haematoxylin and eosin
HIV	Human immunodeficiency virus
H_20	Water
ICZN	The International Code of Zoological Nomenclature
IF	Immunofluorescence
mAB	Monoclonal antibody
mg	Milligrams
$MgCl_2$	Magnesium chloride
Min	Minutes
mL	Millilitre
mM	Millimolar
n	Number of samples
ng	Nanograms
NCBI	National Centre for Biotechnology
NGS	Next generation sequencing
NTC	Non-template control
PCR	Polymerase Chain Reaction
pH	Potential of hydrogen, a logarithmic scale denoting the Acidity or basicity of a solution.
qPCR	Quantitative Polymerase Chain Reaction
RFLP	Restriction fragment length polymorphism
rpm	Revolutions per minute
rRNA	Ribosomal Ribonucleic Acid
SABC	State Agricultural Biotechnology Centre (Murdoch)
s	Seconds

Sp./spp.	Species/species’
TAE buffer	Tris-aceatate, acetic acid and EDTA
u	Micro
ug	Micrograms
µL	Microlitres
WGS	Whole genome sequencing
WHO	World Health Organisation
w/v	Weight of solvent per volume of solvent
3’	Hydroxyl-terminus of DNA molecule
5’	Phosphate-terminus of DNA molecule
18S	18S rRNA locus
°C	Degrees Celsius
°K	Degrees Kelvin
~	Approximately
>	Greater than
<	Less than
%	Percentage
+	Positive
-	Negative

Chapter 1: Introduction and Literature Review

1.1 Introduction

Cryptosporidium are protozoan parasites that infect a wide range of hosts worldwide including fish and have been classified as most closely related to Gregarine parasites (class Gregarinomorphea subclass, Cryptogregaria) (Cavalier-Smith, 2014). *Cryptosporidium* causes the disease cryptosporidiosis by infecting the microvillus border of the gastrointestinal epithelium, associated organs and respiratory system in a wide range of vertebrate hosts. Cryptosporidiosis causes a range of symptoms in humans and clinical signs in animals ranging from asymptomatic to severe diarrhea and death, particularly in young individuals (Striepen, 2013; Ryan et al., 2016; Zahedi et al., 2016b). Infections in all five groups of vertebrate have been observed including humans, livestock, wildlife and fish (Sunnotel et al., 2006; Silva et al., 2013; Cacciò and Widmer, 2014; Ryan et al., 2014). The parasite is transmitted via the faecal-oral contamination route by ingesting environmentally stable oocysts (Ryan et al., 2014). The resulting disease, cryptosporidiosis is mostly self-limiting in healthy adult hosts but can be life-threatening in immunocompromised, malnourished and paediatric populations, particularly in developing countries (Checkley et al., 2015; Aldeyarbi et al., 2016; Daniels et al., 2018). In developed countries the parasite causes economic loss and individual morbidity, particularly during outbreaks (Ryan et al., 2014; Widerstrom et al., 2014; Painter et al., 2015; Ryan et al., 2017a). Water is a major method of transmission of *Cryptosporidium,* as the environmentally robust oocyst is resistant to disinfection including chlorine (Betancourt and Rose, 2004). The successful conventional methods of disinfection are coagulation/flocculation, sedimentation and filtration (Betancourt and Rose, 2004; Sunnotel et al., 2006). Some

species of *Cryptosporidium* are zoonotic while others are more host specific (Osman et al., 2017). Species differ in site of infection, host range and level of intracellular activity (Osman et al., 2017). The majority of infections in humans are caused by *C. parvum* and *C. hominis*, with *C. hominis* mostly anthroponotic and *C. parvum* mostly zoonotic, although both parasites have been found in kangaroos, cattle and sheep (Zahedi et al., 2016a).

Cryptosporidium infections are the second most common cause of diarrheal related death in children in developing countries with rotavirus being the most common (Kotloff et al., 2013; Striepen, 2013). Malnutrition and HIV in developing countries increases the risk of infection with enteric protozoan parasites such as *Cryptosporidium*, causing further malnutrition (due to intestinal damage), ongoing growth retardation, impaired cognitive and immune functions and mortality (Kotloff et al., 2013; Cacciò and Widmer, 2014; Checkley et al., 2015; Daniels et al., 2018). Even asymptomatic patients can develop ongoing symptoms such as irritable bowel syndrome and chronic fatigue (Cacciò and Widmer, 2014; Urrea-Quezada et al., 2017). While there have been numerous studies into the prevalence, pathogenicity and genetic diversity of *Cryptosporidium* in humans and other hosts, relatively little is known about fish and the potential public health implications.

1.2 Taxonomy

The Apicomplexan parasite *Cryptosporidium* possesses features of both subclasses Coccidia and Gregarines with a Gregarine-like feeder organelle but lacking an apicoplast. Until recently, *Cryptosporidium* was classified as a coccidian parasite, however, it has now been formally transferred from subclass Coccidia, class

Coccidiomorphea to a new subclass, Cryptogregaria, within the class Gregarinomorphea (Cavalier-Smith, 2014). *Cryptosporidium* is currently the sole Cryptogregaria within the Gregarine parasites and is described as an epicellular parasite of vertebrates (Cavalier-Smith, 2014). The similarities between *Cryptosporidium* and Gregarines have been supported by extensive microscopic, molecular, genomic and biochemical data (Ryan et al., 2016).

1.2.1 Delimiting species in *Cryptosporidium*

Initial research on *Cryptosporidium,* delimited species based on the oocyst morphology and host occurrence of the parasite (Ryan et al., 2014). Unfortunately, *Cryptosporidium* oocysts are among the smallest of any apicomplexan stage (4-6µm) and lack distinct morphological features that could differentiate the species (Fall et al., 2003; Xiao, 2010). Therefore, molecular characterisation is essential for taxonomic assignment. To allow researchers to delimit *Cryptosporidium* species, a set of guidelines are now routinely followed: (1) morphometric studies of the oocysts; (2) genetic characterisation at two loci and submission of GenBank accession numbers; (3) some evidence of host range and specificity and (4) compliance with International Code of Zoological Nomenclature (ICZN) (Xiao et al., 2004). As a result, 42 valid species of *Cryptosporidium* are currently recognised (Holubová et al., 2016; Ježková et al., 2016; Ryan et al., 2016; Zahedi et al., 2017b; Čondlová et al., 2018; Kváč et al., 2018; Holubová et al., 2019; Horčičková et al., 2019) (Table 1) with > 40 genotypes described from various vertebrate hosts on the basis of morphology and molecular criteria.

Table 1.1. Valid *Cryptosporidium* species.

Species name	Author(s)	Type Host(s)	Major host(s)	Reports in humans
C. occultus	Kváč et al. (2018)	*Rattus norvegicus* (Brown rat)	Rodents and livestock	Ong et al. (2002) and unpublished (HQ822146).
C. apodemi	Čondlová et al. (2018)	*Apodemus agrarius* (striped field mouse*), Apodemus flavicollis* (yellow-necked mouse)	Rodents (*Apodemus* spp)	None reported
C. ditrichi	Čondlová et al. (2018)	*Apodemus flavicollis* (yellow-necked mouse), *Mus musculus* (mouse)	Rodents (*Apodemus* spp)	Unpublished single human infection, reported in Sweden (Acc. No. KU892579)
C. homai	Zahedi et al. (2017a)	*Cavia porcellus* (Guinea pigs)	Rodents (*Apodemus* spp)	None reported
C. ducismarci	Traversa et al. (2008); Ježková et al. (2016)	*Testudo marginata* (Marginated tortoise), *Python* regius (Ball python), *Chamaeleo calyptratus* (Veiled chameleon), *Malacochersus* tornieri (Pancake tortoise), *Agrionemys [Testudo] horsfieldii (Russian tortoise)*	Tortoises	None reported
C. testudinis	Ježková et al. (2016)	*Agrionemys [Testudo] horsfieldii* (Russian tortoise), *Chelonoidis chilensis* (chaco tortoise), *Testudo graeca Linnaeus* (Greek tortoise), *Testudo hermanni gmelin* (Hermann's tortoise), *Geochelone elegans* (Indian star tortoise), *Stigmochelys pardalis* (leopard tortoise), *Testudo marginata* (marginated tortoise), *Astrochelys radiata* (radiated tortoise), *Psammobates oculifer* (serrated tortoise), *Python regius* (Ball python)	Tortoises	None reported
C. avium	Holubová et al. (2016)	*Cyanoramphus novaezelandiae* (red-crowned parakeet), *Agapornis roseicollis* (rosy-faced lovebird), *Gallus gallus* (chicken), *Amazona aestiva* (blue-fronted Amazon)*, Lophochroa leadbeateri* (major Mitchell's cockatoo)*, Nymphicus hollandicus* (Cockatiel), *Melopsittacus undulates* (Budgerigar)	Birds	None reported
C. proliferans	Kváč et al. (2016)	*Equus africanus* (African wild ass), *Equus asinus* (donkey), *Sciurus carolinensis* (eastern gray squirrel), *Syncerus caffer* (African buffalo), *Equus caballus* (horse), *Tachyoryctes splendens* (East African mole rat)	Rodents, Equine	None reported
C. rubeyi	Li et al. (2015)	*Spermophilus beecheyi* (California ground squirrel)	Squirrels	
C. scophthalmi	Alvarez-Pellitero et al. (2004)	*Scophthalmus maximus* (Turbot)	Turbot	None reported
C. huwi	Ryan et al. (2015)	*Poecilia reticulata* (Guppy), *Paracheirodon innesi* (Neon tetra) and *Puntius tetrazona* (Tiger barb)	Fish	None reported
C. erinacei	Kváč et al. (2014)	*Erinaceus europaeus* (European hedgehog)	Hedgehogs, horses	Kváč et al. (2014)

C. scrofarum	Kváč et al. (2013)	*Sus scrofa* (Pig)	Pigs	Kváč et al. (2009a); Kváč et al. (2009b)
C. viatorum	Elwin et al. (2012b)	*Homo sapiens* (Human)	Humans	Rašková et al. (2013)
C. tyzzeri	Tyzzer (1912); Ren et al. (2012)	*Mus musculus* (Mouse)	Rodents	Rašková et al. (2013)
C. cuniculus	Robinson and Chalmers (2010)	*Oryctolagus cuniculus* (European rabbit)	Rabbits	Chalmers et al. (2009); Anson et al. (2010); Molloy et al. (2010); Chalmers et al. (2011); Hadfield and Chalmers (2012); Koehler et al. (2014)
C. ubiquitum	Fayer et al. (2010)	*Bos taurus* (Cattle)	Ruminants, rodents, primates	Commonly reported (cf. Fayer et al. (2010); Elwin et al. (2012a))
C. xiaoi	Fayer and Santín (2009)	*Ovis aries* (Sheep)	Sheep and goats	Adamu et al. (2014)
C. ryanae	Fayer et al. (2008)	*Bos taurus* (Cattle)	Cattle	None reported
C. macropodum	Power and Ryan (2008)	*Macropus giganteus* (Kangaroo)	Marsupials	None reported
C. fragile	Jirku et al. (2008)	*Duttaphrynus melanostictus* (Toad)	Toads	None reported
C. fayeri	Ryan et al. (2008)	*Macropus rufus* (Kangaroo)	Marsupials	Waldron et al. (2010)
C. bovis	Fayer et al. (2005)	*Bos taurus* (Cattle)	Cattle	Khan et al. (2010); Ng et al. (2012); Helmy et al. (2013)
C. suis	Ryan et al. (2004b)	*Sus scrofa* (Pig)	Pigs	Xiao et al. (2002); Leoni et al. (2006); Cama et al. (2007); Wang et al. (2013)
C. galli	Pavlásek (1999); Ryan et al. (2003a)	*Spermestidae, Frangillidae, Gallus gallus, Tetrao urogallus, Pinicola enucleator* (Birds)	Birds	None reported
C. hominis	Morgan - Ryan et al. (2002)	*Homo sapiens* (Human)	Humans	Most common species in humans
C. molnari	Alvarez-Pellitero and Sitjà-Bobadilla (2002)	*Sparus aurata* (Gilt-head sea bream) and *Dicentrarchus labrax* (European seabass)	Fish	None reported
C. canis	Fayer et al. (2001)	*Canis familiaris* (Dog)	Dogs	Many reports (cf. Lucio-Forster et al. (2010))
C. andersoni	Lindsay et al. (2000)	*Bos taurus* (Cattle)	Cattle	Leoni et al. (2006); Morse et al. (2007); Waldron et al. (2011); Agholi et al. (2013); Jiang et al. (2014); Liu et al. (2014)
C. varanii	Pavlasek et al. (1995)	*Varanus prasinus* (Emerald Monitor)	Lizards	None reported
C. baileyi	Current et al. (1986)	*Gallus gallus* (Chicken)	Birds	None reported
C. parvum	Tyzzer (1912)	*Bos taurus* (Cattle)	Ruminants	Commonly reported in humans
C. meleagridis	Slavin (1955)	*Meleagris gallopavo* (Turkey)	Birds and humans	Commonly reported in humans
C. serpentis	Levine (1980)	*Elaphe guttata, E. subocularis, Sanzinia madagascarensus* (Snakes)	Snakes and lizards	None reported
C. felis	Iseki (1979)	*Felis catis* (Cat)	Cats	Many reports (cf. Lucio-Forster et al. (2010))
C. wrairi	Vetterling et al. (1971)	*Cavia porcellus* (Guinea pig)	Guinea pigs	None reported

C. muris	Tyzzer (1907); Tyzzer (1910)	*Mus musculus* (House mouse)	Rodents	Many reports - Guyot et al. (2001); Gatei et al. (2002); Tiangtip and Jongwutiwes (2002); Gatei et al. (2003); Palmer et al. (2003); Gatei et al. (2006); Leoni et al. (2006); Muthusamy et al. (2006); Azami et al. (2007); Al-Brikan et al. (2008); Neira et al. (2012); Hasajová et al. (2014); Petrincová et al. (2015); Spanakos et al. (2015)
C. microti	Horčičková et al. (2019)	*Microtus arvalis* (Common vole)	Voles	None reported
C. alticolis	Horčičková et al. (2019)	*Microtus arvalis* (Common vole)	Voles	None reported
C. proventriculi	Holubová et al. (2019)	*Nymphicus hollandicus* (Cockatiel)	Birds	None reported

1.3 Life cycle of *Cryptosporidium*

Cryptosporidium have a complex life cycle, which involves both asexual and sexual reproduction (Figure 1). Environmentally-resistant oocysts representing the infective life cycle stage of the parasite are excreted in the faeces (Fayer and Xiao, 2008). Ingestion can come from contact with faeces from an infected animal and faecally contaminated water sources, as well as potentially from coughed up oocysts in airborne droplets from hosts with respiratory infections of *Cryptosporidium* (Sponseller et al., 2014; Aldeyarbi et al., 2016). After ingestion, excystation occurs in the intestine with the release of four motile sporozoites that proceed to infect the apical portion of epithelial enterocytes of the gastro-intestinal (GI) tract creating an extracytoplasmic vacuole that sustains the parasite metabolically whilst keeping it safe from the host immune system and allowing development (Fayer and Xiao, 2008). Following the adherence of the anterior end of the sporozoite to the luminal surface of an epithelial cell in the microvilli, each sporozoite matures into a trophozoite. Trophozoites undergo asexual proliferation by merogony to form meronts, marking the beginning of the asexual part of the life cycle (Fayer and Xiao, 2008; Hijjawi, 2010). Two types of meronts have been described in the *Cryptosporidium* life cycle; type I and type II meronts (Hijjawi, 2010). Type I meronts develop six or eight nuclei, each incorporated into a merozoite, which are released from the parasitiphorous vacuole once mature. The mature type I merozoites infect other host cells and either recycle as type I meronts and merozoites, or develop into a type II meront, which produces four merozoites (Hijjawi, 2010). Following the release of mature type II merozoites, a new host cell is invaded and the sexual phase in the life cycle (gametogeny) is initiated. Type II merozoites either enlarge and develop into a uni-

nucleate macrogamont or undergo cellular fission forming a multi-nucleated microgamont containing 14-16 non-flagellated microgametes.

Microgametes are released from ruptured microgamonts; they penetrate host cells containing macrogamonts and subsequently fertilise the macrogamont forming a zygote (Current, 1990; Current and Garcia, 1991; Hijjawi, 2010). The zygote undergoes sporogony, during which both thin-walled and thick-walled oocysts are formed, each containing four potentially infective sporozoites. Thin walled oocysts remain within the host leading to autoinfection and persistent infections, thick walled oocysts are shed in the faeces into the environment, for ingestion by a new host. The environmental thick trilaminar walled oocyst is highly resistant to chemical and mechanical disruption, including chlorine levels used to disinfect drinking water supplies and public swimming pools (Shields et al., 2008).

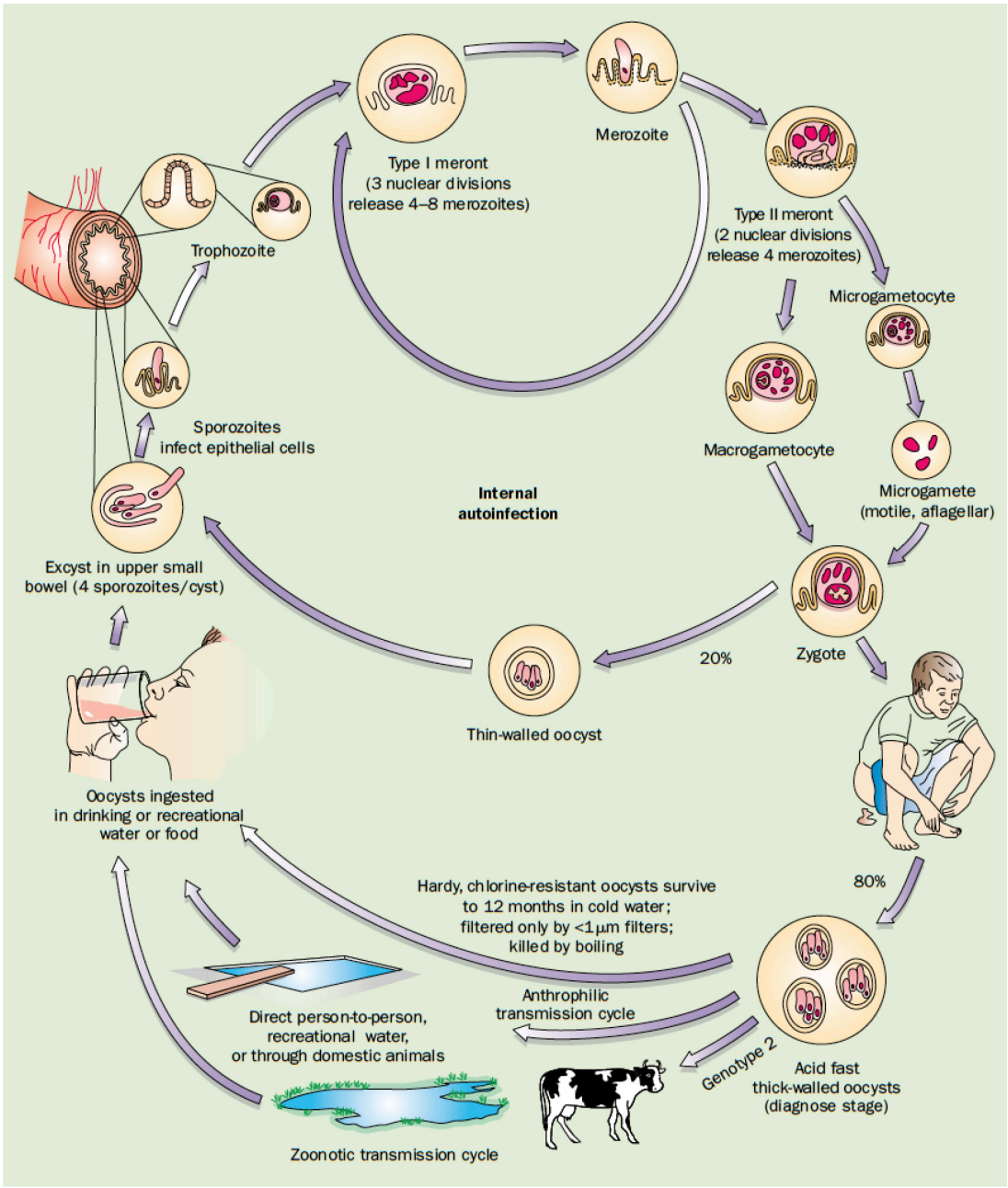

Figure 1.1. The life cycle of *Cryptosporidium parvum*. (Kosek et al., 2001).

1.4 Transmission of *Cryptosporidium*

Cryptosporidium is transmitted via faecal-oral transmission from person to person, animal to person, consumption of contaminated food or water or swimming in contaminated water (Chalmers and Davies, 2010). Transmission can also occur by inhalation resulting in respiratory cryptosporidiosis (Sponseller et al., 2014).

Numerous aspects of the biology of *Cryptosporidium* render the parasite particularly suited to waterborne transmission. These include: (1) oocysts are shed containing fully infective sporozoites and no secondary hosts or maturation conditions are required; (2) the parasite's resistance to disinfection including chlorine (Painter et al., 2015); (3) its ability to be shed in very large quantities, for example, neonatal calves can excrete up to 30 billion oocysts or more over a 1-2 week period (Kuczynska and Shelton, 1999) and (iv) the low infectious dose (10-100 oocysts) (DuPont et al., 1995; Okhuysen et al., 2002; Chappell et al., 2006), means that ingestion of a relatively small amount of contaminated water is sufficient to initiate infection in a susceptible individual. Humans, wildlife and livestock can all potentially contribute infectious oocysts to drinking water (Figure 1.2).

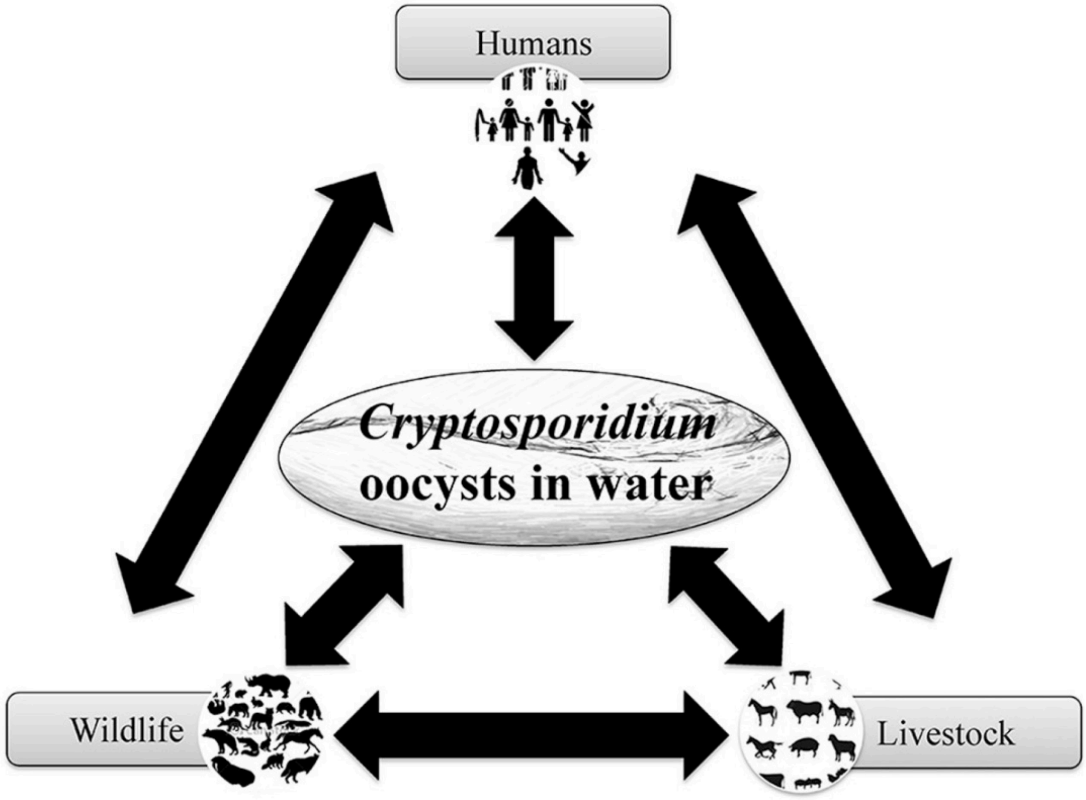

Figure 1.2. Contribution of humans, wildlife and livestock to contamination of drinking water with *Cryptosporidium* oocysts. (Zahedi et al., 2016b).

1.5 Clinical signs and treatment

The symptoms of cryptosporidiosis range from asymptomatic carriage and mild diarrhoea to severe life-threatening illness (Percival, 2014). The general symptoms associated with cryptosporidiosis, in addition to diarrhoea, include vomiting, nausea, inappetence and cramps (Chalmers and Davies, 2010), and cryptosporidiosis is associated with retarded cognitive and functional development in children in developing countries (Kirkpatrick et al., 2002; Valenzuela et al., 2014). Immunocompetent patients generally have self-limiting symptoms but immunocompromised individuals, such as children under 5 years and AIDS patients, can have chronic and severe diarrheal illness that causes stunted growth, malnutrition

and death, particularly in populations of less developed countries (Cacciò and Widmer, 2014).

The mean incubation period is 7 days (ranging 1-15 days) with the prepatent period appearing to decrease in time with an increase of ingested oocysts (Percival, 2014). Clinical signs and symptoms can last between 7 and 22 days, with immunosuppressed patients (such as AIDS/HIV patients) exhibiting prolonged symptoms. In particular, in patients with CD4 T-cell counts <200/mm^3 gastrointestinal symptoms can be severe, chronic, debilitating and life-threatening (Percival, 2014). Prior to the introduction of Highly Active Antiretroviral Therapy (HAART) in 1996, cryptosporidiosis infected 10-15% of AIDS patients with a mortality rate of 50%. HAART has been successful in controlling chronic diarrhoea and wasting due to cryptosporidiosis (Squire and Ryan, 2017). Currently, supportive care and HAART (for HIV/AIDS patients) form the basis for treatment of cryptosporidiosis. There is no effective treatment for cryptosporidiosis in all populations and no vaccine is available (Ryan et al., 2016). The only currently FDA-approved drug, Nitazoxanide, exhibited numerous treatment failures in immunocompetent individuals and is ineffective in immune-compromised populations, even with high doses and prolonged treatment (Amadi et al., 2009). Prevention is mostly based on sanitation and providing clean drinking water, better nutrition and accessible health clinics, particularly in developing countries (Savioli et al., 2006). Guidelines are available for control strategies, following the recommendations of the WHO Neglected Disease Initiative, in 2002 (Savioli et al., 2006).

1.6 Detection and characterisation

Current methods for detection of *Cryptosporidium* include microscopy, immunological assays and molecular testing, each have varying levels of sensitivity and specificity, cost and complexity.

1.6.1 Microscopic methods

Microscopy was originally the only method used to detect and characterise *Cryptosporidium*. It is still used today for histological studies and is a cheap and widely available diagnostic tool, particularly in developing countries (Checkley et al., 2015). This technique however lacks sensitivity, is labour intensive and prone to human error (Fayer et al., 2000). The most common staining techniques include differential-staining methods (eg. Methylene Blue and Ziehl-Neelson), fluorochrome staining and negative staining techniques (e.g. Malachite green and merbromide) (Kawamoto et al., 1987; Chichino et al., 1991; Campbell et al., 1992; Elliot et al., 1999). Due to lack of distinguishing oocyst features however, morphology cannot be used to identify species and therefore molecular characterisation is required to identify to species level (Thompson and Morgan, 1998; Fayer et al., 2000).

1.6.2 Immunological methods

Immunological identification of *Cryptosporidium* offers some advantages over microscopy with increased sensitivity and specificity and include fluorescent antibody staining, latex agglutination reactions, enzyme-linked immunosorbent assays (ELISA), reverse passive haemaglutination (RPH), immunoserology using immunofluorescence (IF) detection and solid phase qualitative immunochromatographic assays (Fayer et al., 2000). A commonly used

immunological assay is the *Cryptosporidium* and *Giardia* Duo-strip immunochromatographic assay (Van den Bossche et al., 2015). However, cross-reactivity with other microorganisms can occur due to the non-specific nature of all antibody-based methods and this can limit their use (Roellig et al., 2017). In addition, in practice, the specificities and particularly the sensitivities of these tests are highly variable, and some *Cryptosporidium* immunochromatographic assays have such low sensitivity and specificity that the US Council of State and Territorial Epidemiologists (CSTE) now exclude cases diagnosed as positive by immunochromatographic assays from cryptosporidiosis surveillance data, and specifies that cases diagnosed with these laboratory tests be considered probable rather than confirmed (Roellig et al., 2017).

1.6.3 Molecular detection and characterisation methods

As microscopy and immunological assays lack specificity and sensitivity and cannot identify *Cryptosporidium* species, molecular detection methods (usually PCR and Sanger sequencing) are the most reliable detection methods (Checkley et al., 2015; Hohweyer et al., 2016). Commonly used loci include the 18S ribosomal RNA (18S) locus and the actin gene (Xiao and Feng, 2017). The 18S is the most common locus used to identify all *Cryptosporidium* species, as it is reliable, multi-copy and contains both conserved regions that identify all *Cryptosporidium* spp. and semi-conserved regions that allow for differentiation between species and genotypes, with the actin locus being used to further confirmation (Xiao and Feng, 2017).

Subtyping (fingerprinting) tools are often used to better understand the transmission dynamics of *Cryptosporidium* species, particularly *C. hominis* and *C. parvum* in humans, animals and wildlife (Xiao, 2010). The 60kDa glycoprotein

(*gp60/40/15*) gene is the most heterogeneous locus in the genome and as this gene encodes a protein that helps in the invasion of gastro-intestinal cells and zoite attachment; it is therefore biologically relevant (Strong and Nelson, 2000; Xiao, 2010). Most of the genetic heterogeneity in the *gp60* gene is the variation in the number of a tri-nucleotide repeat (TCA, TCG or TCT) in the 5' end (*gp40*) of the coding region, although extensive sequence polymorphism is also present in the rest of the gene. The repeats are used to define the subtype families within a species, whereas the remaining polymorphic sites are used to identify subtypes within a subtype family (Ryan et al., 2014). Multilocus fragment typing (MLFT) and is used to enhance the resolution of the subtyping produced by *gp60* sequence analysis (Hotchkiss et al., 2015).

The increasing availability, speed, and decreasing cost per base of next-generation sequencing (NGS) offered by deep sequencing platforms, means that they are increasingly being used for pathogen detection. At present, there are two approaches to NGS. The first (untargeted) approach is shotgun metagenomics, which profiles the entire microbial diversity, or pathobiome (pathogenic microbiome) in a faecal sample. This technique requires the availability of partial or whole reference genomes, which are compared to the shotgun data following quality processing, curation, and assembly of datasets. While this method has the ability to identify mixed microbial infections (correlated to sequence coverage and depth) and novel microbes, until recently, the lack of reference genomes for many of the most important enteric parasites has limited its use. However, with the increasing availability of enteric parasite genomes, including *Cryptosporidium*, shotgun NGS will increasingly be used to identify and develop novel target loci for enteric parasites, particularly those for

which previously only limited diagnostic molecular markers were available (Ryan et al., 2017b).

The second (targeted) approach to NGS is ultra-deep sequencing of PCR products (NGS amplicon sequencing), which allows efficient detection of mixed infection (Ryan et al., 2017b). NGS amplicon sequencing has been used to target predefined loci including the *Cryptosporidium* 18S and *gp60* loci (Paparini et al., 2015; Paparini et al., 2017; Zahedi et al., 2017b; Zahedi et al., 2018).

To date, most genetic characterisation studies of *Cryptosporidium* have utilised Sanger sequencing, however this method cannot resolve mixed infections found in many animals including fish (Yang et al., 2015; Paparini et al., 2017). This is because if a tested sample contains a DNA mixture originating from different *Cryptosporidium* species, then PCR amplification and Sanger sequencing will result in either (1) only DNA of the dominant species being efficiently amplified yielding an unmixed Sanger chromatogram or (2) multiple species will be amplified and mixed chromatogram peaks will render it impossible to identify the species involved (Rieux et al., 2013). NGS overcomes this issue via deep sequencing of the amplicon (i.e. all sequences amplified, even at low levels will be identified) (Paparini et al., 2017). While NGS is more expensive than Sanger sequencing, and currently requires a high level of operator skill, bioinformatic pipeline expertise and knowledge to prevent contamination or corruption of results, it is the method of choice for detecting mixed infection (Paparini et al., 2015). Furthermore, NGS can produce up to 2kb sequences using the Pacific Biosciences platform (Quail et al., 2012) and therefore can be used for evolutionary analysis.

Whole Genome Sequencing (WGS) is an increasingly accessible technology providing extensive bioinformatics data. For the present study, data acquired by WGS would aim to place the evolution of *Cryptosporidium* that infect fish as hosts against those that infect hosts other than fish. WGS achieves this by providing a sequence for the entire genome of a species, all introns and exons and can also be used for finding loci of importance (Xu et al., 2004). Traditional PCR in comparison produces sequences of relatively small sections of a genome (loci) with conserved and variable regions to help identify and characterise species' and is therefore less comprehensive than WGS for creating an evolutionary tree or finding new loci.

1.7 *Cryptosporidium* in fish

Fish as a host for *Cryptosporidium* present a transmission route via (1) being a food source for humans and animals and (2) releasing oocysts into the surrounding water including drinking water. Approximately 9% of global human consumption of protein is provided by fish (Bell, 2019) and almost half of the fish used for human consumption worldwide is provided by Aquaculture (Santos and Ramos, 2018). Parasites can have major economic impacts on aquaculture and zoonotic parasites also represent a significant public health risk (Lafferty et al., 2015). Despite this, relatively little is known about the epidemiology of *Cryptosporidium* infections in fish.

1.7.1 *Cryptosporidium* species and genotypes in fish

Cryptosporidium has been described in both fresh and marine water piscine species with parasitic stages located either on the stomach or intestinal surface, or at both sites (Table 2). The first account of *Cryptosporidium* in a piscine host was

Cryptosporidium nasorum, identified in a Naso tang (*Naso lituratus*), a tropical fish species (Hoover et al., 1981). Hoover and colleagues also noted a similar infection in an unnamed species of marine fish (Hoover et al., 1981). Three years later, Levine (1984) named it *C. nasorum* based on its presumed host specificity. However, no oocyst measurements or helpful taxonomic features were recorded and the fact that only developmental stages on the intestinal microvillous surface were described, has resulted in *C. nasorum* being considered a nomen nudem (i.e., a name that is invalid because an insufficient description was published) (Ryan et al., 2004b; Xiao et al., 2004).

In 1996, Paperna and Vilenkin (1996) proposed a new genus, designated *Piscicryptosporidium*, for *Cryptosporidium*-like species infecting a number of piscine hosts. The genus included two species, *P. reichenbachklinkei* and *P. cichlidaris* previously described as *Cryptosporidium* sp., in cichlid fishes, of the genus *Oreochromis*. Several unique features were cited to support the genus including the covering of the surface of the parasitophorous sac by rudimentary microvilli and the localisation of the oocysts deep within the gastric mucosa (Paperna and Vilenkin, 1996). However, these apparently differential features have also been described in some mammalian *Cryptosporidium* spp. For example, *C. parvum* has been occasionally found within some cells (Marcial and Madara, 1986; Beyer et al., 2000) and microvilli are usually retained in different mammalian species (Alvarez-Pellitero and Sitjà-Bobadilla, 2002).

No molecular data was provided by Paperna and Vilenkin (1996) to support the genus or species, however more recent characterisation of *C. molnari, C.*

scolpthalmi, C. huwi and piscine genotypes indicate that piscine-derived species and genotypes of *Cryptosporidium* are genetically very distinct and primitive to all other species (Ryan et al., 2004b; Palenzuela et al., 2010; Reid et al., 2010; Zanguee et al., 2010; Barugahare et al., 2011; Morine et al., 2012; Ryan et al., 2015; Yang et al., 2015; Yang et al., 2016). However, further studies at additional loci are required to confirm whether or not *Piscicryptosporidium* is valid.

Currently, three species of piscine *Cryptosporidium* are recognised: (1) *Cryptosporidium molnari,* which was originally described in gilthead sea bream (*Sparus aurata*) and European sea bass (*Dicentrarchus labarx*) (Alvarez-Pellitero and Sitjà-Bobadilla, 2002) and was characterised genetically in 2010 (Palenzuela et al., 2010), (2) *C. scophthalmi* was described in turbot in 2004 (*Psetta maxima. sny. Scopthalmus maximus)* (Alvarez-Pellitero et al., 2004) and characterized genetically in 2015 (GenBank accession numbers: KR340588 and KR340589), and (3) *C. huwi* (previously piscine genotype 1) (Ryan et al., 2015).

Molecular characterisation has identified additional piscine genotypes (piscine genotypes 2-8, *C. molnari*-like genotype and seven un-named novel genotypes). While these piscine genotypes appear to be specific for fish hosts, they can frequently infect multiple hosts. For example, piscine genotype 2 was originally identified by Murphy et al. (2009) in histological slides obtained from freshwater angelfish (*Pterophyllum scalare*). The infection in angelfish was described as a myriad of cryptosporidium-like organisms ranging from 1μm to 4.1μm in diameter located along the apical surface of the gastric epithelium. Sporulated oocysts (containing basophilic sporozoites, nearly spherical, 3.4μm + 4μm) and unsporulated oocysts were seen both singly and in

clusters of 4-10 embedded deep within the cytoplasm of the gastric epithelial cells in cytoplasmic vacuoles (parasitophorous vacuoles) surrounded by zones of clearing in gastric epithelial cells (Figure 1.3). DNA was isolated from parasitized visceral tissue and sequenced and a novel genotype was identified; now referred to as piscine genotype 2 (Murphy et al., 2009).

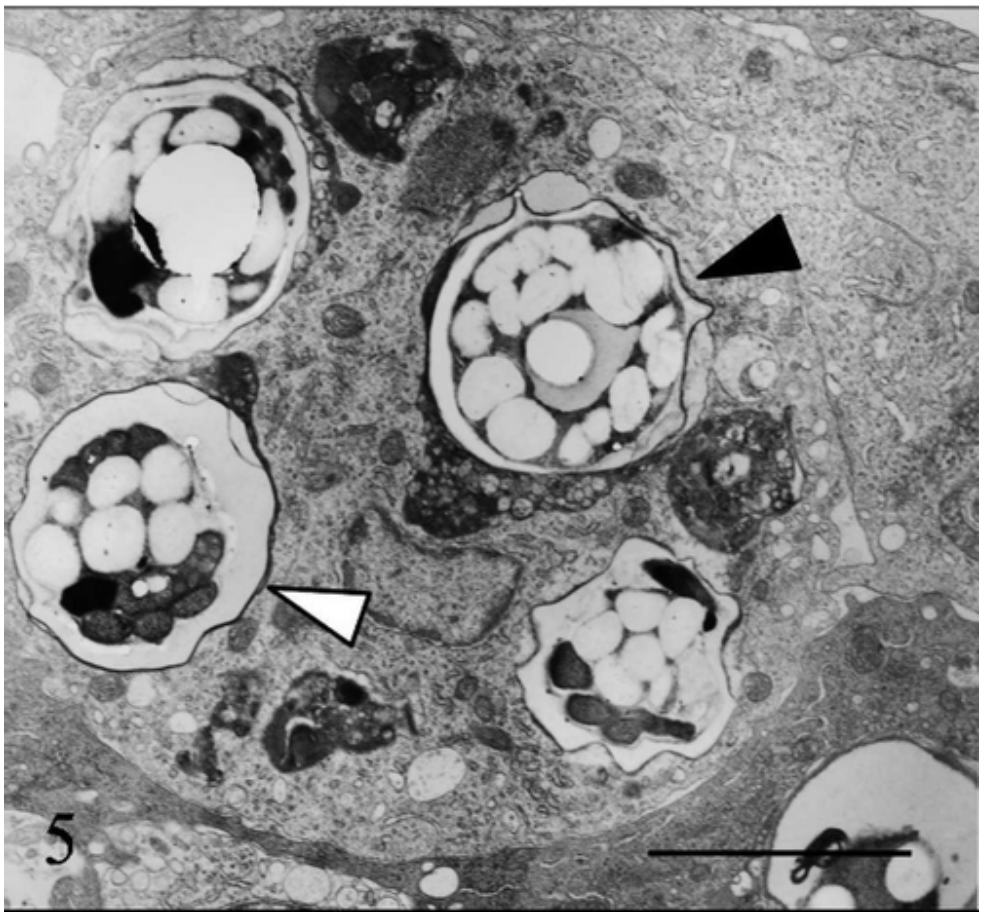

Figure 1.3. *Cryptosporidium* microscopy as seen through a transmission electron micrograph. Sporulated (white arrowhead) and unsporulated (black arrowhead) *Cryptosporidium* embedded in parasitophorous vacuoles within the cytoplasm of gastric mucosa samples taken from infected angelfish. 6,000x magnification. Bar=1μm (Murphy et al., 2009).

In 2010, the same genotype was identified in Oscar fish (*Astronotus ocellatus*) and Neon Tetra (*Paracheirodon innesi*) and was named piscine genotype 2 (Zanguee et al., 2010). Since then piscine genotype 2 has been identified in Mullet (*Mugil cephalus*) and Oscarfish (*Astronotus ocellatus*) (Yang et al., 2015). Further genetic analysis is required at the actin loci to characterise genotype 2 as a valid species.

Molecular characterisation has also identified *C. parvum, C. xiaoi, C. scrofarum, C. hominis* and rat genotype III and more recently, an additional potential

novel species in fish (Reid et al., 2010; Zanguee et al., 2010; Barugahare et al., 2011; Morine et al., 2012; Koinari et al., 2013; Ryan et al., 2014; Certad et al., 2015; Ryan et al., 2015; Yang et al., 2015; Yang et al., 2016).

The identification of *C. hominis* and *C. parvum* in fish has important implications for public health. *C. hominis* has been identified in mackerel scad (*Decapterus maracellus*) in Papua New Guinea (Koinari et al., 2013) and more recently in goldfish (*Carassius auratus*) in Australia (Palermo, 2016). A study in freshwater fish in Lake Geneva of France identified a high prevalence (87%) of *C. parvum* (Certad et al., 2015). In Australia, *C. parvum* has been identified in School whiting (*Sillago vittata*) (Reid et al., 2010) and in goldfish (*Carassius auratus*) (Palermo, 2016).

There are also many mixed infections found in fish that harbour a rich genetic diversity of the parasite with one dominant variant co-inhabiting with far less abundant genotypes (Paparini et al., 2017). Attempts to use nested PCR and Sanger sequencing to characterise mixed infection have been unsuccessful in part due to conflicting results from the two commonly utilised loci, 18S and actin (Yang et al., 2015), and NGS is required to better characterise these mixed infections (Paparini et al., 2017).

Table 1.2. *Cryptosporidium* species and genotypes reported in fish.

Species	Host	Site of Infection	Size (µm) L x W	Reference	GenBank accession number (18S)
C. nasorum	Naso Tang (*Naso literatus*)	Intestine	3.6 x 3.6	Hoover et al. (1981)	-
Cryptosporidium sp.	Carp (*Cyprinus carpio*)	Intestine	-	Pavlásek (1983)	-
Cryptosporidium sp.	Cichlid (*Oreochromis* sp.)	Stomach	-	Landsberg and Paperna (1986)	-
Cryptosporidium sp.	Brown trout (*Salmo trutta*)	Intestine	-	Rush et al. (1987)	-
Cryptosporidium sp.	Barramundi (*Lates calcarifer*)	Intestine	-	Glazebrook and Campbell (1987)	-
Cryptosporidium sp.	Rainbow trout (*Oncorhynchus mykiss*)	Stomach	5-7	Freire-Santos et al. (1998)	-
Cryptosporidium sp.	Red drum (*Sciaenops ocellatus*)	Stomach	7 x 4	Camus and Lopez (1996)	-
Cryptosporidium sp.	Pleco (*Plecostomus* sp.)	Intestine and Stomach	-	Muench and White (1997)	-
Piscicryptosporidium reinchenbachklinkei	Gourami (*Trichogaster leeri*)	Stomach	2.4-3.18 x 2.4-3.0	Paperna and Vilenkin (1996)	-
Piscicryptosporidium cichlidis	Cichlid (*Oreochromis* sp.)	Stomach	4.0-4.7 x 2.5-3.5	Paperna and Vilenkin (1996)	-
Piscicryptosporidium sp.	Gilthead sea bream (*Sparus aurata*)	Stomach	-	Paperna and Vilenkin (1996)	-
C. molnari	Gilthead sea bream (*Sparus aurata*), European sea bass (*Dicentrarchus labrax*), Murray cod (*Maccullochella peelii peelii*)	Stomach (and intestine)	4.72 (3.23–5.45) x 4.47 (3.02–5.04)	Alvarez-Pellitero and Sitjà-Bobadilla (2002); Palenzuela et al. (2010); Barugahare et al. (2011)	HM243548, HM243550, HQ585890
C. molnari-like (LC12)	Peach anthias (*Pseudanthias dispar*)	-	-	Yang et al. (2015)	KR610356
C. scophthalmi	Turbot (*Scophthalmus maximus*)	Intestine	4.44 (3.7–5.03) x 3.91 (3.03–4.69)	Alvarez-Pellitero et al. (2004); Costa (2016)	KR340589
C. huwi (previously piscine genotype 1)	Guppy (*Poecilia reticulata*)	Stomach	4.6 x 4.4	Ryan et al. (2004a); Ryan et al. (2015)	AY524773, KC46997, KC469778
Cryptosporidium sp.	Alewife (*Alosa pseudoharengus*)	-	-	Ziegler et al. (2007)	-
Piscine genotype 2	Angelfish (*Ptertophyllum scalare*), Oscar fish (*Astronatus ocellatis*)	Stomach	3.4 x 4.1	Murphy et al. (2009); Morgan (2015); Yang et al. (2015)	FJ769050, KR610347
Piscine genotype 3	Mullet (*Mugil cephalus*)	Intestine	-	Reid et al. (2010); Yang et al. (2015)	HM989833, KR610348

Piscine genotype 4	Golden algae eater (*Crossocheilus aymonieri*), Kupang damsel (*Chrysiptera hemicyanes)* Oscar	Intestine	-	Reid et al. (2010); Morine et al. (2012)	HM989834, KR610346
Piscine genotype 5	Oscar fish (*Astronatus ocellatis*), Neon tetra *(Paracheirodon innesi*), Angelfish (*Pterophyllum scalare*), Butter bream (*Monodactylidae)*, Golden algae eater (*Crossocheilus aymonieri)*	-	-	Zanguee et al. (2010); Yang et al. (2015)	KR610344
Piscine genotype 5-like (KS05)	Oscar fish (*Astronatus ocellatis*),	-	-	Yang et al. (2015)	KR610345
Piscine genotype 6, piscine genotype 6-like	Guppy (*Poecilia reticulata*), Gourami (*Trichogaster trichopterus)*	-	-	Zanguee et al. (2010); Morine et al. (2012)	HM991857, JQ995776
C. parvum, C. parvum-like, *C. xiaoi* and *C. scrofarum*	Whiting (*Sillago vittata*), Barramundi (*Lates calcarifer*)	-	-	Reid et al. (2010); Gibson-Kueh et al. (2011)	-
Cryptosporidium sp.	Barramundi (*Lates calcarifer*)	Distal stomach and proximal small intestine	-	Gabor et al. (2011)	-
Piscine genotype 7	Red eye tetra (*Moenkhausia sanctaefilomenae*)	-	-	Morine et al. (2012); Yang et al. (2015)	JQ995773, KR610354
Piscine genotype 8	Oblong silver biddy (*Gerres oblongus)*	-	-	Koinari et al. (2013); Yang et al. (2015)	KC807985, KR610349
Cryptosporidium sp. (LC51)	Azure damsel (*Chrysiptera hemicyanea)*	-	-	Yang et al. (2015)	KR610351
Cryptosporidium sp. (CA68)	Platyfish (*Xiphophorus maculatus)*	-	-	Yang et al. (2015)	KR610353
Cryptosporidium sp.(LC38)	Goldfish (*Carassius auratus)*	-	-	Yang et al. (2015)	KR610357
Cryptosporidium sp. (LC01)	Orange clownfish *(Amphiprion percula*)	-	-	Yang et al. (2015)	KR610350
Cryptosporidium sp. (KS02)	Oscar fish (*Astronatus ocellatis*)	-	-	Yang et al. (2015)	KR610352
Cryptosporidium sp.	Koi carp (*Cyprinus carpio*)	Disseminated infection in multiple tissues	-	Yang et al. (2016)	KX033348
Cryptosporidium sp. (JM29)	Goldfish (*Carassius auratus)*	-	-	Morgan (2015); Palermo (2016)	-

1.7.2 Prevalence and clinical signs of piscine *Cryptosporidium*

The prevalence of *Cryptosporidium* in fish is highly variable ranging between 0.8%-100% mostly among juvenile fish (Landsberg and Paperna, 1986; Alvarez-Pellitero et al., 2004; Sitja-Bobadilla, 2005; Murphy et al., 2009; Reid et al., 2010; Zanguee et al., 2010; Morine et al., 2012; Koinari et al., 2013; Certad et al., 2015; Yang et al., 2015; Yang et al., 2016).

Cryptosporidium in fish has been observed in the intestines, stomach, kidneys, spleen, liver and gills (Yang et al., 2016) but normally infects the intestine and stomach of fish (Ryan, 2010). The pathogenesis of *Cryptosporidium* in fish has not been extensively studied, but research has indicated that infected fish exhibit several clinical signs, with morbidity and mortality of parasitised fish dependent on several variables, which include (1) the species of *Cryptosporidium;* (2) the age of the fish; (3) coinfection factors; (4) the size of the fish; and (5) type of fish.

C. molnari was first reported mainly in the stomach epithelium of gilthead sea bream and European sea bass (Alvarez-Pellitero and Sitja-Bobadilla, 2002). Clinical signs included whitish faeces, abdominal swelling and ascites, and *C. molnari* infection was associated with fish mortalities (Alvarez-Pellitero and Sitja-Bobadilla, 2002). The accumulation of *C. molnari* oocysts within the mucosal tissue resulted in cellular injury including consecutive necrosis, vacuolation, and sloughing of epithelial cells (Alvarez-Pellitero and Sitjà-Bobadilla, 2002). Leucocyte inflammatory infiltration has been reported for *C. scolpthalmi* infections (Alvarez-Pellitero et al., 2004) and in gastric cryptosporidiosis in juvenile red drum (*Sciaenops ocellatus*) (Camus and Lopez, 1996).

Other studies of *Cryptosporidium*-infected fish have reported anorexia, regurgitation of food, emaciation, poor growth rates, swollen coelomic cavities, atrophy of skeletal muscle, tucked abdomen, listlessness and increased mortality, particularly in larval and juvenile fish (Camus and Lopez, 1996; Ryan et al., 2004a; Murphy et al., 2009; Gabor et al., 2011). It has also been reported that *Cryptosporidium* distorted the normal mucosal architecture (Landsberg and Paperna, 1986; Paperna, 1987; Camus and Lopez, 1996; Alvarez-Pellitero et al., 2004; Ryan et al., 2004a; Gabor et al., 2011).

A study by Yang et al. (2015) identified a novel *C .molnari*-like genotype in Koi carp (*Cyprinus carpio*), which presented as a disseminated infection throughout the gills, intestine, liver, spleen and kidney. Histological analysis of the Koi carp tissues identified many *Cryptosporidium*-like organisms both free and intracellular (associated with granulomas) in cyst-like structures in the intestine, kidneys, spleen, liver and gills causing severe granulomatous inflammatory lesions (Yang et al., 2016).

1.7.3 Knowledge gaps and conclusion

Morphological and molecular characterisation of piscine genotypes (at two loci) is required in order to characterise them as valid species. For example, piscine genotype 2 has been characterized morphologically and genetically in angelfish at the 18S locus (Morgan et al., 1999), genetically at the 18S locus in Mullet and Oscar fish (Yang et al., 2015), but has yet to be characterised at the actin locus. This is essential to better understand its evolutionary relationships of piscine genotype 2 to other piscine species.

Mixed infections of piscine *Cryptosporidium* spp. have been shown to be common in fish (Yang et al., 2015). It is not known however, whether zoonotic species co-infect fish hosts with piscine species and genotypes and whether fish frequently shed human-infectious oocysts along with host-specific piscine species. It is important to determine this to better understand the public health risks.

1.8 Aims and hypothesis

This project aims to:

1. Screen fish for the presence of *Cryptosporidium* species, and determine the prevalence and diversity of species in farm and aquarium fish from Perth, Western Australia.
2. Characterise piscine genotype 2 and piscine genotype 7 as a valid species using molecular characterisation at the 18S and actin loci and morphological analysis.

The hypotheses of this project are:

1. Phylogenetic analysis of piscine genotype 2 and piscine genotype 7 at the actin locus will confirm its validity as a separate species.
2. Life cycle stages of piscine genotype 2 and piscine genotype 7 will be observed infecting fish gastrointestinal tissue using histological analysis.

Chapter 2: Materials and methods

2.1 Overview

A flow diagram of the methodology used is depicted in Figure 2.1. Briefly, intestine and stomach were dissected and removed with half kept for histology and immunofluorescent antibody staining. The remaining half was used for DNA extraction, followed by quantitative PCR (qPCR). Positives from qPCR were amplified by nested or hemi-nested PCR at the 18S and actin loci and phylogenetic analyses were conducted on the sequences produced. If *C. hominis* or *C. parvum* is detected, then subtyping at the glycoprotein 60 (*gp60*) locus was conducted.

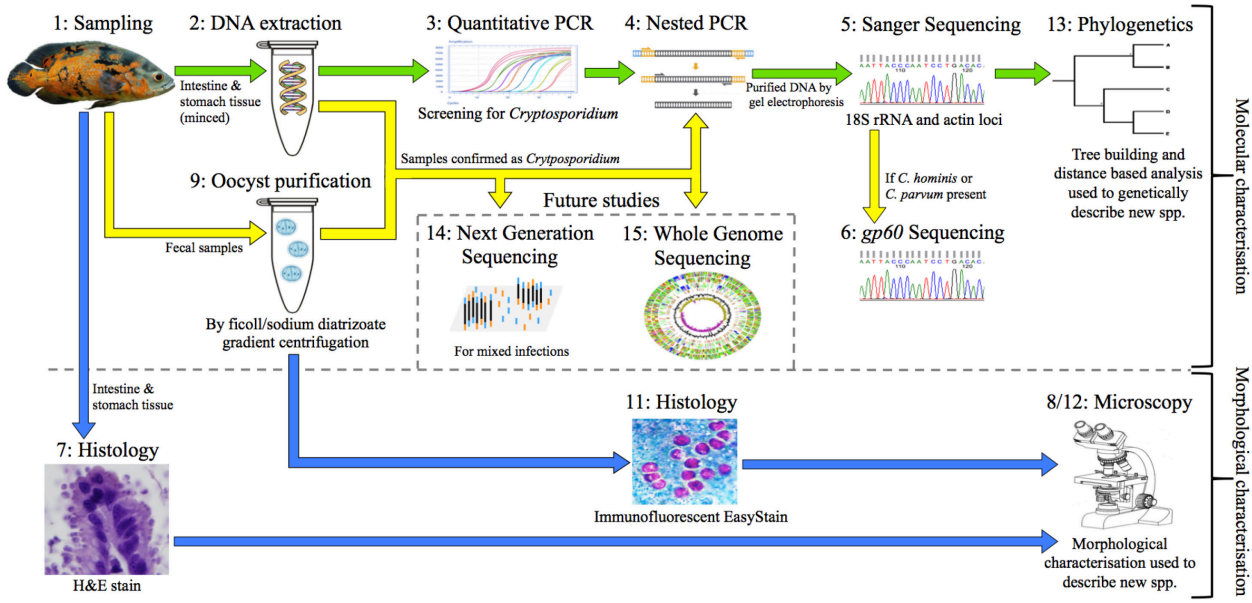

Figure 2.1. Sampling overview. 1) Stomach and intestines were dissected with half was fixed in 10% buffered formalin for histology and the remainder used for DNA extraction. Faecal samples were collected for oocyst purification. 2) DNA was extracted using the DNeasy Blood & Tissue kit (Qiagen, Dusseldorf, Germany). 3) Samples were screened at the 18S locus using *Cryptosporidium*-specific primers by quantitative PCR (qPCR). 4) Samples positive by qPCR were amplified via nested PCR at the 18S and actin loci, amplicons were electrophoresed, positive bands were cut out and sent for Sanger Sequencing. 5 and 6) Sequences are aligned with reference sequences from GenBank for ID of species. 7 and 8) Corresponding tissues from PCR positive samples were processed for H&E stained slides for morphological identification. 9, 10, 11 and 12) Likewise, corresponding faecal samples from PCR

positive samples underwent oocyst purification, histology nested PCR and Sanger sequencing. 13) Phylogenetic analysis was conducted to examine evolutionary relationships. 14) Any mixed infections were identified for future use in NGS. 15) Appropriate samples were reprocessed at tissue level to extract DNA of good quality for WGS.

2.2 Sampling

A total of 467 ornamental freshwater fish were purchased live from local Western Australian aquariums and fish farms between May, 2018 and July, 2019. Multiple ornamental species were obtained from Vebas Aquariums (*n*=233) and consisted of five Angelfish, two Black ghost knife fish, 17 Bronze comets, three Fantails (incidental), eight Golden algae eaters, four Kribensis, 179 Neon tetra, eight Oscar and eight Red-eye tetra (Table 2.1). While Bronze comets (*n*=233) were obtained from Water Garden Life fish farm.

The farmed fish at Water Garden Life fish farm were maintained in an outdoor undercover pond environment. The water supply to the ponds on the fish farm was from underground water table (bore water) and was pumped into outdoor and indoor ponds without any filtration system. Fish were hatched on site and raised separately to other fish species and protected from wildlife by netting and fencing. These fish were collected from the farm in six batches between 4th July, 2018 and 17th April, 2019 over the wet and dry season. The Vebas Aquariums fish were kept in species-specific tanks and were collected in eight batches from the 23rd of May, 2018 to 22nd of July, 2019.

Table 2.1. Fish species screened for *Cryptosporidium.* Fish were sourced locally from either an aquarium (Vebas Aquariums) or a fish farm (Water Garden Life). All samples were obtained alive and euthanized on-site at Murdoch.

Fish common name	Fish scientific name (family)	Habitat	Vebas Aquariums	Water Garden Life fish farm	Total fish
Angelfish	*Pterophyllum altum* (Cichlidae)	Freshwater	5	0	5
Black ghost knife fish	*Apteronotus albifrons* (Apteronotidae)	Freshwater	2	0	2
Bronze comet/Fantail	*Carassius auratus* (Cripinidae)	Freshwater	20	233	253
Golden algae eater	*Gyrinocheilos aymonieri* (Gyrinocheilidae)	Freshwater	8	0	8
Kribensis	*Pelvicachromis pulcher* (Cichlidae)	Freshwater	4	0	4
Neon tetra	*Paracheirodon innesi* (Characidae)	Freshwater	179	0	179
Oscar	*Astronotus ocellatus* (Cichlidae)	Freshwater	8	0	8
Red-eye tetra	*Moenkhausia sanctaefilomenae* (Characidae)	Freshwater	8	0	8
Total			234	233	467

Fish were ethically euthanized in an ice-slurry under Animal Ethics Permit R2949/17. Each fish was weighed, measured (total body length) and dissected using a sterile scalpel blade to remove the stomach, intestines and faeces. Faeces were separated from tissue and kept at 4°C for purifying oocysts. Approximately half of the stomach and intestines from each sample were cut into small sections <1 cm and fixed in 10% buffered formalin for histological examination. These samples were embedded in paraffin and thinly cut sections were used for H & E staining. DNA was extracted from the remaining tissue (≤25mg stomach and intestinal tissue, and homogenised with a clean scalpel blade) using a Qiagen DNeasy Blood and Tissue kits (Dusseldorf,

Germany). Tissue for extraction was preserved at 4°C unless extracted immediately after collection.

2.3 DNA extraction

A Qiagen DNeasy Blood and Tissue Kit (Dusseldorf, Germany) was used to extract DNA from ≤25mg of stomach and intestinal tissue. The manufacturer's instructions were followed for the first batch of fish (*n*=20), which advised elution in 200µL of elution buffer. However, the DNA yield was too dilute, therefore for future extractions, the elution buffer was reduced to between 50-125µL to increase the final DNA concentration. To further optimise DNA elution, the elution buffer was incubated on the DNA elution membrane on the spin column for a minimum of 10 minutes at 37°C and eluted by centrifugation at 11,306 x g for 1 minute. If the available tissue was ≤5 mg, then once eluted, the elution buffer in the spin column was re-applied to the membrane, and the 1 minute spin was repeated to increase DNA yield. Eluted DNA was then stored at 4°C.

If genomic DNA (gDNA) was required for WGS, then during the extraction process an RNase treatment was implemented and an elution buffer such as the Qiagen EB buffer (10 mM Tris-Cl, pH 8.5), that is free of Ethylenediaminetetraacetic acid (EDTA), replaced the Qiagen EA buffer. RNase treatment was applied after adding 180µL ATL buffer and 20µL of proteinase K to digest the tissue sample by adding 1µL of 5µg/µL MasterPure RNase A, vortexing the sample, then incubating at 37°C for 30 min before continuing with the rest of the extraction procedure as described by the Qiagen DNeasy Blood and Tissue handbook. A non-template control (NTC) was added to all extraction runs to act as a negative control and subsequently tested for

contamination during qPCR and PCR runs. This process is for enrichment of DNA and removal of RNA resulting in a DNA pure holobiont sample (host and parasite).

Gel electrophoresis was used on gDNA for WGS to access the extent of undegraded/sheared DNA by electrophoresing at least 5µL of gDNA on a 1% agarose gel a 1 kb DNA ladder at 65-70 volts for 45-50 minutes. A WGS suitable sample should exhibit a bright band above the level 10,000bp ladder band with little to no smearing of product below this (see appendix, Figure A1.1).

2.4 Polymerase Chain Reaction (PCR)

Table 2.2 lists the primers used in the present study. qPCR was used initially to screen all the samples at the 18S locus followed by amplification at the 18S and actin loci using nested and hemi-nested PCR protocols. If *C. parvum* or *C. hominis* were identified, subtyping was conducted at the glycoprotein 60 (*gp60*) locus.

Table 2.2. Primer sets used in the present study.

Locus	Primer name	Direction	Sequence	Amplicon length (base pairs)	Reference
qPCR primers					
18S					
	18SiF	Forward	5'-AGT GAC AAG AAA TAA CAA TAC AGG-3'	298	Morgan et al., 1997
	18SiR	Reverse	5'-CCT GCT TTA AGC ACT CTA ATT TTC-3'		Morgan et al., 1997
Nested/hemi-nested PCR primers					
18S					
Primary Reaction	SHP1	Forward	5'-ACC TAT CAG CTT TAG ACG GTA GGG TAT-3'	773	Silva et al., 2013
	SHP2	Reverse	5'-TTC TCA TAA GGT GCT GAA GGA GTA AGG-3'		Silva et al., 2013

Secondary Reaction	SHP3	Forward	5'-ACA GGG AGG TAG TGA CAA GAA ATA ACA-3'	611	Silva et al., 2013
	SSU-R3	Reverse	5'-AAG GAG TAA GGA ACA ACC TCC A-3'		Xiao et al., 1999
18S					
Primary reaction	18SiCF2	Forward	5'-GAC ATA TCA TTC AAG TTT CTG ACC-3'	763	Ryan et al., 2003
	18SiCR2	Reverse	5'-CTG AAG GAG TAA GGA ACA ACC-3'		Ryan et al., 2003
Secondary reaction	18SiCF1	Forward	5'-CCT ATC AGC TTT AGA CGG TAG G-3'	~587	Ryan et al., 2003
	18SiCR1	Reverse	5'-TCT AAG AAT TTC ACC TCT GAC TG-3'		Ryan et al., 2003
18S					
Primary reaction	SSUF2	Forward	5'-TTC TAG AGC TAA TAC ATG CG-3'	~1325	Xiao et al., 1999
	SSUR2	Reverse	5'-CCC ATT TCC TTC GAA ACA GGA-3'		Xiao et al., 1999
Secondary reaction	SSUF3	Forward	5'-GGA AGG GTT GTA TTT ATT AGA TAA AG-3'	~810	Xiao et al., 1999
	SSUR4	Reverse	5'-CTC ATA AGG TGC TGA AGG AGT A-3''		Xiao et al., 1999
Actin					
Primary reaction	ActinallF1	Forward	5'-GTA AAT ATA CAG GCA GTT-3'	~392	Koinari et al., 2013
Primary and secondary reaction	ActinallR1	Reverse	5'-GGT TGG AAC AAT GCT TC-3'		Koinari et al., 2013
Secondary reaction	ActinallF2	Forward	5'-CCT CAT GCT ATA ATG AG-3'	~278	Koinari et al., 2013
	ActinallR1	Reverse	5'-GGT TGG AAC AAT GCT TC-3'		
Actin					
Primary reaction	ActinF1	Forward	5'-ATG (A/G)G(A/T) GAA GAA G(A/T)A (A/G)(C/T)(A/T)C AA GC-3'	~1095	Sulaiman et al., 2002
	ActinR1	Reverse	5'-AGA A(G/A)C A(C/T)T TTC TGT G(T/G)A CAA T-3'		Sulaiman et al., 2002
Secondary reaction	ActinF2	Forward	5'-CAA GC(A/T) TT(G/A) GTT GTT GA(T/C) AA-3'	~1066	Sulaiman et al., 2002
	ActinR2	Reverse	5'-TTT CTG TG(T/G) ACA AT(A/T) (G/C)(A/T)T GG-3'		Sulaiman et al., 2002
Actin					
Primary reaction	ActinallnewF1	Forward	5'-TAT CCA ATT GAR CAT GG -3'	~1095	Custom made primers
	ActinallnewR1	Reverse	5'- TCA THG TWG ATG GDG CAA -3'		Custom made primers

Secondary reaction	ActinallnewF 1	Forward	5'-TAT CCA ATT GAR CAT GG -3'	~1066	Custom made primers
	ActinR2	Reverse	5'-TTT CTG TG(T/G) ACA AT(A/T) (G/C)(A/T)T GG-3'		Sulaiman et al., 2002
gp60					
Primary reaction	AL3531	Forward	5'-ATA GTC TCG GCT GTA TTC-3'	>850	Glaberman et al., 2002
	AL3535	Reverse	5'-TCC GCT GTA TTC TCA GCC-3'		Glaberman et al., 2002
Secondary Reaction	AL3532	Forward	5'-GGA AGG AAC GAT GTA TCT-3'	800-850	Glaberman et al., 2002
	AL3534	Reverse	5'-GCA GAG GAA CCA GCA TC-3'		Glaberman et al., 2002

All PCRs were run with an extraction reagent blank control (EXB - negative control from the extraction process), a non-template control (NTC - negative control consisting of PCR reagents without template DNA) and a positive control (*C. viatorum* DNA being a *Cryptosporidium* sp. that almost exclusively infects humans (Elwin et al., 2012b)).

2.4.1 Quantitative PCR (qPCR)

All samples were screened by qPCR using the primer pair 18SiF and 18SiR to amplify a ~298 bp product (Table 2.2). PCR was performed in 20µL volume consisting of 1µL gDNA, 2µL of PCR buffer (10x), 3µL $MgCl_2$ (25mM), 1µL dNTPs (10mM), 0.25µL of both forward and reverse primers (10mM), 0.25µL of EUK3 probe, 0.1µL Taq Polymerase (5U/µL), and 12.15µL of Ultra-pure PCR water. Reactions were carried out on a Rotor-Gene-Q 3000 (FisherBiotech, Australia) and subjected to the following PCR conditions: a preliminary cycle of 95°C for 6 minutes followed by 50 cycles of 94°C for 20 seconds and 60°C for 90 seconds. Data was acquired in the green FAM channel at the end of each 60°C step.

2.4.2 Nested PCR

Three sets of 18S nested primers were used in the present study, a set designed by Ryan et al. (2003b) that produced 587bp amplicons, another set designed by Xiao et al. (1999) that produced 810bp amplicons and a primer set by Silva et al. (2013) that produced 611bp amplicons (Table 2.2). Two sets of actin primers are used in the present study, a hemi-nested PCR designed by Koinari et al. (2013) that produced 278bp amplicons and a nested set by Sulaiman (2002) that produced ~1066bp amplicons (Table 2.2). The primers initially used for amplification in the present study were by Silva et al. (2013) for 18S and Koinari et al. (2013) for actin, complimentary primers by Ryan et al. (2003b) and Xiao et al. (1999) for 18S and Sulaiman (2002) were used for further analysis, however, the complimentary primers produced longer and higher quality sequences and became the conclusive primers from which all genetic analysis in the present study was conducted. Amplification conditions for conclusive primers used for analysis in the present study are listed below (Section 2.4.3). For amplification conditions of primers in Table 2.2 not used for analysis please refer to the respective reference n Table 2.2. Custom actin primers were used for complimentary PCR tests but not for analysis, the conditions for use are listed below (Section 2.4.3). Human infective *Cryptosporidium* was not identified in samples from the present study, therefore species subtyping at the *gp60* locus was not conducted.

2.4.3 The 18S locus

Conditions for the 18S primers by Ryan et al. (2003b) consisted of 1µL of DNA, 2.5µL PCR Buffer (10x with dye and 1.5mM Mg at 1X), 0.25µL dNTPs (10 mM), 0.1µL Taq DNA Polymerase (5 units), 19.15µL of PCR grade water and 1µL each of primers 18SiCF2 and 18SiCR2 for the primary PCR (external primers) and

18SiCF1 and 18SiCR1 for the secondary PCR (internal primers) in a 25µL reaction. Cycling conditions were as follows: a preliminary cycle of 94°C for 5 minutes followed by 45 cycles of denaturation, annealing and extension at 94°C for 30 seconds, 58°C for 30 seconds and 72°C for 1 minute, followed by a final extension of 72°C for 10 minutes. These conditions are identical for the primary and secondary PCR with 1µL of product from the primary being used in the secondary.

Conditions for the 18S primers by Xiao et al. (1999) consisted of 1µL of DNA, 2.5µL PCR Buffer (10x with dye and 1.5 mM Mg at 1X), 0.25µL dNTPs (10 mM), 2µL $MgCl_2$ (25 mM), 0.1µL Taq DNA Polymerase (5 units), 17.15µL of PCR grade water and 1µL each of primers SSUF2 and SSUR2 for the primary PCR (external primers) and SSUF3 and SSUR4 for the secondary PCR (internal primers) 18SiCF2 and 18SiCR2 for the primary PCR (external primers) and 18SiCF1 and 18SiCR1 for the secondary PCR (internal primers) in a 25µL reaction. Cycling conditions were as follows: a preliminary cycle of 94°C for 3 minutes followed by 53 cycles of denaturation, annealing and extension at 94°C for 45 seconds, 58°C for 1 minute and 30 seconds and 72°C for 1 minute, followed by a final extension of 72°C for 7 minutes. These conditions are identical for the primary and secondary PCR with 1µL of product from the primary being used in the secondary.

2.4.4 The actin locus

Conditions for the Sulaiman (2002) nested actin primers were 1µL of DNA, 2.5µL PCR Buffer (10x with dye and 1.5mM Mg at 1X), 0.25µL dNTPs (10 mM), 2µL $MgCl_2$ (25 mM), 0.1µL Taq DNA Polymerase (5 unit), 17.15µL of purified water and 1µL each of primers ActinF1 and ActinR1 for the primary PCR (external primers)

and ActinF2 and ActinR2 for the secondary PCR (internal primers) in a 25µL reaction. Cycling conditions were 94°C for 5 minutes followed by 45 cycles of denaturation (this was increased to 45 cycles, which produced better results), annealing and extension at 94°C for 45 seconds, 50°C for 45 seconds and 72°C for 1 minute, followed by a final extension of 72°C for 10 minutes. For the secondary PCR, the conditions for the annealing temperature changed from 50°C for 45 seconds to 45°C for 45 seconds, all other conditions remained the same, with 1µL of product from the primary used in the secondary PCR.

A set of primary nested actin primers, ActinallnewF1 and ActinallnewR2, were custom designed for the present study from an actin sequence of genotype 2 using Amplify version 4 (https://engels.genetics.wisc.edu/amplify/). These custom actin primers were only complimentary to the conclusive primers and sequences produced were not used in genetic analysis, however, if future studies require their use the conditions used were as follows. Conditions for these primers were 1µL of DNA, 2.5µL PCR Buffer (10x with dye and 1.5mM Mg at 1X), 0.25µL dNTPs (10 mM), 2µL $MgCl_2$ (25 mM), 0.1µL Taq DNA Polymerase (5 unit), 17.15µL of purified water and 1µL each of primers ActinF1 and ActinR1 for the primary PCR (external primers) and ActinF2 and ActinR2 for the secondary PCR (internal primers) in a 25 µL reaction. Cycling conditions were 94°C for 5 minutes followed by 45 cycles of denaturation, annealing and extension at 94°C for 45 seconds, 50°C for 45 seconds and 72°C for 1 minute, followed by a final extension of 72°C for 10 minutes. For the secondary PCR the condition for the annealing temperature changed from 50°C for 45 seconds to 45°C for 45 seconds, all other conditions remained the same, with 1µL of product from the primary used in the secondary PCR.

2.4.5 *gp*60 PCR

The human infective *Cryptosporidium* species *C. hominis* or *C. parvum* were not identified in samples from the present study and therefore *gp*60 subtyping was not conducted.

2.5 Gel electrophoresis

PCR products were separated according to size on a 1% (w/v) agarose gel (Fisher Biotech, Australia) containing 5µL of SYBR® Safe (Invitrogen™, Australia) via gel electrophoresis. The gel was placed into a bath of 1x TAE buffer (40mM Tris-HCL, 20mM EDTA at pH 7.0) buffer and 20 µL of PCR product was loaded into the wells. A 100bp molecular weight ladder (Axygen, FisherBiotech, Australia) (8µL) was used. Gels were run at 65-70 volts for 45-50 minutes and then placed on an AlphaDigiDoc ultra-violet transillumination system (BioRad, Hercules, CA, USA) to visualise bands. A Cannon C-5060 Wide Zoom digital camera was used to capture images using the AlphaDigiDoc software.

2.6 DNA purification

Visualised bands of the required size for each set of secondary primers (see Table 2.2) were purified using the filter tip method by Yang et al. (2013) for Sanger sequencing. Briefly, P200 aerosol barrier pipette tips with filters (Interpath Services, Australia) were prepared by cutting the narrow end off about 3mm from the filter and placed into 1.5ml tubes (Eppendorf™, Germany). Bands were precisely excised from agarose gel using individual sterilised scalpel blades and placed into prepared pipette tips with filters intact. Tubes were then spun at full speed on a microfuge, filter tips

were discarded and the eluent (purified DNA) was stored at -20°C to be used for Sanger sequencing.

2.7 Sanger sequencing

Sanger sequencing was conducted both on-site at the Murdoch University (Western Australia) State Agriculture Biotechnology Centre sequencing facility and externally at the Australian Genome Research Facility (AGRF).

Sequencing conducted on PCR positives at Murdoch used an ABI Prism™ Dye Terminator cycle sequencing kit (Applied Biosystems, Foster City, California) and was conducted according to the manufacturer's instructions using an ABI 373096 sequencer (Life Technologies, USA).

Sequencing reactions were 10 µL in volume and consisted of 1µL Big Dye, 1.5µL of 5x PCR buffer, 6.5µL purified DNA and 1µL of secondary primer (forward or reverse). The PCR conditions were a preliminary denaturation of 95°C for 2 minutes, followed by 27 cycles of 95°C for 10 seconds, 55°C for 5 seconds and 60°C for 4 minutes, with a final hold temperature of 12°C. Samples were stored at -20°C unless immediately processed. Ethanol precipitation was conducted on the 10 µL PCR products by pipetting the reactions into plates containing 1µL of 125mM EDTA, 1µL of 3M sodium acetate and 35µL of 100% ethanol and mixing by vortexing for 15 seconds. Plates were incubated at room temperature for 20 minutes then spun in a microfuge at 4100 rpm for 30 minutes. Plates were then opened and the ethanol removed and placed upside down in the centrifuge on paper towel and spun at 1000 rpm to remove supernatant and leave DNA pellets on the inner surface of the tubes. Plates were washed with 35µL of 70% ethanol, and mixed by vortexing for 20 seconds

before being spun with lids closed at 3300 rpm for 15 minutes. Plates were air-dried and sent directly for sequencing or stored at -20°C for sequencing at a later stage.

Sequencing was also conducted at AGRF over the summer period due to the shutdown of the Murdoch University campus but continued throughout 2019 due to the reliable and time saving service that was provided by AGRF.

2.8 Sequence alignment and NCBI BLAST

Sequences were initially assessed using the FinchTV chromatogram viewer version 1.5 (https://digitalworldbiology.com/FinchTV), to confirm quality and resolve ambiguities or sequencing artifacts. Sequencing chromatograms were imported into Geneious (Kearse et al., 2012) and primers were trimmed before being run through the NCBI database using the Basic Local Alignment Search Tool (BLAST). The species identity was confirmed against the highest % Blast result with a significant query cover and by phylogenetic analyses.

2.9 Phylogenetic analysis

Sanger sequencing chromatogram files were imported into Geneious (Kearse et al., 2012), and the nucleotide sequences of each gene was curated, analysed and aligned with reference sequences from GenBank using MAFFT v7.071 (Katoh and Toh, 2010) and realigned using MUSCLE (Edgar, 2004). Phylogenetic analysis of aligned sequences was conducted using Neighbor Joining and Maximum Likelihood analysis with MEGA version 7 (http://www.megasoftware.net) (Tamura et al., 2013) with the most suitable nucleotide substitution model for each analysis selected according to jModelTest2 (Darriba et al., 2012). Bootstrap support was based on 1000

replications. Phylogenetic analyses were conducted on sequences from the 18S locus, the actin locus and concatenated sequences from the 18S and actin loci.

2.10 Oocyst purification

Cryptosporidium oocysts were purified from faecal samples using Ficoll/sodium diatrizoate gradient centrifugation in a method adapted from Boxell et al. (2008).

Faeces were resuspended in cold PBS and mixed vigorously; ~10 mL/g of faeces. The sample was strained through prewetted surgical gauze and resuspended in cold PBS and 0.05 grams of sputosol (oxoid)/10 mL of faecal suspension added. Samples were then left at room temperature (~23°C) on a mixer for 60-90 minutes. Samples were washed in cold PBS by centrifugation at 2000 x g for 8 minutes at 4°C, this was repeated until supernatant became clear. Samples were again resuspended in cold PBS and ~2.5mL of ether per 10 mL of suspension was added, samples were mixed vigorously for 10-15 seconds and centrifuged at 2000 x g for 8 min at 4°C. Supernatant was removed and washed twice in cold sterile PBS at 2000g for 4-5 minutes at 4°C. Samples were resuspended in 2-3 mL of cold sterile PBS and 2-3mL of oocyst suspension was carefully layered on top of a cold gradient at 4°C and samples were centrifuged for 20 minutes at 2000g at room temperature (~23°C). The interface was transferred between the 0.5% and the 1.0% phases to a 50 mL tube, samples were topped up to 50mL with PBS and centrifuged at 2000g for 5 minutes at 4°C. Pellet is washed in 10% bleach then spun at 2000g at 4°C for 8 minutes. The supernatant was removed and 1-2mL of PBS was added. Samples were then resuspended in 1-2mL of cold sterile PBS and 15µL of antibiotic solution (5,000 units

penicillin and 5mg streptomycin/mL) per mL of resuspended oocysts was added and samples were stored at 4°C.

2.11 Microscopy

2.11.1 Histology preparation from tissue

Intestinal and gastric tissue from corresponding PCR positives, previously collected and placed in 10% formalin, was suspended in paraffin wax blocks and thin slides were cut and stained with Hematoxylin and eosin (H&E) and examined by microscopy to identify life cycle stages of *Cryptosporidium*.

2.11.1 Histology preparation from purified oocysts

Easy Stain™ (BTF, Sydney), which binds to *Cryptosporidium* oocyst walls, and DAPI (4',6-diamindino-2-phenylindole), which readily binds to areas of DNA with a high percentage of adenine and thymine, was applied for enhanced visibility via immunofluorescence in a method adapted from Boxell et al. (2008).

Samples were placed in wells on glass slides then dried at 37°C (maximum drying time 1 hour). After drying 50µL methanol was added to the wells and allowed to dry for approximately 30 minutes. 1-2 drops of EasyStain™ DAPI *(or 50µL working strength DAPI) solution was added to the wells and left on for 2 minutes, excess solution was removed by tilting the well slide (long edge down) and placing an absorbent material at the edge of the well slide to soak it up. 50 µL of distilled water was added to the wells and left for 1 minute, which was followed by removal of excess solution (as previously discussed). 1 drop (50µL) of EasyStain™ (or enough to cover the well) was added to the wells and slides were incubated at room temperature for 30

minutes followed by removal of excess solution (as previously discussed). 100-250µL of ice cold (4°C) Fixing Buffer was added to the wells and allowed to flow to the well edges and left for 2 minutes, excess solution was then removed (as previously discussed). 5µL of EasyStain™ Mounting Medium was added to the wells and cover slips were applied to the wells. Visualisation was conducted with an Olympus D21 digital camera magnified by an Olympus BX51 fluorescence microscope. Unfortunately oocysts were not seen in processed slides, most likely due to the small volume of faecal samples and high number of PBS washes where oocysts can become lost. In future studies smaller volumes of PBS is recommended along with less washes.

2.12 Statistical analysis

Prevalence was expressed as the percentage of samples amplified by PCR at the 18S locus, with 95% confidence intervals (traditional Clopper-Pearson CI) calculated assuming a binomial distribution, using the software Quantitative Parasitology 3.0 (Reiczigel et al., 2019).

Student's t-tests were performed using PAST version 3.24 (Hammer et al., 2001) to determine whether there was a significant difference in the weight and length of fish that were infected with *Cryptosporidium* spp. and those that were not. Homogeneity of variance will be determined using the F test, if variances are unequal unequal-variance *t*-values and *p*-values will be used to determine significance.

Chapter 3: Results

3.1 Parasite prevalence in fish

Of 467 fish samples screened for *Cryptosporidium* at the 18S locus, 20 were positive for the parasite (20/467, 4.3%, 95% CI; 2.6-6.5). In total, one *Cryptosporidium* species (*C. huwi* from Neon tetra; *n*=11), three genotypes including piscine genotype 2 (from Oscarfish; *n*=3), piscine genotype 4 (from a Black ghost knife fish; *n*=1), and piscine genotype 7 (from Red eye tetra; *n*=5), and one mixed infection were detected (Table 3.1). In addition, due to non-specific amplification at the 18S locus, two other parasite genera were detected including ten sequences genetically similar to *Goussia* spp. (10/467, 2.1%, 95% CI; 1.0-3.9) (see Chapter 3.3), and a single sequence from a free-living alveolate *Colpodella* sp. (1/467, 0.21%, 95% CI; 0.0-1.2) (see Chapter 3.4).

Of the 20 samples confirmed to be positive for *Cryptosporidium* by Sanger sequencing at the 18S locus, only seven produced clean chromatograms at the actin locus. In total, one *Cryptosporidium* species (*C. huwi* from Neon tetra; *n*=3), two genotypes including piscine genotype 2 (from Oscarfish; *n*=1) and piscine genotype 7 (from Red eye tetra; *n*=1), and one novel *Cryptosporidium* sequence in a Red eye tetra were detected (Table 3.1). One sample produced a sequence for *C. huwi* at the actin loci that did not amplify at the 18S locus. The sample that amplified a novel *Cryptosporidium* sequence at the actin locus had previously been identified as piscine genotype 7 at the 18S locus, indicating a mixed infection. In total there were two mixed infections found in fish in the present study, both in Red eye tetra.

Table 3.1. Prevalence of *Cryptosporidium* detected in freshwater fish at the 18S locus. (95% confidence intervals are given in parenthesis).

Fish Common name	Fish Scientific name (family)	Aquarium	Fish farm	Total no sampled	Prevalence of *Cryptosporidium* by PCR at the 18S locus (%, 95% CI)	No of *Cryptosporidium* sp. confirmed by PCR at the actin locus	*Cryptosporidium* species at the 18S locus
Angelfish	*Pterophyllum altum* (Cichlidae)	5	0	5	0 (0%, 0-52.2)	0	-
Black ghost knife fish	*Apteronotus albifrons* (Apteronotidae)	2	0	2	1/2 (50%, 1.3-98.7)	0	Piscine genotype 4 (*n*=1)
Bronze comet/Fantail (goldfish)	*Carassius auratus* (Cripinidae)	20	233	253	0 (0%, 0-1.4)	1*	-
Golden algae eater	*Gyrinocheilos aymonieri* (Gyrinocheilidae)	8	0	8	0 (0%, 0-36.9)	0	-
Kribensis	*Pelvicachromis pulcher* (Cichlidae)	4	0	4	0 (0%, 0-60.2)	0	-
Neon tetra	*Paracheirodon innesi* (Characidae)	179	0	179	11/179 (6.1%, 3.1-10.7)	3	*C. huwi* (*n*=11)
Oscar	*Astronotus ocellatus* (Cichlidae)	8	0	8	3/8 (37.5%, 8.5-75.5)	1	Piscine genotype 2 (*n*=3)
Red eye tetra	*Moenkhausia sanctaefilomenae* (Characidae)	8	0	8	5/8 (62.5%, 24.5-91.5)	2**	Piscine genotype 7 (*n*=5)
Total		234	233	467	20/467 (4.3%, 2.6-6.5)	7	

*Note 1 *C. huwi* was sequenced by PCR at the actin loci from a goldfish that did not amplify at the 18S locus.
**Note a conflicting novel *Cryptosporidium* sequence was amplified from the same Red eye tetra that produced a piscine genotype 7 sequence at the 18S loci.

3.2 *Cryptosporidium* in fish

3.2.1 Differences in size and length of fish with *Cryptosporidium* infections

A student's t-test was performed on fish with appropriate sample numbers to determine whether there was a correlation between length or weight of fish identified as positive for *Cryptosporidium* by PCR and sequencing and those that tested negative. Statistical tests were conducted separately for different species of fish hosts. A p-value of $P<0.05$ was deemed as the significant.

The student's t-test was performed on both Neon tetra and Oscarfish. The t-test was not performed on goldfish, Angelfish, Golden algae eater or Kribensis as no positive samples were identified in these species. Black ghost knife fish or Red eye tetra samples were not analysed either regardless of infections due to the small sample sizes (n=2) (one tested positive for *Cryptosporidium*) and n=8 (6/8 tested positive for *Cryptosporidium*) respectively; the t-test cannot be performed unless there are three samples from each group (positive and negative).

The F test determined homogeneity of variance between groups of Neon tetra screened for *Cryptosporidium* and was equal for both weight ($F(177)=2.3029$, $p=0.1438$) and length ($F(177)=1.0096$, $p=0.9074$). Homogeneity of variance between groups of Oscarfish were also equal for both weight ($F(6)=11.6140$, $p=0.1623$) and length ($F(6)=25.1000$, $p=0.0775$).

The student's t-test determined no significance ($p<0.05$) between Neon tetra (n=179) that tested positive or negative for *Cryptosporidium* and a difference in weight ($t(177)=1.589$, $p=0.1132$) or length ($t(177)=1.0132$, $p=0.3119$) (Table 3.2).

The students' t-test determined no significance ($p<0.05$) between Oscarfish (n=8) that tested positive or negative for *Cryptosporidium* and a difference in weight ($t(6)=0.6967$, $p=0.5179$) or length ($t(6)=0.6930$, $p=0.51422$) (Table 3.2).

Table 3.2. Statistical analysis of the correlation between the presence of *Cryptosporidium* and the length and weight. Results of the t-test were not significant with a p-value < 0.05 being deemed significant.

Fish sp.	Variable	*p*-value	*t*-value	Uneq. Var. *p*-value	Uneq. Var. *t*-value	Degrees of freedom
Neon tetra	Weight	0.2467	1.1624	0.1184	1.6699	177
Neon tetra	Length	0.5758	0.5605	0.5845	0.5629	177
Oscarfish	Weight	0.5179	0.6867	0.2296	1.3271	6
Oscarfish	Length	0.51422	0.6930	0.4178	0.8728	6

Neon tetra (*Paracheirodon innesi*) (n=179) samples that tested negative for *Cryptosporidium* (n=168) had a mean weight of 0.23g and mean length of 2.72cm, while the samples that tested positive (n=11) had a mean weight of 0.21g and a mean length of 2.75cm (Figure 3.1). As the age of juvenile Neon tetra was unknown, fish age was not a consideration of this statistical analysis.

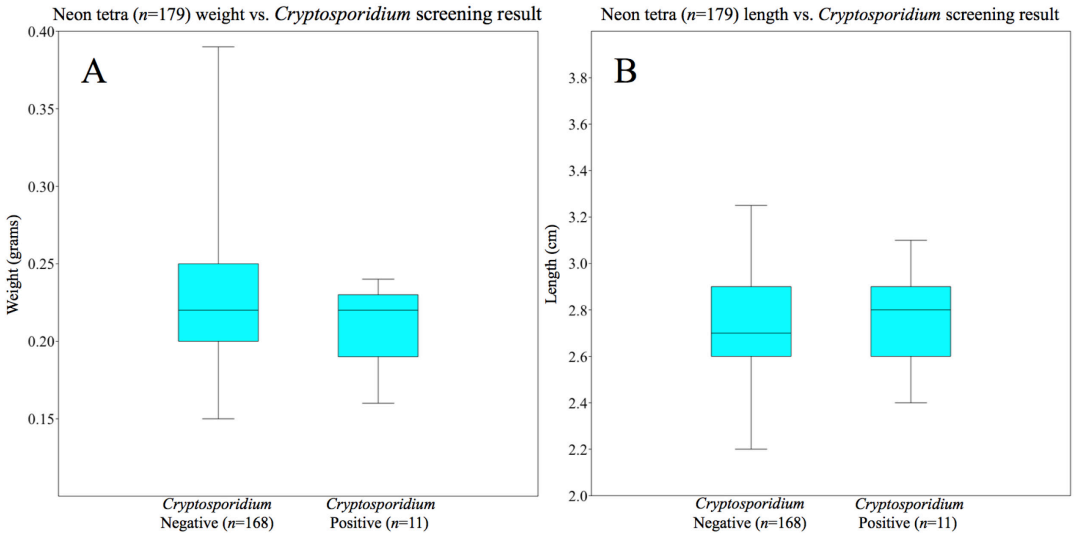

Figure 3.1. Boxplot of Neon tetra weight in grams (A) and length in cm (B) comparing fish found to be negative and positive for *Cryptosporidium* by PCR. Shown are the range, median and quartiles with a drop in both weight and length of fish with infections.

Oscarfish (*Astronotus ocellatus*) (*n*=8) samples that tested positive for *Cryptosporidium* (*n*=3) had a mean weight of 6.55g and mean length of 7.16cm, while the samples that tested negative (*n*=11) had a mean weight of 7.49g and a mean length of 7.37cm (Figure 3.2). All Oscarfish used in the present study were juvenile fish with adults growing over 36cm and weighing over 1.4kg.

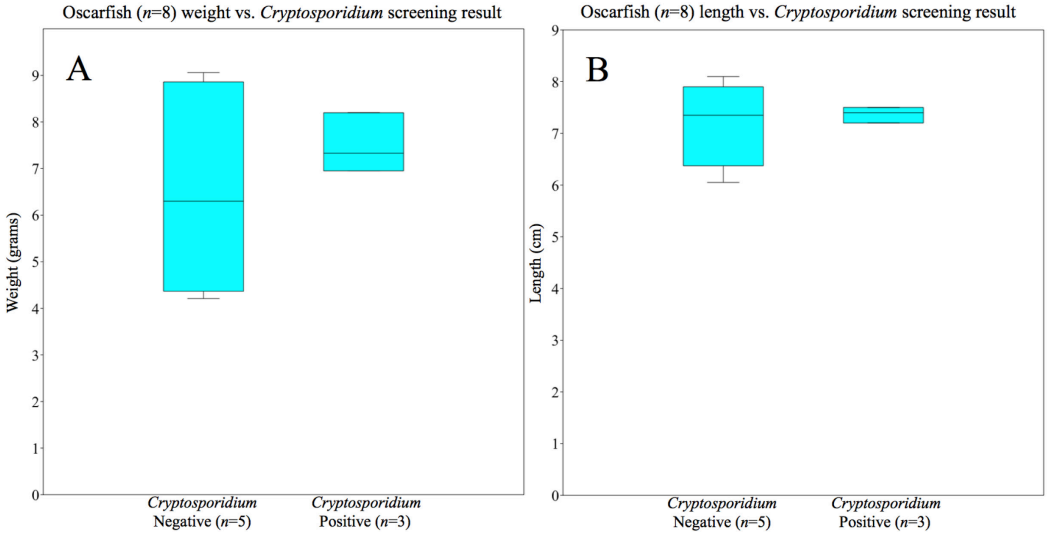

Figure 3.2. Boxplot of Oscarfish weight in grams (A) and length in cm (B) comparing fish found to be negative and positive for *Cryptosporidium* by PCR. Shown are the range, median and quartiles with a drop in both weight and length of fish with infections.

3.2.2 Species of *Cryptosporidium* in fish

At the 18S locus, clean chromatograms of *Cryptosporidium* sequences were generated for 20 samples; 11 were *C. huwi* (isolates NT184, NT207, NT214, NT216, NT218, NT232, NT406, NT411, NT418, NT428, NT432), three were piscine genotype 2 (isolates OF447, OF448, OF449), one was piscine genotype 4 (isolate BGKF462), five were piscine genotype 7 (isolates RET438, RET439, RET441, RET442, RET443, RET445), and one was a mixed infection RET438 (Table 3.3). At the actin locus, seven isolates (NT207, NT214, NT218, GF314, RET441, RET445 and OF448) were amplified (Table 3.3).

Table 3.3. *Cryptosporidium* species sequenced at the 18S and actin loci and identified by morphology. Samples starting with GF are goldfish, NT are Neon tetra, RET are Red eye tetra, OF are Oscarfish and BGKF are Black ghost knife fish.

Sample ID	18S locus sequence (Xiao, 1999) ~810bp	18S locus sequence (Ryan, 2003) ~578bp	Actin locus sequence (Sulaiman 2002) ~1066bp	Morphology
NT184	-	*C. huwi*	-	-
NT207	-	*C. huwi*	*C. huwi*	-
NT214	-	*C. huwi*	*C. huwi*	(H&E stain) (Figures 3.6-8)
NT216	-	*C. huwi*	-	-
NT218	-	*C. huwi*	*C. huwi*	-
NT232	-	*C. huwi*	-	-
GF324	-	-	*C. huwi*	-
NT406	-	*C. huwi*	-	-
NT411	-	*C. huwi*	-	-
NT418	-	*C. huwi*	-	-
NT428	*C. huwi*	*C. huwi*	-	-
NT432	-	*C. huwi*	-	-
RET438	-	Mixed infection	-	(H&E stain) (Figure A1.1)
RET439	-	Piscine genotype 7	-	-
RET441	Piscine genotype 7	Piscine genotype 7	Novel sequence	-
RET442	-	Piscine genotype 7	-	-
RET443	-	Piscine genotype 7	-	-
RET445	Piscine genotype 7	Piscine genotype 7	Piscine genotype 7	-
OF447	-	Piscine genotype 2	-	-
OF448	Piscine genotype 2	Piscine genotype 2	Piscine genotype 2	-
OF449	-	Piscine genotype 2	-	-
BGKF462	-	Piscine genotype 4	-	-

3.2.1 Phylogenetic analysis of *Cryptosporidium* at the 18S locus

Phylogenetic analysis at the 18S locus based on 736 bp of sequence data, using parsimony, neighbour-joining and maximum likelihood (ML) produced trees with similar topologies (Figure 3.3A, ML tree shown); *Monocystis agilis* (AF457127) was used as the outgroup. Pairwise genetic distance analyses (Table 3.4) indicated that piscine genotype 2 shared between 12.2%-12.6% and 13.0% genetic distance from *C. molnari* and *C. huwi* respectively, and 18.8% (*C. muris*) to 22.3% (*C. scophthalmi*) genetic distances from all other *Cryptosporidium* species. Piscine genotype 7 was closest to *C. huwi* with a genetic distance of 2.9%. Phylogenetic analysis at the18S locus was also conducted on shorter (488 bp) sequences (Figure 3.3B, maximum likelihood tree shown), which included piscine genotypes 2-7 and other piscine-derived *Cryptosporidium* species. In that analysis, all piscine genotype 2 isolates

(OF447, OF448 and OF449) were identical and were most closely related to piscine genotype 4 (3.7% genetic distance) followed by piscine genotype 3 (6.0% genetic distance) (Table 3.4). In addition, all piscine genotype 7 isolates (RET439, RET441, RET442, RET443, RET445) were identical and again grouped closest to *C. huwi* (2.9%) and shared between 11.2% (piscine genotype 5) and 13.4% (piscine genotype 3) genetic distance from the other piscine genotypes (Table 3.4).

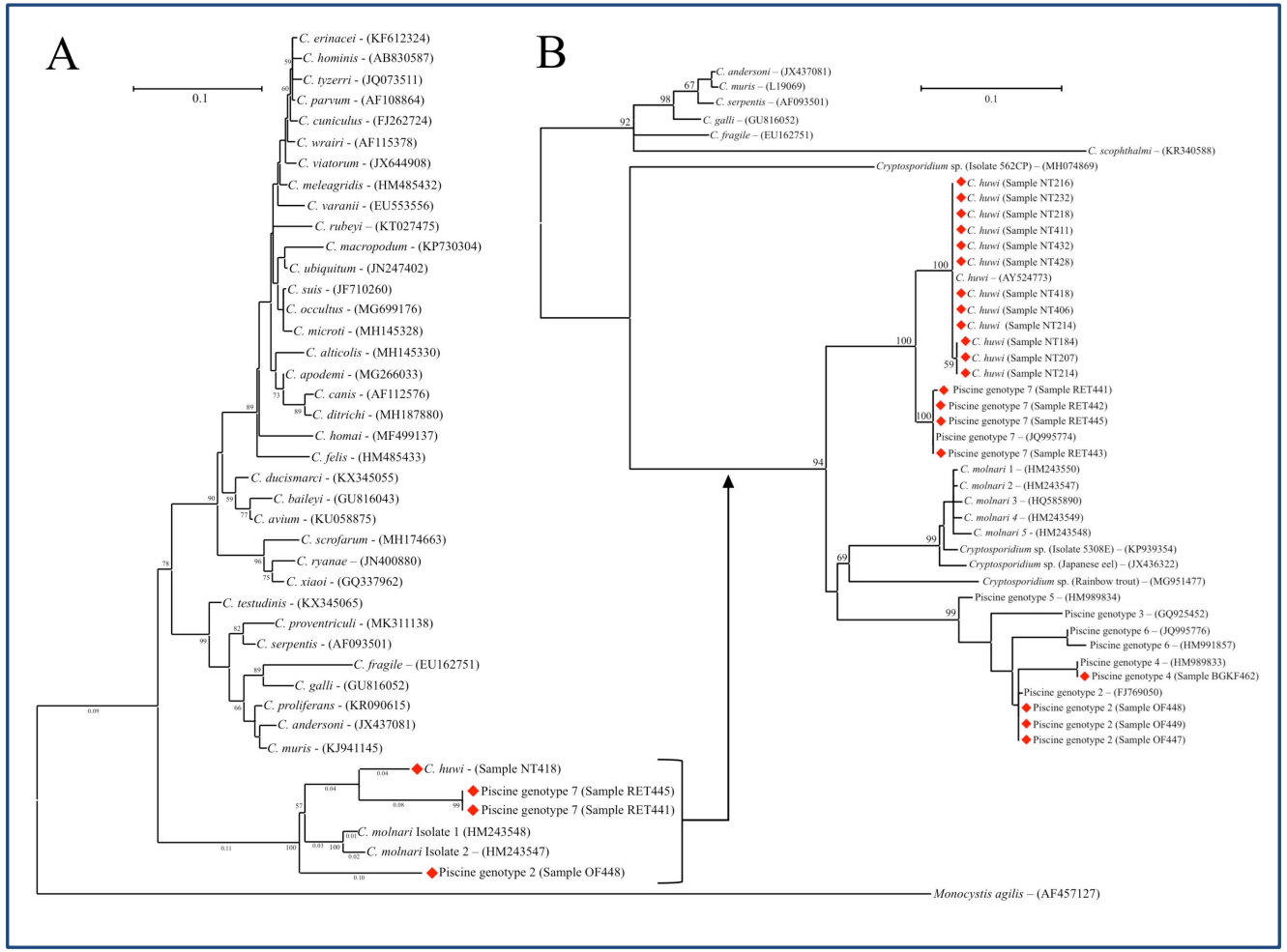

Figure 3.3. Evolutionary relationships of *Cryptosporidium* spp. using sequences from the 18S locus inferred by distance analysis. (A) Phylogenetic relationship of *Cryptosporidium* using 736bp sequences. (B) Analysis of just piscine *Cryptosporidium* spp. using 488bp sequences. Percentage support (>50%) indicated at left of supported node from 1000 pseudoreplicates. Diamonds indicate samples from the present study.

Table 3.4. Pairwise genetic distances (%) between the piscine *Cryptosporidium* species and genotypes found in the present study at the 18S locus. Using maximum composite likelihood method (gamma distributed), using 1000 bootstrap replicates based on the Tamura 3-parameter model. Substitutions include transitions and transversions.

	C. muris	*C. scophthalmi*	*C. molnari*	*C. huwi* (NT428)	PG2 (OF448)	PG3	PG 4 (BGKF462)	PG5	PG6	PG7
C. muris	0									
C. scophthalmi	15.2	0								
C. molnari	15.7-17.0	20.8-21.8	0							
C. huwi (NT428)	16.1	20.0	9.1-9.5	0						
Piscine genotype 2 (OF448)	18.8	20.8	12.2-12.6	13.0	0					
Piscine genotype 3	19.2	21.2	12.9-14.2	13.0	6.0	0				
Piscine genotype 4 (BGKF462)	18.8	19.9	13.4-13.9	13.0	3.7	5.7	0			
Piscine genotype 5	18.0	19.1	10.7-11.2	12.9	3.8	6.6	7.0	0		
Piscine genotype 6	17.6	21.6	13.0-13.5	13.3	3.8	7.6	6.7	6.7	0	
Piscine genotype 7	17.3	20.8	10.3-10.7	2.9	12.3	13.4	13.1	11.2	13.0	0
Piscine genotype 8	14.5	20.2	12.4-18.8	8.2	10.3	10.8	11.7	10.0	11.1	7.7

3.2.2 Phylogenetic analysis of *Cryptosporidium* at the actin locus

Phylogenetic analysis at the actin locus based on 816 bp of sequence data, using parsimony, neighbour-joining and maximum likelihood (ML) analyses produced trees with similar topologies (Figure 3.3A, ML tree shown), *Toxoplasma gondii* (AF054932) was used as the outgroup. Pairwise genetic distance analyses (Table 3.5) revealed that piscine genotype 2 exhibited 18.1-18.2% genetic distance from *C. molnari*, 20.0% genetic distance from *C. huwi* and 26.1% genetic distance from *C. scolpthalmi* (Figure 3.4A) and 22.3% (*C. meleagridis)* to 32.0% (*C. felis*) genetic distances from all other *Cryptosporidium* species. At the actin locus piscine genotype 7 grouped closest to *C. huwi* at 9.4%, with 20%-20.4% genetic distance from *C. molnari*, 28.2% from *C. scophthalmi* and 29.7% from *C. hominis*. A novel sequence was amplified at the actin locus from sample RET441, that grouped within the piscine clade but exhibited between 15.7% (*C. molnari*) and 23.3% (*C. scophthalmi*) from other piscine-derived *Cryptosporidium* sp., with 23.2% (*C. muris*) and 24.1% (*C. hominis*) distance from other species of *Cryptosporidium* (Table 3.5). Analysis of shorter actin sequences available for piscine genotypes (206bp) (Table 3.6) revealed that piscine genotype 2 grouped most closely with piscine genotype 4 (7.2% genetic distance), followed by piscine genotype 3 (15.1%) (Figure 3.4B). A phylogenetic tree was built using the shorter 206bp sequences (see appendix, Figure A1.2), however, the sequences were too short for robust phylogenetic analysis (see appendix).

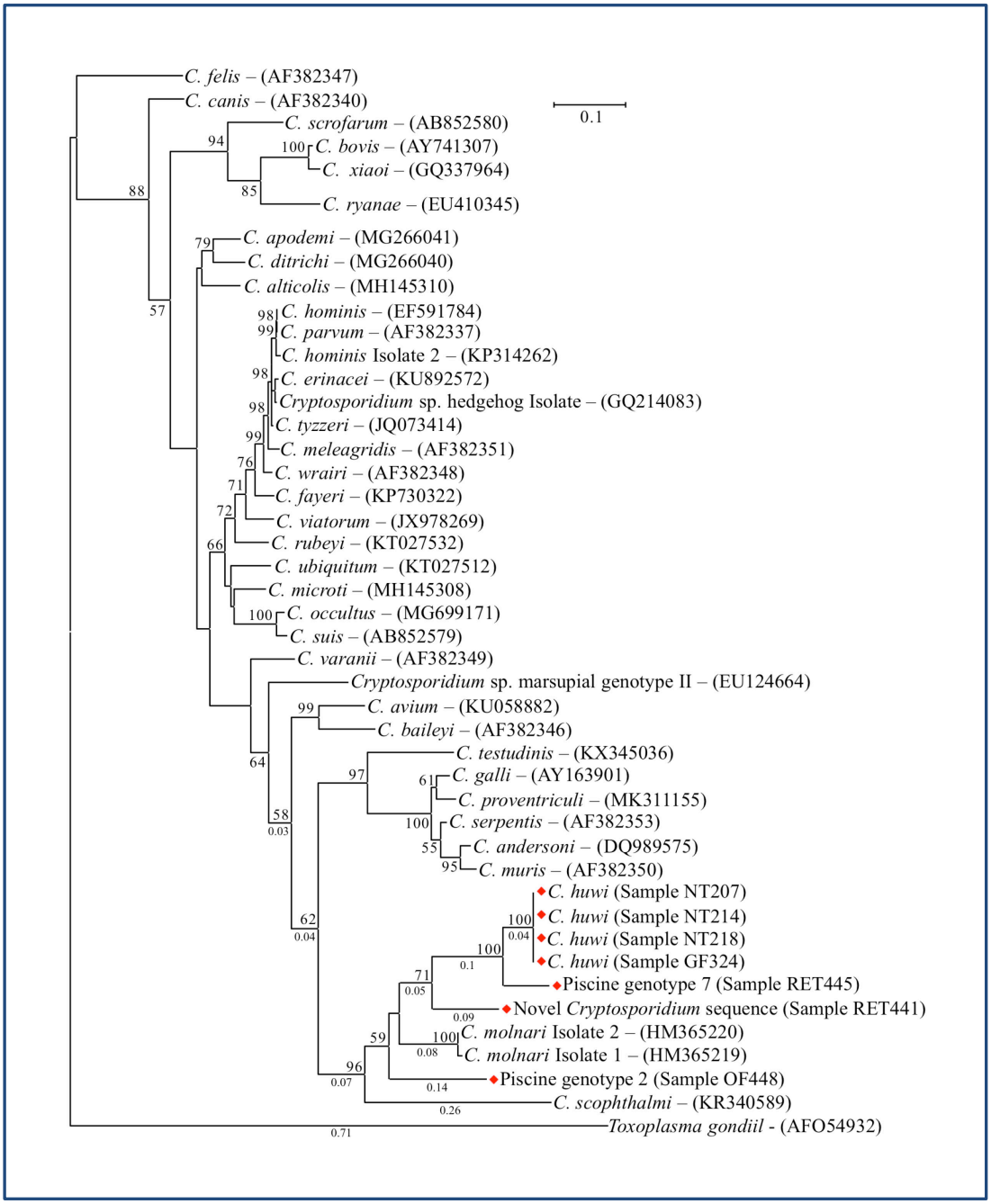

Figure 3.4. Phylogenetic analysis of *Cryptosporidium* genotypes and established spp. using sequences from the actin locus (816 bp). Pairwise-distances were calculated by the Maximum Likelihood method using the General Time Reversible model (GTR and gamma distributed) Percentage support (>50%) from 1000 pseudoreplicates is indicated to the left of the supported node. Diamonds indicate *Cryptosporidium* samples from the present study.

Table 3.5. Pairwise genetic distances (%) between the piscine *Cryptosporidium* species and genotypes found in the present study at the actin locus using 816bp sequences.

	PG2 (OF448)	N. seq (RET441)	PG7 (RET445)	*C. huwi*	*C. hominis*	*C. muris*	*C. scophthalmi*
Piscine genotype 2 (OF448)	0						
Novel sequence (RET441)	18.5	0					
Piscine genotype 7 (RET445)	21.8	16.7	0				
C. huwi (NT218)	20.0	16.7	9.4	0			
C. hominis	25.9	24.1	29.7	27.1	0		
C. muris	23.8	23.2	29.5	26.6	22.5	0	
C. scophthalmi	26.1	23.3	28.2	29.9	27.0	28.8	0
C. molnari	18.1-18.2	15.7-16.3	20-20.4	19.4-19.8	22.7	22.7-22.9	20.8-21.1

Table 3.6. Pairwise genetic distances (%) between the piscine genotypes of *Cryptosporidium* and the genotypes found in the present study at the actin locus using 206bp sequences.

	PG2 (OF448)	PG3	PG4	PG5	PG7 (RET445)	PG8
Piscine genotype 2 (OF448)	0					
Piscine genotype 3	15.1	0				
Piscine genotype 4	7.2	16.1	0			
Piscine genotype 5	17.4	6.9	17.4	0		
Piscine genotype 7 (RET445)	30.2	16.3	22.8	14.8	0	
Piscine genotype 8	26.1	19.5	20.2	13.3	21.8	0
Novel sequence (RET441)	20.2	14.2	16.3	13.2	22.3	17.1

Note no sequence is available for piscine genotype 6 at the actin locus.

3.2.3 Phylogenetic analysis of *Cryptosporidium* using sequence concatenation

Concatenated sequences were constructed by joining sequences amplified from the same sample at the 18S and actin loci. Phylogenetic analysis using 1,476 bp of concatenated sequence data, using parsimony, neighbour-joining and maximum likelihood (ML) produced trees with similar topologies (Figure 3.3A, ML tree shown), concatenated *Monocystis agilis* 18S (AF457127) and actin (AY391264) sequences were used as the outgroup. When analysed by genetic pairwise distance (Table 3.7) piscine genotype 2 exhibited 12.5% and 14.0% distance from *C. molnari* and *C. huwi,* respectively (Figure 3.5A). Piscine genotype 2 exhibited 14.2% genetic distance from piscine genotype 7 and exhibited between 18.4% (*C. hominis*) and 21.1% (*C. scophthalmi*) genetic distance from all other *Cryptosporidium* spp. (Table 3.7). Piscine genotype was closest to *C. huwi* at 7.5% genetic distance and genetic distance ranged from 13.4% (*C. molnari*) to 23.1% (*C. scophthalmi*) from other species of *Cryptosporidium*. Analysis of shorter concatenated actin and 18S sequences available for piscine genotypes (614bp), revealed that piscine genotype 2 was closest to piscine genotype 4 (4.8% genetic distance), followed by piscine genotype 5 (8.4%) (Figure 3.5B). Piscine genotype 7 grouped closest to *C. huwi* at 7.5% genetic distance, with genetic distances to other piscine species ranging from 13.2% (piscine genotype 5) to 26.9% (*C. scophthalmi*) (Table 3.8).

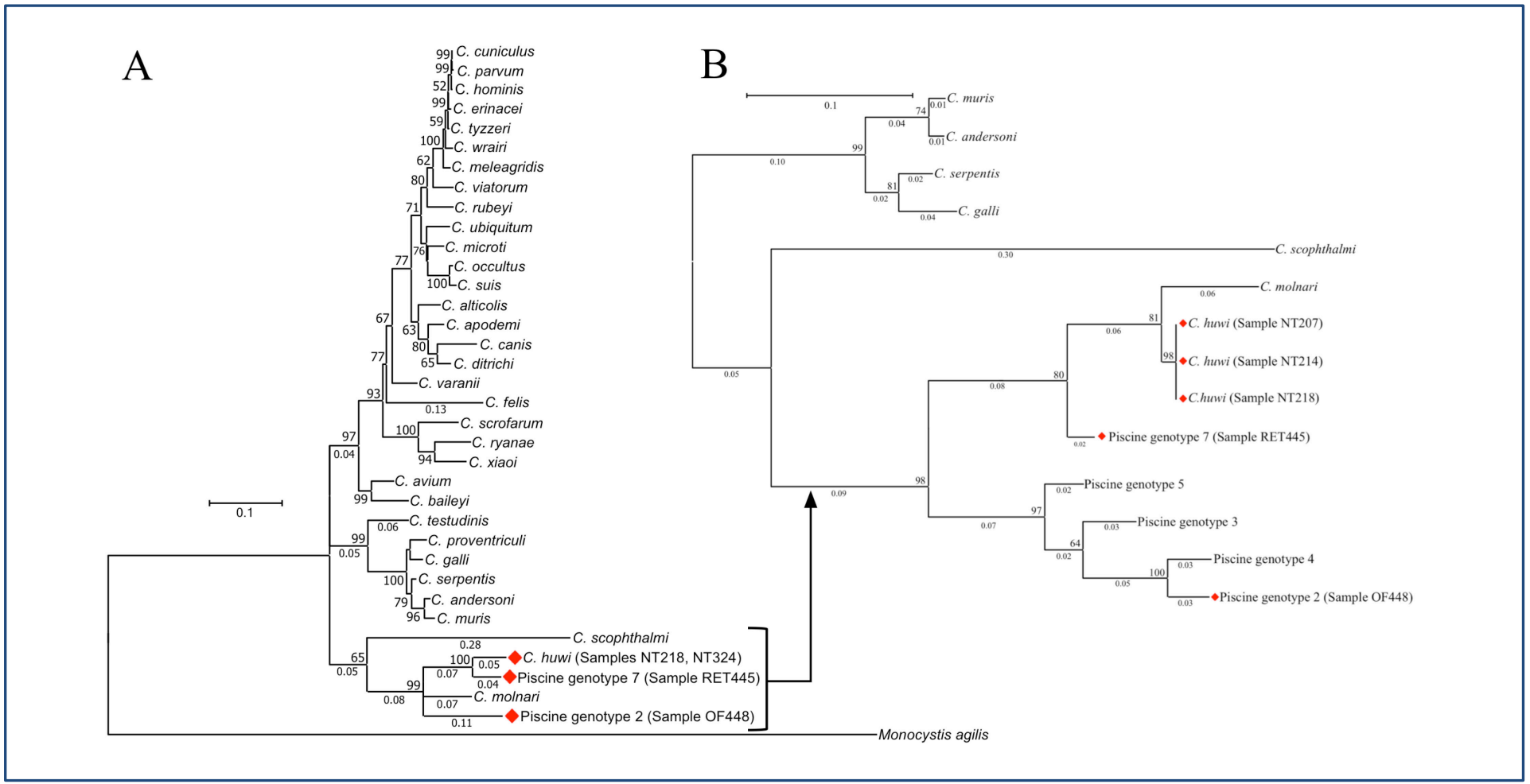

Figure 3.5. Evolutionary relationships of *Cryptosporidium* using concatenated sequences from the actin and 18S loci. With (A) 1476 base pairs for a large range of spp. and (B) 614 base pairs for piscine spp. Percentage support (>50%) indicated at left of supported node from 1000 pseudoreplicates. Distances are included under branches where convenient. Diamonds indicate *Cryptosporidium* samples from the present study.

Table 3.7. Pairwise genetic distances (%) between the piscine *Cryptosporidium* species and genotypes using concatenated sequences 1476 base pairs long from the 18S and actin loci.

	PG2 (OF488)	PG7 (RET445)	*C. huwi* (NT218, NT418)	*C. hominis*	*C. parvum*	*C. scophthalmi*
Piscine genotype 2 (OF448)	0					
Piscine genotype 7 (RET445)	15.4	0				
C. huwi (NT218, NT418)	14.9	7.5	0			
C. hominis	19.7	22.7	19.8	0		
C. parvum	19.6	22.3	19.7	6.9	0	
C. scophthalmi	22.2	23.1	25.0	21.6	21.5	0
C. molnari	14.0	13.4	13.3	18.4	18.3	20.2

Table 3.8. Pairwise genetic distances (%) between the piscine *Cryptosporidium* species and genotypes using concatenated sequences 614 base pairs long from the 18S and actin loci.

	PG2 (OF488)	PG7 (RET445)	*C. huwi* (NT218, NT418)	*C. scophthalmi*	*C. molnari*	Piscine genotype 3	Piscine genotype 4
Piscine genotype 2 (OF448)	0						
Piscine genotype 7 (RET445)	18.8	0					
C. huwi (NT218, NT418)	19.1	7.2	0				
C. scophthalmi	29.9	26.9	28.0	0			
C. molnari	17.2	11.6	5.8	29.5	0		
Piscine genotype 3	9.6	14.9	16.9	28.9	15.7	0	
Piscine genotype 4	4.8	17.2	18.7	30.2	18.0	9.3	0
Piscine genotype 5	8.4	13.2	16.47	25.0	14.9	6.8	10.5

Note concatenated sequences piscine genotype 6 or piscine genotype 8 were not of appropriate length and quality and therefore not included. For pairwise genetic distances of the piscine genotypes and piscine genotype 6 at the 18S loci refer to Table 3.4, for piscine genotype 8 please refer to the 18S (Table 3.4) and actin (Table 3.6) distance tables.

3.2.4 Microscopy

Histological slides (H&E) were made from all samples positive for *Cryptosporidium* at the 18S loci. Positive identification of *Cryptosporidium* life cycles was made by microscopy on sample NT214 only, which was positive for *C. huwi*. Unfortunately no piscine genotypes were clearly identified through histology, however histology from sample RET438 did reveal some *Cryptosporidium*-like organisms along the brush border of the gastric epithelium and deep within the epithelia of the GI tract. However, these images were not convincing due to the lack of clustered life cycle stages and histology images from RET438 were moved to the appendix (see appendix, Figure A.1.3). Rapid autolysis of fish gastrointestinal tissue on some histological slides made positive morphological analysis difficult.

Morphological analyses of sample NT214 (positive for *C. huwi* by PCR at the 18S locus) revealed a heavy infection of *C. huwi*, with life cycle stages seen along the surface of the gastric epithelium and also sporogonal stages embedded deep in the epithelium, a feature characteristic of piscine *Cryptosporidium* species (Figure 3.6). The gastric epithelium was damaged and sloughing of epithelium cells and necrosis was seen throughout (Figure 3.6). *Cryptosporidium* life cycle stages are seen lining the gastrointestinal epithelium in tightly clustered patches (Figure 3.7).

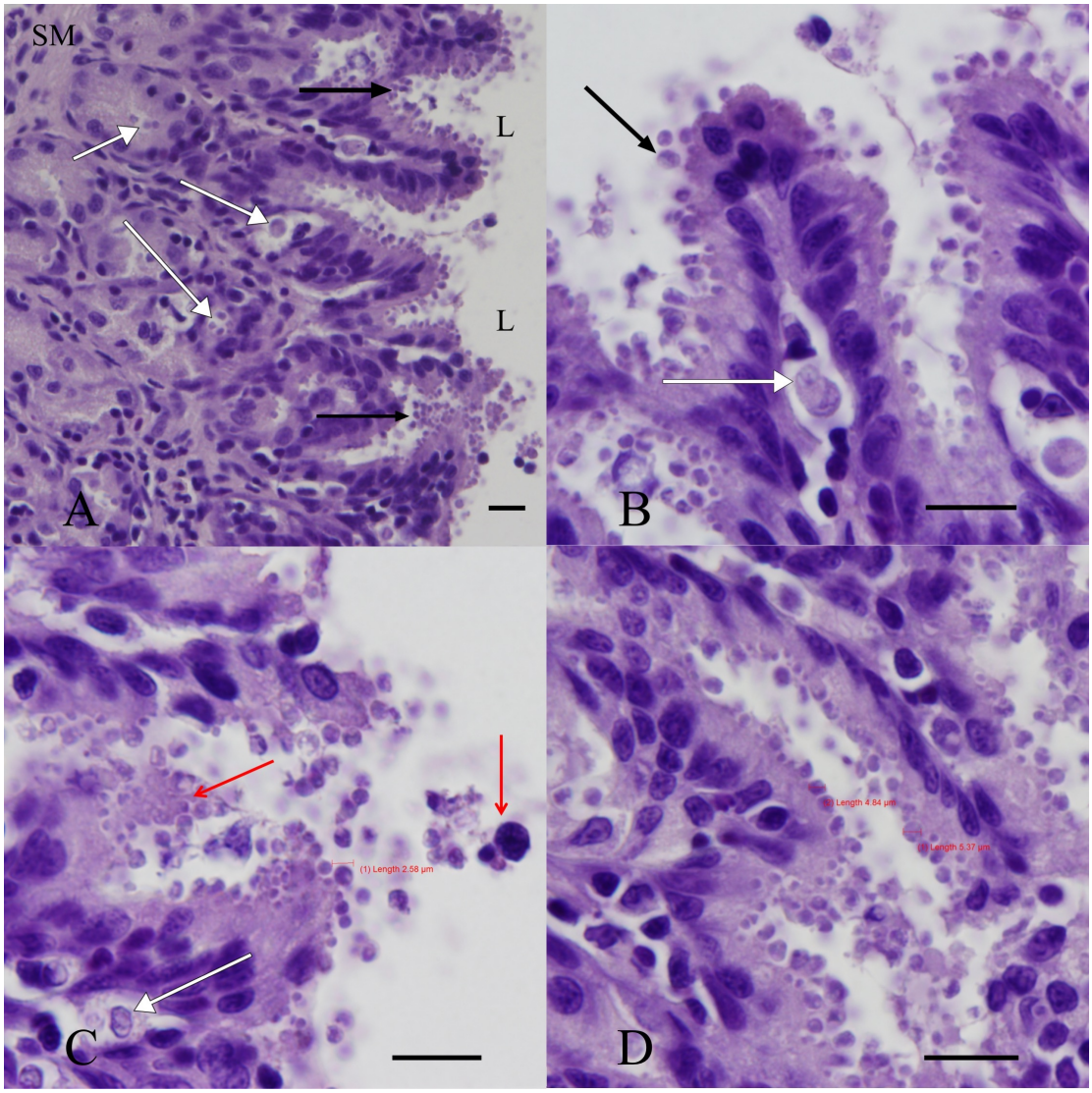

Figure 3.6. Hematoxylin and eosin-stained sections of Neon tetra stomach exhibiting a *Cryptosporidium* infection. Sample NT214 with a heavy infection of *C. huwi* organisms along the epithelial lining of the stomach (black arrows) (A and B). Oogonial and sporogonial stages are clustered deep toward the basolateral side of the gastric epithelium (white arrows) (A, B and C), which is characteristic of piscine sp. of *Cryptosporidium*. Loose cell debris in the gastric lumen can be seen due to sloughing of epithelial cells by oocysts (red arrows) (C and D). SM = submucosa, L = lumen. All scale bars = 10µm.

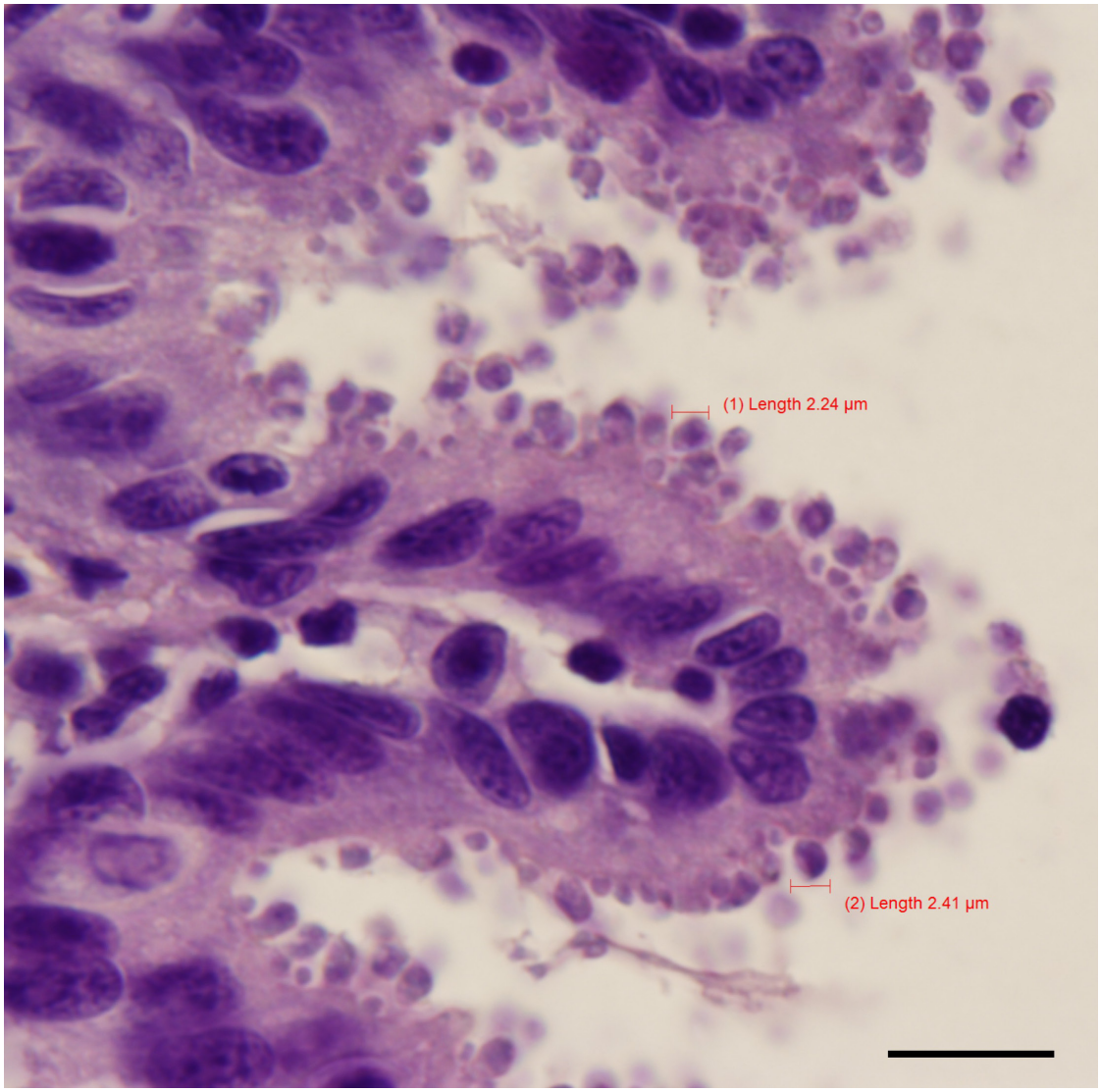

Figure 3.7. Histology showing *C. huwi* oocysts and life cycle stages lining the brush border of the gastric epithelium. Scale bar = 10µm.

The *Cryptosporidium* oocysts observed were spherical. Sporulated oocysts contain sporozoites that can be seen as darks points within the translucent oocysts (Figure 3.8).

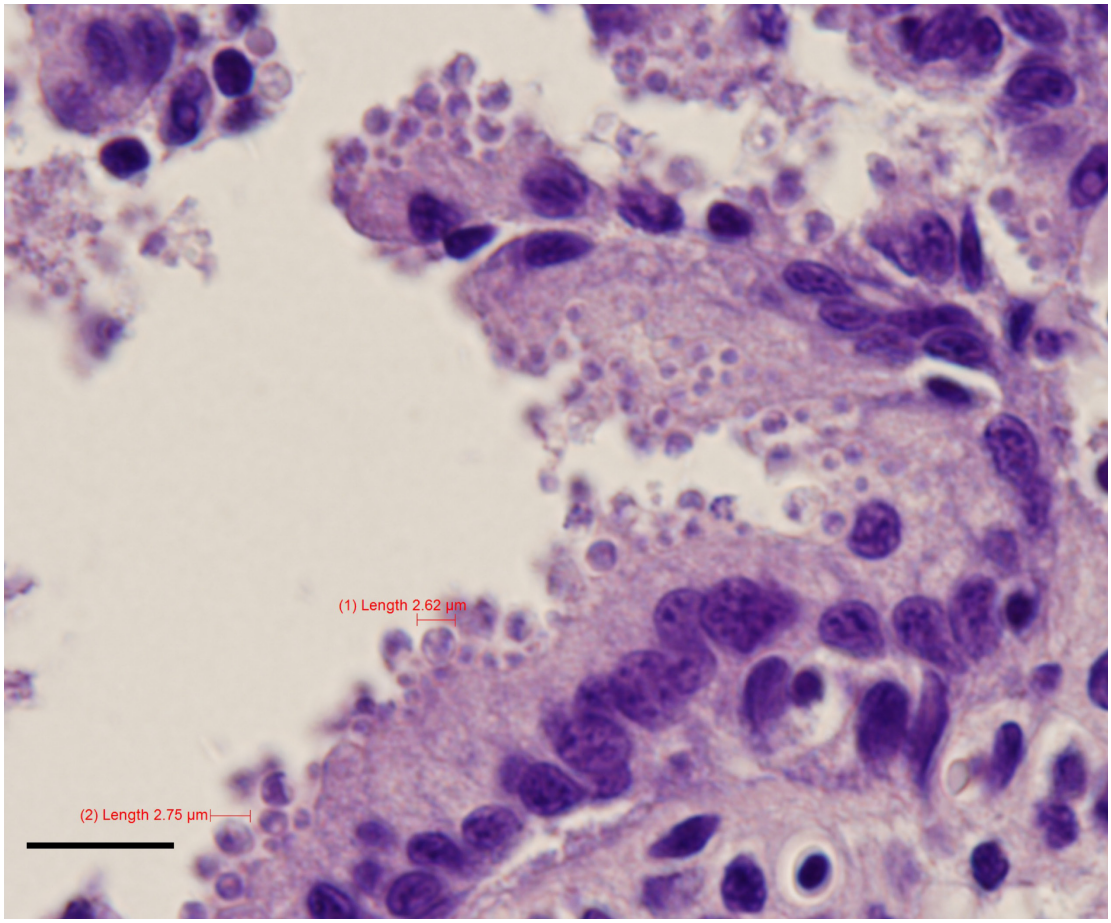

Figure 3.8. Histology showing spherical oocysts containing sporozoites. Scale bar = 10µm.

3.3 *Goussia*

Goussia were identified in goldfish (*Carassius auratus*) taken from the fish farm at a prevalence of 4.0% (10/253, 95% CI; 1.9-7.1). The overall prevalence of *Goussia* in fish from the present study was 2.1% (10/467, 2.1%, 95%CI; 1.0-3.9). Interestingly, the results, as shown in Table 3.9 and Figure 3.7, indicate that all nine

Goussia isolates sequenced did not align with any established species or nucleotide sequences available in GenBank.

Table 3.9. *Goussia* sequences identified at the 18S locus.

Sample ID	18S locus sequence ~578bp
GF112	*Goussia* (novel sequence 1)
GF305	*Goussia* (novel sequence 2)
GF315	*Goussia* (novel sequence 3)
GF317	*Goussia* (novel sequence 4)
GF330	*Goussia* (novel sequence 5)
GF342	*Goussia* (novel sequence 5)
GF354	*Goussia* (novel sequence 6)
GF366	*Goussia* (novel sequence 7)
GF375	*Goussia* (novel sequence 8)
GF377	*Goussia* (novel sequence 9)

3.3.1 Differences in weight and length of fish with *Goussia* infections

Goldfish (n=253) that screened positive for *Goussia* had a 34.3% lower mean weight and a 19.7% lower mean length. The F test determined homogeneity of variance was equal for both weight (F(251)=2.1179, p=0.1859) and length (F(251)=1.5261, p=0.4697). The t-test determined no significance ($p<0.05$) between goldfish that tested positive or negative for *Goussia* and a difference in weight. (t(251)=1.589, p=0.1132). The t-test determined significance ($p<0.05$) between goldfish that tested positive or negative for *Goussia* and a difference in length (t(251)=2.2756, p=0.0237) (see Table 3.10 below).

Table 3.10. Statistical analysis of the correlation between the presence of *Goussia* and the length and weight of the fish.

Fish sp.	Variable	*p*-value	*t*-value	Uneq. Var. *p*-value	Uneq. Var. *t*-value	Degrees of freedom
Goldfish	Weight	0.1132	1.589	0.02595	2.5393	251
Goldfish	Length	0.02371	2.2756	0.0180	2.7604	251

Goldfish that tested negative for *Goussia* (n=243) had a mean weight of 7.77g and a mean length of 8.85cm while those that tested positive for *Goussia* (n=10) had

a mean weight of 4.91g and a mean length of 7.03cm (Figure 3.9). Therefore, goldfish that tested positive had a mean weight 2.86g lower and mean length 1.82cm lower than those that tested negative (Figure 3.7).

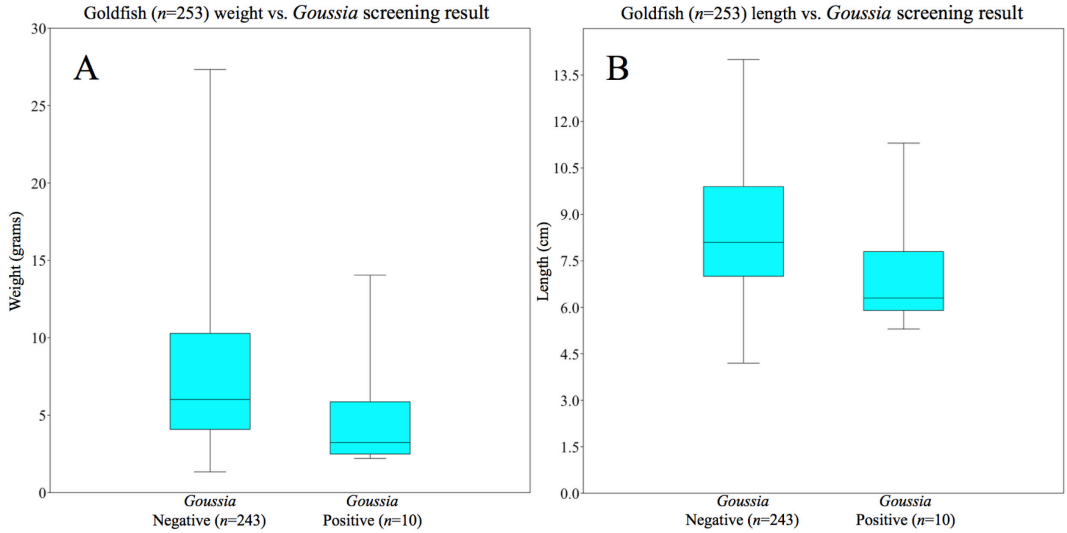

Figure 3.9. Boxplot of goldfish weight in grams (A) and length in cm (B) comparing fish found to be negative and positive for *Goussia* by sequencing by PCR. Shown are the range, median and quartiles with a drop in both weight and length of fish with infections.

3.3.2 *Goussia* phylogenetic analysis at the 18S Locus

At the 18S locus using the Ryan et al. (2003) primers, 10 *Goussia* isolates (GF112, GF305, GF315, GF317, GF330, GF342, GF354, GF366, GF375 and GF377) were amplified. Histological slides (H&E) were produced from all *Goussia* positive samples, unfortunately, no oocysts or life-cycle stages were observed possibly due to the rapid rate of fish tissue autolysis. None of the *Goussia* sequences aligned closely to any sequences available in GenBank. Evolutionary relationships were analysed using phylogenetic analyses (Figure 3.10) and pairwise genetic distance analysis (Table 3.11) at the 18S locus comparing 516 base pair long sequences from established species of *Goussia* and the novel sequences discovered in the present study. All the novel *Goussia* sequences grouped closest to dispersed types of *Goussia*, GF112

grouped closest to *G. bohemica* (reference GU479654) (Figure 3.7) at 5.5% genetic distance, all other novel sequences (GF305, GF315, GF317, GF330, GF342, GF354, GF366, GF375 and GF377) were closest to *G. carpelli* (reference GU479640) (Figure 3.10) with between 1.9% to 3.9% genetic distance (Table 3.11). GF330 and GF342 were 100% identical to each other. Of the novel sequences, GF112 was the most genetically distinct and was closest to GF305 at 7.0%, all other novel sequences exhibited distances to each other between 0.4% (GF366, GF375, GF330 or GF342, GF377 and GF330 or GF342) and 3.9% (GF315 and GF375) at the 18S locus (Table 3.11). Overall the novel *Goussia* sequences exhibited between 1.9% to 14.8% genetic distance to established species of *Goussia.* However, while all isolates were genetically most related to *Goussia*, some sequences also exhibited relatively close relationships to *Eimeria* (2.9% to 9.3% genetic distance) (Table 3.11), this is also reflected by the apparent paraphyly in Figure 3.10, where *Eimeria* appears to group with the *Goussia* isolates.

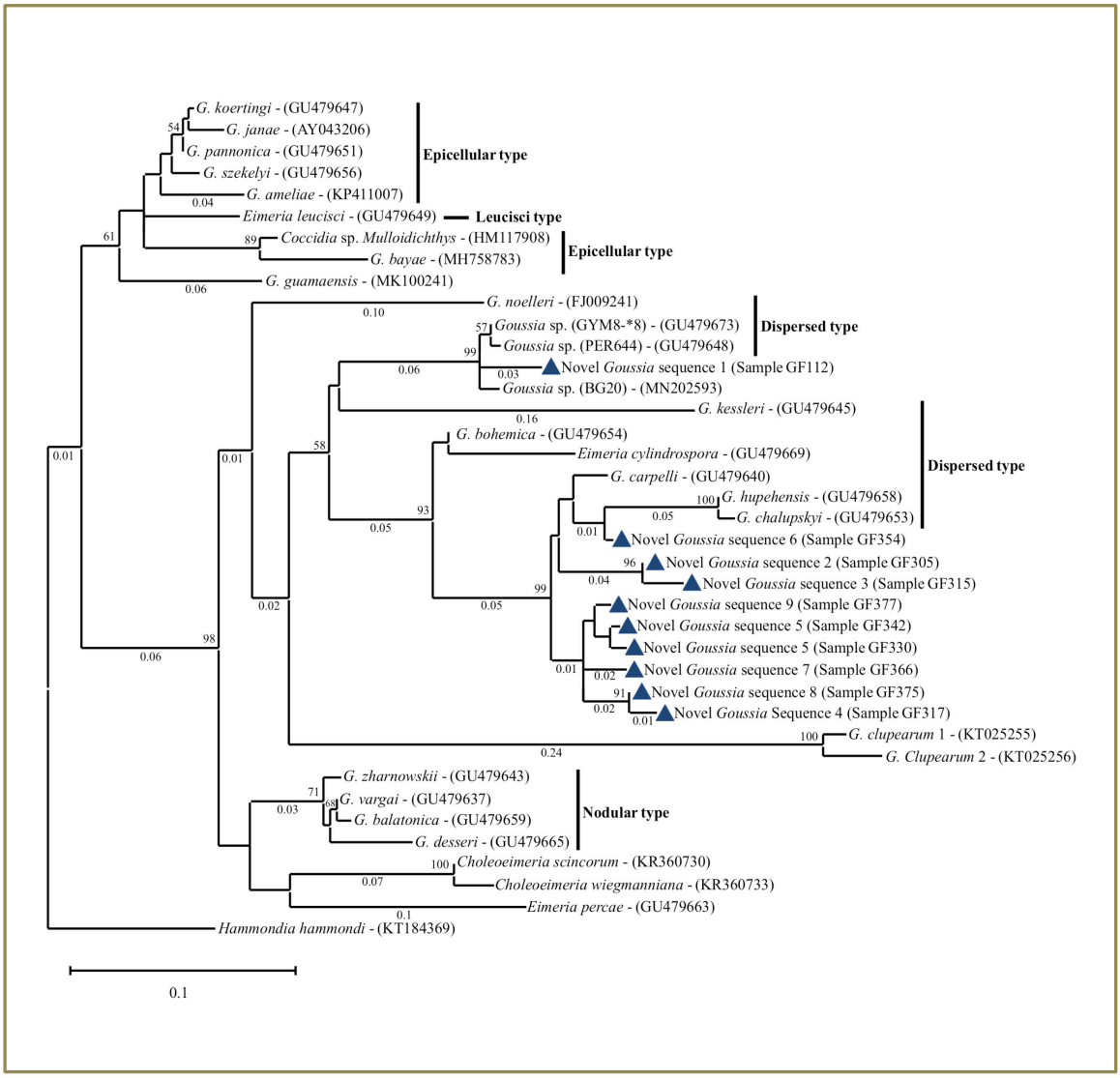

Figure 3.10. Maximum Likelihood phylogenetic tree comparing novel sequences and established *Goussia* spp. at the 18S locus. Phylogenetic relationships of 516 bp sequences were calculated using the Tamura 3-parameter model (T93, gamma distributed, 1000 bootstrap replicates). Triangles indicate novel sequences of *Goussia* from the present study.

Table 3.11. Pairwise genetic distances (%) between the established *Goussia* species and novel sequences identified in the present study at the 18S locus (516 bp). Column numbers denote the sequences of each row with the same number.

	GF112 (n seq. 1)	GF305 (n seq. 2)	GF315 (n seq. 3)	GF317 (n seq. 4)	GF330 (n seq. 5)	GF354 (n seq. 6)	GF366 (n seq. 7)	GF375 (n seq. 8)	GF377 (n seq. 9)	*G. clupearum*	*G. balatonica*	*G. pannonica*	*G. vargai*	*G. guamaensis*	*G. janae*	*G. szekelyi*	*G. ameliae*	*G. koertingi*	*G. bohemica*	*G. chalupskyi*	*G. carpelli*	*G. hupehensis*	*G. kessleri*	*E. leucisci*
GF112 (n seq. 1)	0																							
GF305 (n seq. 2)	7.0	0																						
GF315 (n seq. 3)	8.7	1.5	0																					
GF317 (n seq. 4)	7.8	2.8	3.4	0																				
GF330 (n seq. 5)	7.3	1.9	3.0	1.7	0																			
GF354 (n seq. 6)	7.5	2.1	3.6	2.9	2.7	0																		
GF366 (n seq. 7)	7.5	2.1	3.7	1.5	0.6	2.1	0																	
GF375 (n seq. 8)	7.2	2.3	3.9	0.8	1.2	2.7	0.6	0																
GF377 (n seq. 9)	7.5	2.1	3.4	2.1	0.6	3.0	0.8	1.5	0															
G. clupearum	14.3	13.1	14.8	13.6	14.0	12.8	13.1	13.3	14.3	0														
G. balatonica	8.8	7.2	9.0	7.2	7.5	6.5	6.7	6.5	7.7	11.5	0													
G. pannonica	10.6	10.8	12.8	11.3	11.7	10.0	10.8	10.8	11.9	14.0	7.1	0												
G. vargai	8.2	7.0	8.8	6.7	7.2	6.0	6.5	6.2	7.5	11.0	0.4	6.6	0											
G. guamaensis	12.6	12.0	14.0	12.5	12.8	11.1	12.0	11.9	13.1	16.7	7.4	4.3	6.9	0										
G. janae	10.6	10.5	12.5	11.1	11.4	9.7	10.5	10.5	11.7	13.7	6.9	0.2	6.4	4.6	0									
G. szekelyi	10.0	11.8	13.8	11.9	12.2	11.0	11.3	11.3	12.5	15.0	7.8	1.4	7.3	5.0	1.7	0								
G. ameliae	11.1	11.3	13.3	12.1	12.2	10.5	11.3	11.5	12.5	13.7	7.4	1.9	6.9	4.5	2.1	2.3	0							
G. koertingi	10.9	11.1	13.1	11.6	12.0	10.3	11.1	11.1	12.2	14.1	7.4	0.2	6.9	4.6	0.4	1.7	2.1	0						
G. bohemica	5.5	3.6	5.3	4.1	3.7	3.0	3.6	3.9	4.9	11.1	5.2	7.9	4.8	8.9	7.6	8.4	8.1	8.2	0					
*G. chalupskyi_*	8.7	3.2	4.8	4.3	4.1	3.4	3.6	4.3	6.1	12.9	6.9	10.6	6.7	11.8	10.3	11.6	10.6	10.8	0.6	0				
G. carpelli	7.5	2.3	3.9	2.7	2.5	1.9	2.5	2.8	3.5	12.8	6.9	10.5	6.4	11.6	10.2	11.0	11.0	10.8	2.1	4.6	0			
G. hupehensis	10.7	5.2	6.1	6.3	5.8	4.5	6.0	6.0	5.8	5.8	9.1	12.1	8.5	13.7	11.2	12.9	12.0	12.0	6.0	5.4	4.4	0		
G. kessleri	10.6	10.3	11.7	9.2	10.0	8.7	9.3	9.0	9.8	9.8	11.2	11.5	11.0	14.0	12.9	11.4	11.9	11.9	8.6	9.0	8.1	9.1	0	
E. leucisci	14.1	14.5	15.5	14.6	13.9	12.7	13.1	14.5	14.4	18.3	10.3	3.8	10.1	7.2	4.2	11.9	12.7	12.3	3.3	12.9	13.3	13.1	14.5	0
E. cylindrospora	5.2	3.7	5.5	3.3	3.5	3.1	2.9	3.1	3.8	5.2	6.0	7.8	5.5	9.3	7.8	8.0	8.0	8.0	1.3	3.8	2.6	3.8	6.4	8.6

3.4 *Colpodella*

A single goldfish (isolate GF357) was identified as positive for the free-living predatory non-parasitic protist *Colpodella*, a prevalence in all fish from the present study of 0.2% (1/467, 0.2%, 95%CI; 0.0-1.2) and a prevalence in goldfish of 0.4% (1/253, 0.4%, 95%CI; 0.0-2.2). At the 18S locus, the closest matches to GF357 in GenBank using BLAST (https://blast.ncbi.nlm.nih.gov/Blast.cgi) were unclassified *Colpodellidae* sequences uploaded by Yuan et al. (2012) (GQ411073) and Han et al. (2018) (MG012044) both at 100% query cover over 551 base pairs of sequence.

3.5 *Schyzocotyle* (*Bothriocephalus*) *acheilognathi*

Schyzocotyle (syn. *Bothriocephalus*) *acheilognathi* (Asian fish tapeworm) was identified in two goldfish from the Water Garden Life fish farm (Samples GF035 and GF131). The prevalence of *S. acheilognathi* in all fish samples from the present study was 0.4% (2/467, 0.4%, 95%CI; 0.1-1.5). The prevalence of *S. acheilognathi* in goldfish only (the species it was found infecting), was 0.8% (2/253, 0.79%, 95%CI; 0.1-2.8).

At first observation, infected goldfish exhibited enlarged, distended abdomens and during dissection, mature *S. acheilognathi* were observed throughout the alimentary canal and through the transparent intestinal wall as well as emerging into the abdominal cavity through intestinal ruptures and perforations. The worms caused intestinal occlusion (see Figure 3.10) and pressure necrosis in the intestines. Morphological identification using the *Bothriocephalus* revision (Scholz, 1997) and fish cestode species key (Chubb et al., 1987) as well as the striking similarity to *S.*

acheilognathi found by Košuthová et al. (2015) led to identification of these organism as *S. acheilognathi*.

Morphology was limited to identifying features on the scoleces, neck and gross structures of *S. acheilognathi*, as the segments of the body were irreversibly affected when live worms were placed in fixative. Fixative (e.g. formaldehyde or ethanol) causes the tapeworm's segments to concertina, this makes identification of species via staining mature and gravid proglottids and imaging internal structures difficult (Scholz et al., 1998). Worms from samples GF035 and GF101, shared the unique morphological features characteristic of *S. acheilognathi* such as the heart shaped scolex and absence of a neck (see Figure 3.8).

Figure 3.11. Microscopy of an Asian fish tapeworm. *S. acheilognathi* has a distinct heart-shaped scolex (1.18mm long and 1.07mm wide) containing dorsally and ventrally situated borthria (b) while the neck is absent (A). Worm is 14.6mm long (B),

however fixation caused concertina of segments likely reducing overall length. Posterior end shows mature proglottids (C). Apical/terminal disc is very poorly developed or absent and armless (black arrows) (B and D). Scale bars for A, C, D = 200µm. Scale bar for B = 1mm.

The bothria of *S. acheilognathi* is distinct, deep, with narrow, small openings; simple (non-crenulate) margins and located dorsally and ventrally on the scolex (see Figure 3.9).

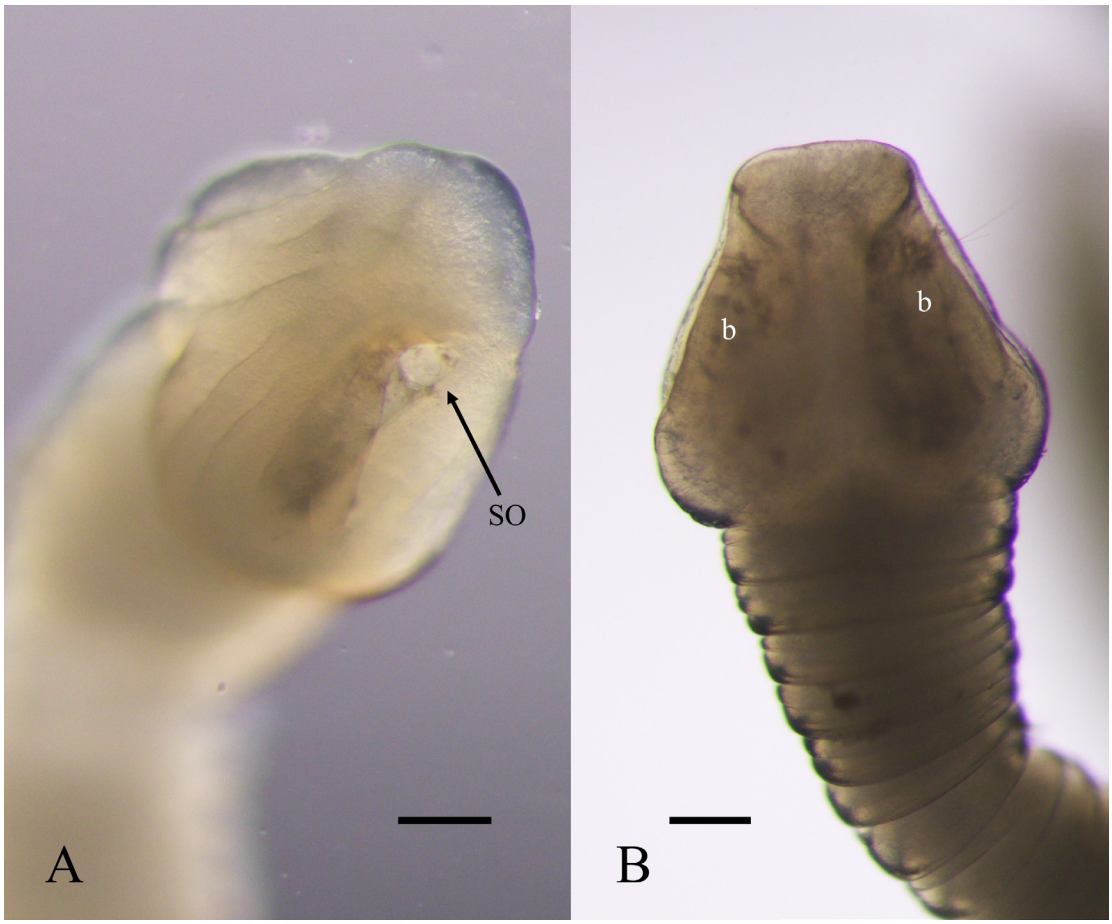

Figure 3.12. Scolex of the Asian fish tapeworm. *S. acheilognathi* has characteristic deep bothria (b) with narrow small openings (SO), located dorsally and ventrally on the scolex. All scale bars = 200µm.

Samples GF035 and GF131 were parasitised by *S. acheilognathi* to the extent that their intestines were completely blocked with parasites (see Figure 3.10) and during

dissection it was clear that the intestinal walls were perforated leading to the presence of *S. acheilognathi* in the abdominal cavity.

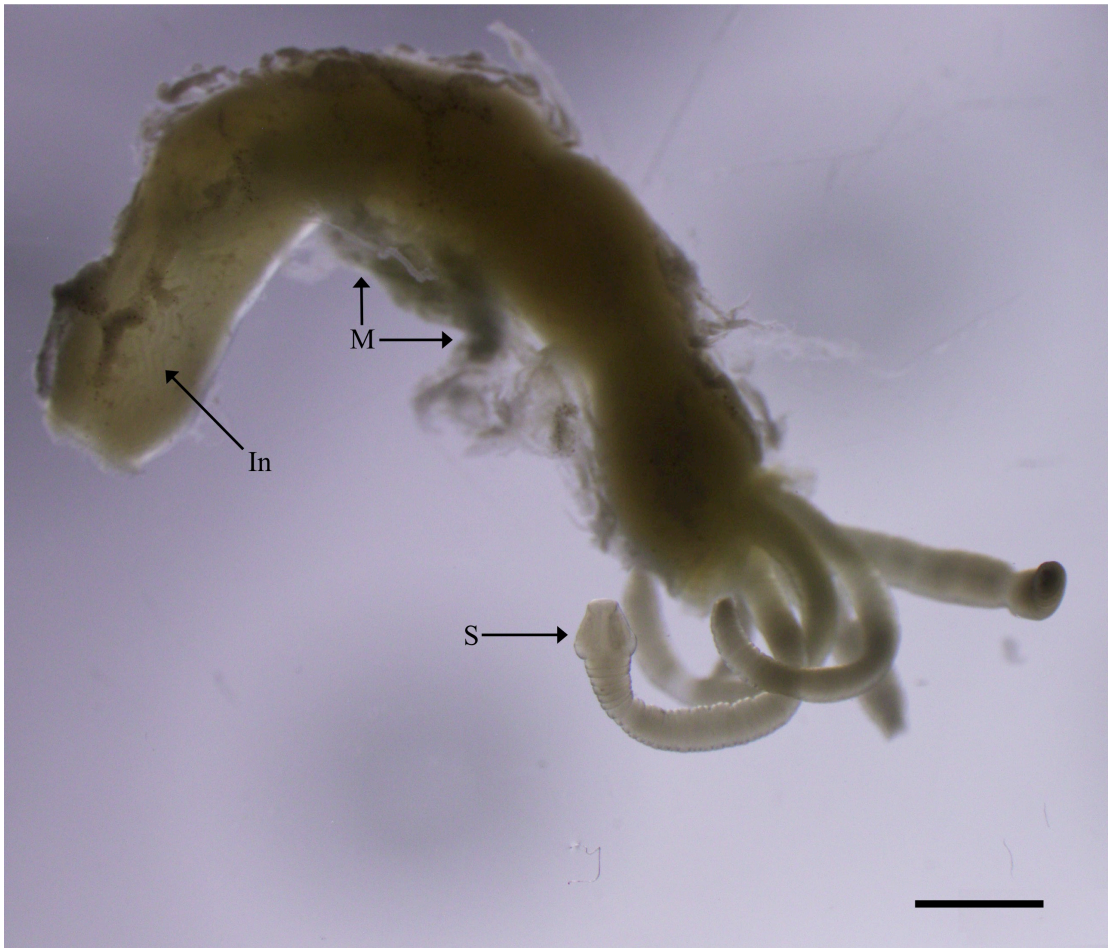

Figure 3.13. Microscopy of Asian fish tapeworm causing intestinal occlusion. Fish intestine (In) (sample GF131) heavily parasitised by *S. acheilognathi* to the point of blocking the lumen and causing intestinal perforations. The scolex of one tapeworm can be seen (S). The intestinal mesentery (M) is seen still attached to the intestine. Scale bar = 2mm.

Chapter 4: Discussion

4.1 Prevalence of *Cryptosporidium* in fish

There are currently 42 valid *Cryptosporidium* species (Holubová et al., 2016; Ježková et al., 2016; Ryan et al., 2016; Zahedi et al., 2017b; Čondlová et al., 2018; Kváč et al., 2018; Holubová et al., 2019; Horčičková et al., 2019), however, the genetic diversity of *Cryptosporidium* species in piscine hosts is still largely unknown and it is vital to bridge this knowledge gap to better understand the taxonomy and public health implications of piscine-derived *Cryptosporidium* species. Due to the morphological similarity between *Cryptosporidium* species, delimiting new species requires genetic analysis at multiple loci in combination with morphological analysis (Xiao et al., 2004). The 18S and actin are the most common loci used for delimiting species of *Cryptosporidium,* as both contain both conserved and variable regions that produce reliable phylogenies (Xiao, 2010).

In the present study, *Cryptosporidium* species were amplified at the 18S locus from 20 of 234 aquarium fish at a prevalence of 8.5% (20/234) and only one was detected in 233 farmed fish at the actin locus, a prevalence of 0.4% (1/233) the one *Cryptosporidium* positive detected at the actin locus in farmed fish was not detected at the 18S locus. The overall prevalence of *Cryptosporidium* in the 467 samples of fish a the 18S locus was 4.3%, when including the actin locus the prevalence increased to 4.5%. In previous studies, the prevalence of *Cryptosporidium* ranged from 0.8% to 100% in parasitised fish (Sitja-Bobadilla, 2005; Murphy et al., 2009; Reid et al., 2010; Zanguee et al., 2010; Morine et al., 2012; Koinari et al., 2013; Certad et al., 2015; Ryan et al., 2015; Yang et al., 2015; Palermo, 2016; Yang et al., 2016). Within species sampled in the present study, the prevalence ranged from 0% to 75%, however, sample

sizes for some species were small (*n*=2-8), and so prevalence estimates for these species are unreliable (Table 3.1). In the present study, ornamental fish samples were obtained from a local aquarium that provides ornamental fish to a customer base distributed across the state. From this customer base, there is a high risk of introduction of these non-native fish into local natural water systems that are often subject to high levels of anthropogenic interactions (Costanza et al., 1998; Morgan and Gill, 2000; Morgan et al., 2004; Rahel, 2007) where they pose a major threat to native fish (Courtenay Jr and Stauffer Jr, 1990; Canonico et al., 2005; Dudgeon et al., 2006). Furthermore, bodies of water used as drinking water for livestock are a potential source of contamination by zoonotic *Cryptosporidium* species' (Zahedi et al., 2016a). Introduced fish harbouring *Cryptosporidium* could hypothetically contaminate these bodies of water and infect native species. The role of fish in zoonotic *Cryptosporidium* outbreaks involving livestock and public drinking water is unknown (Zahedi et al., 2016a; Zahedi et al., 2018).

The prevalence of piscine *Cryptosporidium* may be higher in aquarium and farmed fish than in wild populations. For example, a large scale screening of 1,853 wild marine fish off the coast of France by Certad et al. (2019) reported a prevalence of 2.3-3.2%, compared to a prevalence of 5.3% in 775 captive marine and freshwater fish screened by Yang et al. (2015), in which prevalence's ranged from 1.5-100% within individual host species. It is possible restricted water flow and high-density living environments increase the exposure of healthy fish to infected individuals, which increases infection rates. A study by Sitja-Bobadilla (2005) posited that recirculation systems and fish cannibalism would likely contribute to the presence and

dispersion of oocysts in aquaculture facilities. However, a study of *Cryptosporidium* in wild fish from Lake Geneva reported a prevalence of 36.6% (Certad et al., 2015).

In the present study, student's t-tests were conducted on Oscarfish and Neon tetra samples to determine if there were length and weight differences between the *Cryptosporidium* infected and non-infected groups. The t-tests determined no significance, although it should be noted that the sample size for infected fish was low and this adds to the noise of the t-test, which decreases the likelihood that a positive difference between groups is identified. A similar study by Palermo (2016) reported no significance in difference of length and weight between fish infected with *Cryptosporidium* and those not infected (Palermo, 2016). Age of fish may contribute to susceptibility to *Cryptosporidium* infections with previous studies reporting higher prevalence in juveniles (Alvarez-Pellitero et al., 2004; Sitja-Bobadilla, 2005). For example, in some studies, prevalence has been higher in juvenile fish as opposed to adults, for example, in juvenile Turbot, a 100% prevalence was reported by Alvarez-Pellitero et al. (2004) and Sitja-Bobadilla (2005) reported higher infection rates in pre-growing and early on-growing juvenile fish compared to adults. Of the samples tested for *Cryptosporidium* in the present study, it was not possible to conduct an analysis between infections and growing stages of fish due to a number of factors; (1) all Oscar fish were juveniles (2) Neon tetra are difficult to age and sex, and (3) no other species were infected at a prevalence sufficiently high enough to conduct a statistically valid age analysis. Further studies are required to determine whether infection in juveniles is associated with increased *Cryptosporidium* prevalence and a difference in adult fish weight and length.

Previous studies have reported that other piscine-derived *Cryptosporidium* species can also have serious clinical impacts on their hosts. For example, (Yang et al., 2016) described a piscine species of *Cryptosporidium* infecting a Koi carp (*Cyprinus carpio*), causing severe granulomatous inflammatory lesions and granulomas were found in the gills, liver, spleen, kidneys, intestine and through the subcutaneous layer. The pathogenicity of piscine genotype 2 was described in angelfish in a study conducted by Murphy et al. (2009). In that study, a cryptosporidiosis outbreak occurred in predominantly larval angelfish in which 80% of fish died (400/500). Clinical signs noted included fish with varied levels of emaciation, poor growth rates, swollen coelomic cavities, anorexia, spiralling and listlessness (Murphy et al., 2009). In the present study, no noticeable change in general appearance or health was observed in fish that later tested positive for *Cryptosporidium*. However, the epithelium infected by *Cryptosporidium* in the gastrointestinal system of fish can become necrotic with sloughing of epithelial cells causing abundant cell debris throughout the lumen (Alvarez-Pellitero and Sitjà-Bobadilla, 2002). In the present study, histology of a sample positive for *C. huwi* (Figure 3.6-8) revealed similar epithelial damage.

The two most common *Cryptosporidium* species found infecting humans worldwide, *C. hominis* and *C. parvum* (Xiao, 2010), were not found in the current study, however, previous studies have identified both species in fish. For example, Koinari et al. (2013) found zoonotic subtypes of *C. parvum* and *C. hominis* infecting cultured, wild marine and freshwater fish from Papua New Guinea. Palermo (2016) reported zoonotic *C. parvum* and *C. hominis* in goldfish from a fish farm in Perth (Australia). Two French studies by Certad et al. (2015); Certad et al. (2019) identified

zoonotic *C. parvum* in fish from a lake in France as well as from edible marine fish in the surrounding European seas of France. Further studies are required to determine the prevalence of zoonotic *Cryptosporidium* species in fish and the public health implications.

4.2 Characterising *Cryptosporidium* in fish

Sequencing at the 18S locus identified *C. huwi* (*n*=11) and three genotypes; piscine genotype 2 (PG2) (*n*=3), piscine genotype 4 (PG4) (*n*=1) and piscine genotype 7 (PG7) (*n*=5) and one mixed infection. At the actin locus, *C. huwi* (*n*=4), piscine genotype 2 (PG2) (*n*=1), (PG7) (*n*=1) and one novel *Cryptosporidium* sequence were identified. All samples that produced positive *Cryptosporidium* sequences at the 18S and actin loci were sourced from Vebas Aquarium, except for one *C. huwi* sequenced at the actin locus from a goldfish sourced from the fish farm.

Earlier phylogenetic analysis presented two broad branches of *Cryptosporidium*; gastric and intestinal (Xiao et al., 2004). More recent phylogenetic analysis, including the present study, provides growing evidence of a piscine clade that includes piscine-derived *Cryptosporidium* species including *C. molnari, C. huwi*, *C. scophthalmi* and piscine genotypes which branch off at a basal position relative to all other *Cryptosporidium* species (Palenzuela et al., 2010; Reid et al., 2010; Zanguee et al., 2010; Morine et al., 2012; Koinari et al., 2013). The present study also includes novel genotypes previously reported found parasitising a variety of wild marine fish (Certad et al., 2019). The present study placed piscine-derived *Cryptosporidium* basal at both the actin and 18S phylogenetic trees, which suggests that piscine species may be the evolutionary ancestors of all known *Cryptosporidium* species followed by

species that primarily infect the stomach (e.g. *C. serpentis*) followed by species that infect respiratory organs (e.g. *C. baileyi*) and most recently evolved are species that primarily infect the intestine (e.g. *C. hominis*)

Samples RET441 and RET445 were both positive at the 18S locus for piscine genotype 7, however, when sequenced at the actin locus, while isolate RET445 matched at 100% similarity to a piscine genotype 7 actin sequence on GenBank (KR610335), isolate RET441 showed no similarity to the same sequence. Instead, at the actin locus, RET441 exhibited 17.7% pairwise genetic distance from the RET445 genotype 7 actin sequence. Therefore RET441 is likely a mixed infection of piscine genotype 7 (18S locus) and a novel genotype (actin locus). This finding along with the mixed sequence (RET338) from the same batch of fish provides evidence of a high likelihood that the actin sequence found in RET441 is from a novel species different to piscine genotype 7, but still within the piscine clade and coinfecting sample RET441 along with piscine genotype 7. These results further support the idea that a wide genetic variety exist within the piscine clade (Murphy et al., 2009; Reid et al., 2010; Zanguee et al., 2010; Morine et al., 2012; Koinari et al., 2013) and that mixed infections are common (Paparini et al., 2017) and can result in different species being sequenced at the 18S and actin loci (Yang et al., 2015).

4.2.1 Prevalence of piscine genotypes

Piscine genotype 2 has been found previously in Angelfish, Oscarfish and Mullet with prevalence's ranging from 0.5-5% (Murphy et al., 2009; Reid et al., 2010; Yang et al., 2015). The prevalence of piscine genotype 2 in the present study was considerably higher at 37.5%. Furthermore, Oscar fish in the present study were

juveniles and juveniles and neonates have been reported to have higher levels of infections then their respective adult counterparts (Alvarez-Pellitero et al., 2004; Sitja-Bobadilla, 2005). The prevalence of piscine genotype 4 in the present study was 50% (1/2) and it was only found in Black ghost knife fish. Two previous studies reported prevalence's of 1.8% in wild marine Sea mullet (2/111) (Reid et al., 2010) and 25% in Neon tetra from the same Perth aquarium (1/4) (Morine et al., 2012). The prevalence of piscine genotype 7 found in Red eye tetra in the present study was 62.5% (5/8), which was higher than the 27.3% (3/11) found in Red eye tetra in a study by Morine et al. (2012) and much higher than the 0.7% found in Neon tetra in a study by Yang et al. (2015)

4.2.2 Characterising piscine genotypes at the 18S locus

In the present study, at the 18S locus using 736 base pairs of genetic data, the closest genetic match of a described species to piscine genotype 2 was *C. molnari* at 12.2% followed by *C. huwi* at 12.8%, The present study places piscine genotype 2 at 12.2% genetic distance from *C. molnari*, similar to the 12.8% genetic distance previously calculated by Morine et al. (2012). Yang et al. (2015) reported that piscine genotype 2 exhibited 9% genetic distance from *C. molnari* at the 18S locus. At the 18S locus, piscine genotype 4 was most closely related to piscine genotype 2 (3.7%) followed by piscine genotype 3 (5.7%) and exhibited 13.0% (*C. huwi*) to 19.9% (*C. scophthalmi*) genetic distance to all other species. At the 18S locus piscine genotype 7 grouped closest to *C. huwi* at 2.9% genetic distance, similar to previous studies at the same locus (Morine et al., 2012; Yang et al., 2015). Across the shorter 18S sequences, and compared to the piscine genotypes, genotypes 2-6 had genetic

distances closer to each other (3.7-7.6%) than to any established *Cryptosporidium* species (10.7%-21.6%).

4.2.3 Characterising piscine genotypes at the actin locus

At the actin locus, with 816 bp sequences and comparing to established species, piscine genotype 2 was again most closely related to *C. molnari* at 18.1%-18.2% followed by *C. huwi* at 20.0%, however, the novel *Cryptosporidium* actin sequence (RET441) from the present study had a genetic distance of 18.5% from piscine genotype 2. Similar to Yang et al. (2015), piscine genotype 7 was once again closest to *C. huwi* at 8.9% genetic distance, with the novel *Cryptosporidium* sequence from sample RET441 exhibiting 16.7% genetic distance from piscine genotype 7.

Analysis of shorter actin sequences again grouped piscine genotype 2 closest to piscine genotype 4 (7.2% genetic distance). Piscine genotype 7 remained grouped closest to *C. huwi* at 8.9% genetic distance.

4.2.4 Characterising piscine genotypes using concatenated sequences

Phylogenetic analysis of longer concatenated 18S and actin sequences (1,476 bp) also confirmed the genetic distinctness of piscine genotype 2 which grouped closest to *C. molnari* at 13.4% and exhibited 14.9% (*C. huwi*) to 22.2% (*C. scophthalmi*) genetic distance from piscine *Cryptosporidium*, with 16.5% (*C. rubeyi*) and 22.4% (*C. canis*) genetic distances from all non-piscine *Cryptosporidium* species. The concatenated sequences placed piscine genotype 7 closest to *C. huwi* at 7.5% and exhibited 13.4% (*C. molnari*) to 23.1% (*C. scophthalmi*) genetic distances from piscine *Cryptosporidium*, with 17.9% (*C. testudinis*) to 22.6% (*C. canis*) genetic

distance from all non-piscine *Cryptosporidium*. Piscine genotype 2 exhibited 14.6% genetic distance from piscine genotype 7. Across the shorter concatenated sequences (614 bp) and compared to the piscine genotypes, piscine genotype 2 grouped closest to piscine genotype 4 at 4.8% followed by piscine genotype 5 at 8.4% and piscine genotype 3 at 9.6%, with *C. molnari* grouping at 17.2%. Piscine genotype 7 grouped closest to *C. huwi at* 7.2% genetic distance followed by *C. molnari* at 11.6% then piscine genotype 5 at 13.2%.

The 18S locus contains conserved, variable and hyper-variable regions, however, at least two loci are required to be sequenced to describe a novel species and actin is another common locus for further characterisation. An issue that can arise when using PCR and Sanger sequencing to describe a species is mixed infections producing different sequences at the 18S and actin loci (Yang et al., 2015). A mixed infection in Sample RET441 was detected when amplifications from the 18S and actin loci were incongruent and produced sequences from piscine genotype 7 and a novel *Cryptosporidium* sequence respectively.

The genetic distances reported in the present study clearly support piscine genotype 2, piscine genotype 4 and piscine genotype 7 as separate species from any established *Cryptosporidium* species as these genetic differences are greater than between many currently accepted species. For example, the genetic distance at the 18S and actin loci between *C. hominis* and *C. cuniculus* is 0.4% and 1.6%, respectively (Kvác et al., 2014), and the genetic distance between *C. muris* and *C. andersoni* at the 18S, actin, *hsp70* loci is 0.7%, 3.5% and 2.2%, respectively (Holubová et al., 2016).

The host range of piscine genotype 2, piscine genotype 4 and piscine genotype 7 and its zoonotic potential are also currently unknown, but it has not been previously reported in non-piscine hosts, suggesting that it may be piscine specific, however, further analysis is required to determine this.

4.2.4 Histology and immunohistological staining

A characteristic of piscine-derived *Cryptosporidium* infections is the presence of oocysts located deep within the epithelium (Alvarez-Pellitero and Sitjà-Bobadilla, 2002; Ryan et al., 2004a; Palenzuela et al., 2010), as opposed to the less invasive (epicellular) mucosal locations of most of non-piscine derived *Cryptosporidium* sp. Piscine *Cryptosporidium* infections have also been associated with vast sloughing and necrosis of epithelial cells. In the present study, morphological analysis was conducted on histological slides from a Neon tetra (NT214) infected with *C. huwi* to compare the infection to the previous descriptions by (Ryan et al., 2015) and the same morphological characteristics were present including oogonial and sporogonial life-cycle stages deeply embedded in the gastric epithelium and significant epithelial cell damage causing loose detritus in the gastric lumen (Figure 3.6).

A previous study by Murphy et al. (2009) characterised piscine genotype 2 using histology and EM and reported that the parasite was observed in gastric locations only and all life cycle stages were described, with oocysts measuring 3.4 µm in diameter (n=64). As with previous descriptions of piscine-derived *Cryptosporidium* species, oocysts were observed embedded deep within the epithelial cell cytoplasm.

Unfortunately *Cryptosporidium* infections were not observed in other sections and no morphological data is available in the present study for piscine genotypes 2, 4 and 7. A common issue with fixation of fish gastrointestinal tissue for histology is the rapid rate of autolysis after dissection compared to homeotherms (Zanguee et al., 2010; Roberts, 2012). While morphological characterisation is important, oocysts do not contain features that can be used to reliably distinguish between species and therefore more reliance is placed on molecular characterisation (Morgan et al., 1998; Fayer et al., 2000).

4.3 *Goussia*

Out of the 253 samples of goldfish sequenced, 10 from the fish farm were identified as the parasitic protist *Goussia* from the phylum Apicomplexa (class Conoidasida, subclass Coccidiasina). Many organisms of the phylum Apicomplexa cause disease and are of veterinary and medical importance with parasites of the subclass Coccidiasina being obligate intracellular Apicomplexa and include parasites of aquatic organisms that have a significant pathological impact on natural stocks of a number of fish species (Azevedo et al., 1995; Abollo et al., 2001; Morrison and Marryatt, 2012; Lovy and Friend, 2015). *Goussia* sp. parasitise reptiles, amphibians, fish and arthropods and are a taxonomically diverse genus (Lee et al., 2000; Jirků et al., 2002; Dogga et al., 2015). They can cause significant damage to the digestive tract and heavy infections may cause mortalities (Azevedo, 2001; Gestal and Azevedo, 2005). *Goussia* are a neglected pathogen due to the limited number studies on their diversity and dynamics (da Costa Maia, 2015; Dogga et al., 2015), and the extent of impact of *Goussia* on natural fish stocks is unknown and the taxonomic uncertainty of coccidia infecting aquatic hosts is high relative to their terrestrial counterparts (Xavier

et al., 2018), hence there is a great need to expand the database on the diversity of this group (da Silva et al., 2019). There are approximately 50 known species of *Goussia* and sequenced data loci from the 18S locus are commonly used to advance the taxonomic data of *Goussia* (Jirků et al., 2002; Matsche et al., 2019a). In the present study, nine novel 18S *Goussia* sequences of *Goussia* were identified, all of which were from the fish farm goldfish.

There are four subgroups of *Goussia* based on where they are found infecting their host, an epicellular type (intracellular but extracytoplasmal), a nodular type (found in nodules) and a dispersed type (found throughout the gut) and the leucisci type (*G. leucisci*, found in the renal tubules) (Rosenthal et al., 2016; Xavier et al., 2018). The novel sequences found in the present study at the 18S locus grouped closely to the dispersed type of *Goussia*. Using pairwise genetic distances novel sequences 2-9 (Samples GF305, GF315, GF317, GF330, GF342, GF354, GF366, GF375 and GF377) grouped closest to *G. carpelli* (usually found in cyprinid fish, including the fish host of these samples, *Carassius auratus*), which is found dispersed throughout the gut. In piscine hosts, *C. carpelli* can cause acute or chronic enteritis (Matsche et al., 2019b). Novel genotype 6 (sample GF354) was most similar to *G. carpelli* at 1.9% genetic distance, while novel sequences 2, 3, 4, 5, 7, 8, and 9 ranged from 2.3-3.9%. Novel sequence 1 (GF112) grouped closer to *G. bohemica* (5.5% genetic distance) than the other novel sequences (7-8.7%) (See Table 3.8 and Figure 3.7). However, overall novel sp. 1 grouped closest to four undescribed *Goussia* species (reference MN202593, GU479673, GU479636, GU479648), all of which are dispersed types along with *G. bohemica* (which has been found to inhabit the goblet and epithelial cells of the intestine) (Lukeš, 1994). *G. leucisci* is the only known

leucisci type (infect renal tubules) within the *Goussia* genus, currently there is only morphological data on *G. leucisci* (Rosenthal et al., 2016; Matsche et al., 2019a). It should be noted that while all novel sequences from goldfish in the present study were most genetically similar to established species of *Goussia*, the genus *Eimeria* (apicomplexan parasites) is closely related to *Goussia* (Figure 3.10), While all the novel *Goussia* sequences were genetically most closely related to *Goussia*, they also exhibited genetic similarity to *Eimeria* and clearly further morphological and phylogenetic analyses is required to better understand their evolutionary relationships. *Eimeria* have a wider range of hosts including birds, mammals, reptiles and fish (Chapman et al., 2013) and are an important cause of gastrointestinal illness in livestock and Australian marsupials (Hillman et al., 2016).

The students t-test found a significance in the difference of length in fish infected with *Goussia*, however, there was no significant difference in weight. The sample size of *Goussia* positive fish was small at 10 in comparison to the negative samples at 243, the t-test is still feasible with sample sizes as small as n=2 (De Winter, 2013), however, it is important to note that small sample sizes or large variance can reduce the accuracy of the t-test (Kim, 2015). It is not known whether *Goussia* infections are correlated with a difference in size of fish. Research into the pathology caused by *Goussia* reports symptoms ranging from mild intestinal damage in koi carp experimentally administered *Goussia* oocysts to extreme gut pathology, high mortality rates and listlessness in gourami (Szekely and Molnar, 1992; Steinhagen et al., 1997; Hemmer et al., 1998). In future, research questions that could be asked include, investigating if *Goussia* infections causes stunted growth of fish or if juveniles have a higher likelihood of infections.

H&E stained slides were made from the intestine and stomach from samples positive with *Goussia* and while no organisms were seen it is possible they were parasitising an organ other than the GI tract. *Goussia* have historically been associated with the GI epithelium of both freshwater and marine piscine hosts but can parasitise other organs such as the spleen, bile ducts, gall bladder, liver and swim bladder (Li and Desser, 1985; Diouf and Toguebaye, 1993; Morrison et al., 1993; Molnár et al., 2004; Dogga et al., 2015; Matsche et al., 2019b). The present study involved the collection of fish gastric and intestinal tissue for histological purposes and while *Goussia* are commonly found in the GI tract of fish in future studies a recommendation would be to include other organs known to be parasitised by *Goussia* for future studies.

4.4 *Schyzocotyle* (*Bothriocephalus*) *acheilognathi*

Samples GF035 and GF131 were identified by microscopy as positive for *Schyzocotyle* (*Bothriocephalus*) *acheilognathi* (Asian fish tapeworm), an invasive piscine cestode of veterinary and environmental importance first described by Yamaguti (1934).

Although identification was made by morphology only, the distinctive features made morphological identification reliable include; deep bothria, narrow openings with simple (non-crenulate) margins, located dorsally and ventrally on the scolex; heart shaped scolex, absence of a neck and absence of or poorly developed apical disc, unarmed (Chubb et al., 1987; Scholz, 1997; Košuthová et al., 2015). However, some difficulties were encountered in the present study, Freshly collected tapeworms were placed into fixative (in this case, 4% formaldehyde and absolute ethanol), which

caused segments to contract or concertina making accurate length calculations difficult. Future studies should soak freshly sampled tapeworms in distilled water or saline first to allow the segments to relax and expand so that staining can reveal internal structures more reliably (Chubb et al., 1987; Scholz, 1997; Scholz et al., 1998; Košuthová et al., 2015). Fixation in hot (almost boiling) 4% formaldehyde also prevents segment contraction (Scholz et al., 1998). Future studies should also conduct molecular analysis to confirm the species identify. Genetic identification of *S. acheilognathi* has previously been conducted successfully using primers to amplify loci from the internal transcribed spacer (ITS), cytochrome c oxidase (CO) and 18S regions (Marcogliese et al., 2016; Boonthai et al., 2017; Hansen and Alarcon, 2019).

The Asian fish tapeworm, *Schyzocotyle acheilognathi* was previously named *Bothriocephalus acheilognathi* when Akhmerov (1960) erroneously placed the genus in the family Cyathocephalidae due to misinterpreting the scolex morphology of the species. The genus *Schyzocotyle* was resurrected to accommodate the Asian fish tapeworm (Brabec et al., 2015), which is of veterinary importance as it is a generalist invasive fish parasite with fish serving as the final host where infection causes significant damage by intestinal occlusion and rupture leading to substantial mortality (Boonthai et al., 2017). Recently, the global spread of invasive *S. acheilognathi* has been investigated and highlighted as a significant global concern by countries including China, USA, Mexico, Madagascar and Brazil (Boonthai et al., 2017; Brabec et al., 2018; de León et al., 2018; Scholz et al., 2018; Souza et al., 2018) and has been of significant concern in Australia, Britain and America for decades (Chubb et al., 1987; Scholz, 1997; Dove and Fletcher, 2000).

In Australia (New South Wales and Victoria), Asian fish tapeworm was discovered for the first time by Dove and Fletcher (2000) in the fish host *Carassius auratus*, where the authors reported low host specificity for Asian fish tapeworm (including hosts from six orders and 11 families, inclusive of native sp.). In particular, fish collected sympatrically with a principle host, from the family *Cripinidae*, were more likely to be infected with Asian fish tapeworm (Dove and Fletcher, 2000). *Carassius auratus* are an imported exotic sp. of ornamental fish that find their way to rivers, estuaries and lakes from pet owners or fish farms either through drainage systems or otherwise. Asian fish tapeworm has caused mass mortalities in cultured fish (Körting, 1975) and its high pathogenicity in known hosts combined with the low host specificity is a current threat to native fish of the Murray-Darling basin (Dove and Fletcher, 2000), in part due to the abundance of feral goldfish. Feral goldfish are also found in freshwater bodies in Western Australia and they could help spread the Asian fish tapeworm to native fish of Western Australia. However, whether it is pathogenic to native species is unknown and more data are required. The presence of Asian fish tapeworm could pose a threat to the native freshwater fish species of Western Australia.

Asian fish tapeworm is found worldwide in freshwater fish, its principle hosts are from the family *Cripinidae* and include *Carassius auratus* (the same host species positive for Asian fish tapeworm in the present study, GF035 and GF131). Asian fish tapeworm was discovered in 2018 in Western Australia for the first time by a Murdoch researcher in feral goldfish removed from Lake Joondalup (Palermo et al., unpublished). The present study observed Asian fish tapeworm in Western Australia from a commercial fish farm with a varied customer base. It can thus be suggested that

improved quarantine and prophylactic measures are required for imported ornamental fish to prevent the spread of Asian fish tapeworm. In addition, treatment of farmed and pet fish using 2mg per litre of praziquantel immersions have been shown to be well tolerated and efficacious (Košuthová et al., 2015).

4.5 Conclusions

Cryptosporidium is an important parasite, it is the second leading cause of diarrheal deaths in children under the age of five in developing countries (Cacciò and Widmer, 2014) and outbreaks are recurrent in the developed world. Piscine *Cryptosporidium* forms a phylogenetic clade within the genus with many species yet to be characterised, and veterinary and public health implications unclear. Piscine genotype 2 is genetically most similar to piscine genotype 4 at 3.7% pairwise genetic distance at the 18S locus and 7.2% at the actin locus. Piscine genotype 7 was closest to *C. huwi* at 5.7% genetic distance at the 18S locus and 8.9% at the actin locus.

The present study benefits the global effort to describe and track species of *Cryptosporidium* and understand the complicated patterns of host associations within this genus (Kissinger, 2019). Particularly useful is the genetic data offered from the present study that describes both piscine genotype 2 and piscine genotype 7 at both the 18S and actin loci with sequences longer than any to date (818bp for 18S and 1,050bp for actin). The findings also include a 1,050bp actin sequence from a novel piscine *Cryptosporidium* actin sequence, ten 583bp 18S sequences from 9 novel sequences of *Goussia* and an 583bp 18S sequence of piscine genotype 4, all sequences will be uploaded to GenBank for public use. Future genetic work on *Cryptosporidium* should aim at characterising novel piscine genotypes as well as collecting

morphological data to help describe the unique pathologies of piscine *Cryptosporidium*.

4.6 Future research and considerations

While PCR and histology are excellent tools for describing new species of *Cryptosporidium* it is vital to acknowledge the limits of this process. PCR is labour intensive and costly with potential for contamination, non-specific amplification and conflicting sequences from the same sample. More than one gene is required for sufficiently describing species (DeSalle et al., 2005) and Sanger sequencing can only generate one sequence for each locus. Furthermore, PCR and Sanger sequencing cannot resolve *Cryptosporidium* species and genotypes of low relative abundance or mixed infections unless cloning is performed. PCR and Sanger sequencing are very useful tools for describing species but would benefit from being used in combination with technologies such as NGS and WGS to further understand the extent of mixed infections and describe the entire genomes of *Cryptosporidium* species. Histology is useful for visualising life-cycle stages, however, finding infections can be difficult due to the nature of patchy infections and the speed of fish tissue autolysis.

The advent of second generation, high-throughput NGS platforms have allowed fast and efficient sequencing of genes, genomes and metagenomes (Metzker et al, 2010). By applying this technique to the host samples of mixed *Cryptosporidium,* it may be possible to identify the specific infections responsible for the parasitisation at a reduced cost (Taniuchi et al, 2011).

NGS can be conducted on samples with mixed infections of *Cryptosporidium* using indexed primers at the 18S locus on an Illumina MiSeq. The majority of

molecular characterisation techniques, to date, have been based on Sanger Sequencing (chain termination) (Sanger et al, 1977). NGS has been used recently by Paparini et al. (2017) to uncover mixed infections present in 11 ornamental fish, which revealed mixed infections were common and consisted of a more dominant species coinfecting with rarer species and genotypes. The present study produced one mixed sample (RET438) and another sample produced piscine genotype 7 sequence at the 18S locus and a novel piscine genotype 7-like sequence at the actin locus (RET441). Therefore, performing NGS on all samples would elucidate the level of mixed infections.

Extensive bioinformatics data are provided through WGS, the data gained can also describe the evolution of piscine *Cryptosporidium* with respect to other species of *Cryptosporidium* by providing the entire genome of a species. Similar to how WGS has been used to elucidate evolution of anthroponosis in *Cryptosporidium* (Kissinger, 2019; Nader et al., 2019), WGS of piscine *Cryptosporidium* can provide enough genetic data to confidently describe the evolution of the piscine clade in regards to other species of *Cryptosporidium*. PCR and amplicon-based NGS, in comparison, mostly aim to provide sequences of relatively small sections of a genome (loci) that contain preserved and variable regions to identify and characterise species, and in the case of NGS, mixed infections also (Paparini et al., 2017). WGS data is also suitable for finding new loci of significance, for example, Li et al. (2014) used WGS to subtype *C. ubiquitum* and Feng et al. (2011) scanned WGS data to develop a multilocus sequencing tool for high resolution typing of both *C. muris* and *C. andersoni*.

Finally, transmission studies regarding piscine *Cryptosporidium* would reveal a great deal about not only the process of infection in water but their zoonotic potential

and host specificity (de Lucio et al., 2017). Transmission studies could be conducted by monitoring infection rates of various *Cryptosporidium* spp. between fish-hosts experimentally kept in tanks while regulating the environments and contact between samples, furthermore, infected water from the tanks could be administered as drinking water for non-piscine hosts to determine susceptibility to infection.

References

Abollo, E., Calvo, M., Pascual, S., 2001. Hepatic coccidiosis of the blue whiting, *Micromesistius poutassou* (Risso), and horse mackerel, *Trachurus trachurus* (L.), from Galician waters. Journal of Fish Diseases 24, 335-343.

Adamu, H., Petros, B., Zhang, G., Kassa, H., Amer, S., Ye, J., Feng, Y., Xiao, L., 2014. Distribution and clinical manifestations of *Cryptosporidium* species and subtypes in HIV/AIDS patients in Ethiopia. PLoS Neglected Tropical Diseases 8, e2831.

Agholi, M., Hatam, G.R., Motazedian, M.H., 2013. HIV/AIDS-associated opportunistic protozoal diarrhea. AIDS Research and Human Retroviruses 29, 35-41.

Akhmerov, A.K., 1960. The tapeworms of fishes in the Amur river. Trudi Gelmintologicheskoi Laboratorii. Akademiya Nauk SSSR. 10, 15-31.

Al-Brikan, F.A., Salem, H.S., Beeching, N., Hilal, N., 2008. Multilocus genetic analysis of *Cryptosporidium* isolates from Saudi Arabia. J Egypt Soc Parasitol 38, 645-658.

Aldeyarbi, H.M., Abu El-Ezz, N.M.T., Karanis, P., 2016. *Cryptosporidium* and cryptosporidiosis: the African perspective. Environmental Science and Pollution Research 23, 13811-13821.

Alvarez-Pellitero, P., Quiroga, M.I., Sitjà-Bobadilla, A., Redondo, M.J., Palenzuela, O., Padrós, F., Vázquez, S., Nieto, J.M., 2004. *Cryptosporidium scophthalmi* n. sp. (Apicomplexa: Cryptosporidiidae) from cultured turbot *Scophthalmus maximus*. Light and electron microscope description and histopathological study. Diseases of Aquatic Organisms 62, 133-145.

Alvarez-Pellitero, P., Sitjà-Bobadilla, A., 2002. *Cryptosporidium molnari* n. sp. (Apicomplexa: Cryptosporidiidae) infecting two marine fish species, *Sparus aurata* L. and *Dicentrarchus labrax* L. International Journal for Parasitology 32, 1007-1021.

Amadi, B., Mwiya, M., Sianongo, S., Payne, L., Watuka, A., Katubulushi, M., Kelly, P., 2009. High dose prolonged treatment with nitazoxanide is not effective for cryptosporidiosis in HIV positive Zambian children: a randomised controlled trial. BMC Infectious Diseases 9, 195-195.

Anson, V., Whipp, M., Haydon, S., Gasser, R., 2010. *Cryptosporidium cuniculus* e new records in human and kangaroo in Australia. Parasit. Vectors 7, 492.

Azami, M., Moghaddam, D., Salehi, R., Salehi, M., 2007. The identification of *Cryptosporidium* species (protozoa) in Ifsahan, Iran by PCR-RFLP analysis of the 18S rRNA gene. Molekuliarnaia Biologiia 41, 934-939.

Azevedo, C., 2001. Fine structure of sporogonic stages of *Goussia clupearum* (Apicomplexa: Eimeriidae) in the liver of infected fish (*Belone belone* L.), using light and electron microscopy. Parasitology Research 87, 326-330.

Azevedo, C., Matos, E., Matos, P., 1995. Ultrastructural data on sporogony of the coccidian parasite *Calyptospora spinosa* from the liver of the Amazonian fish, *Crenicichla lepidota* Heckel. Journal of Fish Diseases 18, 475-479.

Barugahare, R., Dennis, M.M., Becker, J.A., Šlapeta, J., 2011. Detection of *Cryptosporidium molnari* Oocysts from Fish by Fluorescent-Antibody Staining Assays for *Cryptosporidium* spp. Affecting Humans. Applied and Environmental Microbiology 77, 1878.

Bell, F.W., 2019. Food from the sea: The economics and politics of ocean fisheries. Routledge.

Betancourt, W.Q., Rose, J.B., 2004. Drinking water treatment processes for removal of *Cryptosporidium* and *Giardia*. Veterinary Parasitology 126, 219-234.

Beyer, T.V., Svezhova, N.V., Sidorenko, N.V., Khokhlov, S.E., 2000. *Cryptosporidium parvum* (Coccidia, Apicomplexa): Some new ultrastructural observations on its endogenous development. European Journal of Protistology 36, 151-159.

Boonthai, T., Herbst, S.J., Whelan, G.E., Van Deuren, M.G., Loch, T.P., Faisal, M., 2017. The Asian fish tapeworm *Schyzocotyle acheilognathi* is widespread in baitfish retail stores in Michigan, USA. Parasites & Vectors 10, 618.

Boxell, A., Hijjawi, N., Monis, P., Ryan, U., 2008. Comparison of various staining methods for the detection of *Cryptosporidium* in cell-free culture. Experimental Parasitology 120, 67-72.

Brabec, J., Scholz, T., Štefka, J., 2018. Development of polymorphic microsatellites for the invasive Asian fish tapeworm *Schyzocotyle acheilognathi*. Parasitology International 67, 341-343.

Brabec, J., Waeschenbach, A., Scholz, T., Littlewood, D.T.J., Kuchta, R., 2015. Molecular phylogeny of the Bothriocephalidea (Cestoda): molecular data challenge morphological classification. International Journal for Parasitology 45, 761-771.

Cacciò, S.M., Widmer, G., 2014. *Cryptosporidium*: parasite and disease. Springer, Vienna.

Cama, V.A., Ross, J.M., Crawford, S., Kawai, V., Chavez-Valdez, R., Vargas, D., Vivar, A., Ticona, E., Navincopa, M., Williamson, J., 2007. Differences in clinical manifestations among *Cryptosporidium* species and subtypes in HIV-infected persons. The Journal of Infectious Diseases 196, 684-691.

Campbell, A.T., Robertson, L.J., Smith, H.V., 1992. Viability of *Cryptosporidium* parvum oocysts: correlation of in vitro excystation with inclusion or exclusion of fluorogenic vital dyes. Applied and Environmental Microbiology 58, 3488-3493.

Camus, A.C., Lopez, M.K., 1996. Gastric Cryptosporidiosis in Juvenile Red Drum. Journal of Aquatic Animal Health 8, 167-172.

Canonico, G.C., Arthington, A., McCrary, J.K., Thieme, M.L., 2005. The effects of introduced *tilapias* on native biodiversity. Aquatic Conservation: Marine and Freshwater Ecosystems 15, 463-483.

Cavalier-Smith, T., 2014. Gregarine site-heterogeneous 18S rDNA trees, revision of gregarine higher classification, and the evolutionary diversification of Sporozoa. European Journal of Protistology 50, 472-495.

Certad, G., Dupouy-Camet, J., Gantois, N., Hammouma-Ghelboun, O., Pottier, M., Guyot, K., Benamrouz, S., Osman, M., Delaire, B., Creusy, C., Viscogliosi, E., Dei-Cas, E., Aliouat-Denis, C.M., Follet, J., 2015. Identification of *Cryptosporidium* Species in Fish from Lake Geneva (Lac Leman) in France. PLOS ONE 10, e0133047.

Certad, G., Follet, J., Gantois, N., Hammouma-Ghelboun, O., Guyot, K., Benamrouz-Vanneste, S., Fréalle, E., Seesao, Y., Delaire, B., Creusy, C., Even, G., Verrez-Bagnis, V., Ryan, U., Gay, M., Aliouat-Denis, C., Viscogliosi, E., 2019. Prevalence, Molecular identification, and risk factors for *Cryptosporidium* infection in edible marine fish: A Survey Across Sea Areas Surrounding France. Frontiers in Microbiology 10.

Chalmers, R.M., Davies, A.P., 2010. Minireview: Clinical cryptosporidiosis. Experimental Parasitology 124, 138-146.
Chalmers, R.M., Elwin, K., Hadfield, S.J., Robinson, G., 2011. Sporadic human cryptosporidiosis caused by *Cryptosporidium cuniculus*, United Kingdom, 2007–2008. Emerging Infectious Diseases 17, 536.
Chalmers, R.M., Robinson, G., Elwin, K., Hadfield, S.J., Thomas, E., Watkins, J., Casemore, D., Kay, D., 2009. Detection of *Cryptosporidium* species and sources of contamination with *Cryptosporidium hominis* during a waterborne outbreak in north west Wales. Journal of Water and Health 8, 311-325.
Chapman, H.D., Barta, J.R., Blake, D., Gruber, A., Jenkins, M., Smith, N.C., Suo, X., Tomley, F.M., 2013. A selective review of advances in coccidiosis research, In: Advances in parasitology. Elsevier, pp. 93-171.
Chappell, C.L., Okhuysen, P.C., Langer-Curry, R., Widmer, G., Akiyoshi, D.E., Tanriverdi, S., Tzipori, S., 2006. *Cryptosporidium hominis*: Experimental challenge of healthy adults. American Journal of Tropical Medicine and Hygiene 75, 851.
Checkley, W., White, A.C., Jaganath, D., Arrowood, M.J., Chalmers, R.M., Chen, X.-M., Fayer, R., Griffiths, J.K., Guerrant, R.L., Hedstrom, L., Huston, C.D., Kotloff, K.L., Kang, G., Mead, J.R., Miller, M., Petri, W.A., Priest, J.W., Roos, D.S., Striepen, B., Thompson, R.C.A., Ward, H.D., Van Voorhis, W.A., Xiao, L., Zhu, G., Houpt, E.R., 2015. A review of the global burden, novel diagnostics, therapeutics, and vaccine targets for *Cryptosporidium*. The Lancet Infectious Diseases 15, 85-94.
Chichino, G., Bruno, A., Cevini, C., Atzori, C., Gatti, S., Scaglia, M., 1991. New rapid staining methods of *Cryptosporidium* oocysts in stools. The Journal of Protozoology 38, 212S.
Chubb, J., Pool, D., Veltkamp, C., 1987. A key to the species of cestodes (tapeworms) parasitic in British and Irish freshwater fishes. Journal of Fish Biology 31, 517-543.
Čondlová, Š., Horčičková, M., Sak, B., Květoňová, D., Hlásková, L., Konečný, R., Stanko, M., McEvoy, J., Kváč, M., 2018. *Cryptosporidium apodemi* sp. n. and *Cryptosporidium ditrichi* sp. n.(Apicomplexa: Cryptosporidiidae) in *Apodemus* spp. European Journal of Protistology 63, 1-12.
Costa, 2016. Characterization of a *Cryptosporidium scophthalmi*-like isolate from farmed turbot (*Scophthalmus maximus*) using histological and molecular tools. Diseases of Aquatic Organisms.
Costanza, R., De Groot, R., Farber, S., Grasso, M., Hannon, B., Limburg, K., Naeem, S., Paruelo, J., Raskin, R., Sutton, P., 1998. The value of the worlds ecosystem services and natural capital. Ecological Economics 25, 3-15.
Courtenay Jr, W.R., Stauffer Jr, J.R., 1990. The introduced fish problem and the aquarium fish industry. Journal of the World Aquaculture Society 21, 145-159.
Current, W., 1990. Techniques and laboratory maintenance of *Cryptosporidium*. Cryptosporidiosis of Man and Animals, 31-49.
Current, W.L., Garcia, L.S., 1991. Cryptosporidiosis. Clinical Microbiology Reviews 4, 325-358.
Current, W.L., Upton, S.J., Haynes, T.B., 1986. The life cycle of *Cryptosporidium baileyi* n. sp.(Apicomplexa, Cryptosporidiidae) infecting chickens. The Journal of Protozoology 33, 289-296.
da Costa Maia, J.P.M., 2015. Diversity, infection patterns and host-parasite associations of apicomplexan parasites in reptiles.

da Silva, M.F., de Araújo, R.S., da Silva, D.T., Sanches, O., Hamoy, I., Matos, E., 2019. Gastric coccidiosis in *Thoracocharax stellatus* caused by *Goussia guamaensis* n. sp.(Apicomplexa: Eimeriidae) from the Amazon region. Journal of Fish Diseases 42, 905-912.

Daniels, M.E., Smith, W.A., Jenkins, M.W., 2018. Estimating *Cryptosporidium* and *Giardia* disease burdens for children drinking untreated groundwater in a rural population in India. PLoS Neglected Tropical Diseases 12, e0006231.

Darriba, D., Taboada, G.L., Doallo, R., Posada, D., 2012. jModelTest 2: more models, new heuristics and parallel computing. Nature Methods 9, 772.

de León, G.P.-P., Lagunas-Calvo, O., García-Prieto, L., Briosio-Aguilar, R., Aguilar-Aguilar, R., 2018. Update on the distribution of the co-invasive *Schyzocotyle acheilognathi* (= *Bothriocephalus acheilognathi*), the Asian fish tapeworm, in freshwater fishes of Mexico. Journal of Helminthology 92, 279-290.

de Lucio, A., Bailo, B., Aguilera, M., Cardona, G.A., Fernández-Crespo, J.C., Carmena, D., 2017. No molecular epidemiological evidence supporting household transmission of zoonotic *Giardia* duodenalis and *Cryptosporidium* spp. from pet dogs and cats in the province of Álava, Northern Spain. Acta Tropica 170, 48-56.

De Winter, J.C., 2013. Using the Student's t-test with extremely small sample sizes. Practical Assessment, Research & Evaluation 18.

DeSalle, R., Egan, M.G., Siddall, M., 2005. The unholy trinity: taxonomy, species delimitation and DNA barcoding. Philosophical Transactions of the Royal Society B: Biological Sciences 360, 1905-1916.

Diouf, J.N., Toguebaye, B.S., 1993. Studies of coccidian parasites of fish from the coast of Senegal (West Africa): new species of the genus *Goussia* (Apicomplexa, Eucoccidiida, Calyptosporidae). Zoologica scripta 22, 117-126.

Dogga, S.K., Bartošová-Sojková, P., Lukeš, J., Soldati-Favre, D., 2015. Phylogeny, morphology, and metabolic and invasive capabilities of epicellular fish coccidium *Goussia janae*. Protist 166, 659-676.

Dove, A.D.M., Fletcher, A.S., 2000. The distribution of the introduced tapeworm *Bothriocephalus acheilognathi* in Australian freshwater fishes. Journal of Helminthology 74, 121-127.

Dudgeon, D., Arthington, A.H., Gessner, M.O., Kawabata, Z.-I., Knowler, D.J., Lévêque, C., Naiman, R.J., Prieur-Richard, A.-H., Soto, D., Stiassny, M.L., 2006. Freshwater biodiversity: importance, threats, status and conservation challenges. Biological Reviews 81, 163-182.

DuPont, H.L., Chappell, C.L., Sterling, C.R., Okhuysen, P.C., Rose, J.B., Jakubowski, W., 1995. The Infectivity of *Cryptosporidium parvum* in Healthy Volunteers. The New England Journal of Medicine 332, 855-859.

Edgar, R.C., 2004. MUSCLE: multiple sequence alignment with high accuracy and high throughput. Nucleic Acids Research 32, 1792-1797.

Elliot, A., Morgan, U.M., Thompson, R.C.A., 1999. Improved staining method for detecting *Cryptosporidium* oocysts in stools using malachite green.

Elwin, K., Hadfield, S., Robinson, G., Chalmers, R., 2012a. The epidemiology of sporadic human infections with unusual cryptosporidia detected during routine typing in England and Wales, 2000–2008. Epidemiology & Infection 140, 673-683.

Elwin, K., Hadfield, S.J., Robinson, G., Crouch, N.D., Chalmers, R.M., 2012b. *Cryptosporidium viatorum* n. sp.(Apicomplexa: Cryptosporidiidae) among

travellers returning to Great Britain from the Indian subcontinent, 2007–2011. International Journal for Parasitology 42, 675-682.
Fall, A., Thompson, R.C.A., Hobbs, R.P., Morgan-Ryan, U., 2003. Morphology Is Not a Reliable Tool for Delineating Species Within *Cryptosporidium*. Journal of Parasitology 89, 399-402.
Fayer, R., Morgan, U., Upton, S.J., 2000. Epidemiology of *Cryptosporidium*: transmission, detection and identification. International Journal for Parasitology 30, 1305-1322.
Fayer, R., Santín, M., 2009. *Cryptosporidium xiaoi* n. sp.(Apicomplexa: Cryptosporidiidae) in sheep (Ovis aries). Veterinary Parasitology 164, 192-200.
Fayer, R., Santín, M., Macarisin, D., 2010. *Cryptosporidium ubiquitum* n. sp. in animals and humans. Veterinary parasitology 172, 23-32.
Fayer, R., Santín, M., Trout, J.M., 2008. *Cryptosporidium ryanae* n. sp.(Apicomplexa: Cryptosporidiidae) in cattle (Bos taurus). Veterinary Parasitology 156, 191-198.
Fayer, R., Santín, M., Xiao, L., 2005. *Cryptosporidium bovis* n. sp.(Apicomplexa: Cryptosporidiidae) in cattle (Bos taurus). The Journal of Parasitology, 624-629.
Fayer, R., Trout, J., Xiao, L., Morgan, U., Lal, A., Dubey, J., 2001. *Cryptosporidium canis* n. sp. from domestic dogs. Journal of Parasitology 87, 1415-1423.
Fayer, R., Xiao, L., 2008. *Cryptosporidium* and cryptosporidiosis, 2nd Edition. CRC Press, London;Boca Raton;.
Feng, Y., Yang, W., Ryan, U., Zhang, L., Kváč, M., Koudela, B., Modrý, D., Li, N., Fayer, R., Xiao, L., 2011. Development of a multilocus sequence tool for typing *Cryptosporidium muris* and *Cryptosporidium andersoni*. Journal of Clinical Microbiology 49, 34-41.
Freire-Santos, F., Vergara-Castiblanco, C.A., Tojo-Rodriguez, J.L., Santamarina-Fernandez, T., Ares-Mazas, E., 1998. *Cryptosporidium parvum*: An attempt at experimental infection in rainbow trout Oncorhynchus mykiss. The Journal of Parasitology 84, 935-938.
Gabor, L.J., Srivastava, M., Titmarsh, J., Dennis, M., Gabor, M., Landos, M., 2011. Cryptosporidiosis in Intensively Reared Barramundi (Lates Calcarifer). Journal of Veterinary Diagnostic Investigation 23, 383-386.
Gatei, W., Ashford, R.W., Beeching, N.J., Kamwati, S.K.e., Greensill, J., Hart, C.A., 2002. *Cryptosporidium muris* infection in an HIV-infected adult, Kenya. Emerging Infectious Diseases 8, 204.
Gatei, W., Greensill, J., Ashford, R.W., Cuevas, L.E., Parry, C.M., Cunliffe, N.A., Beeching, N.J., Hart, C.A., 2003. Molecular analysis of the 18S rRNA gene of *Cryptosporidium* parasites from patients with or without human immunodeficiency virus infections living in Kenya, Malawi, Brazil, the United Kingdom, and Vietnam. Journal of Clinical Microbiology 41, 1458-1462.
Gatei, W., Wamae, C.N., Mbae, C., Waruru, A., Mulinge, E., Waithera, T., Gatika, S.M., Kamwati, S.K., Revathi, G., Hart, C.A., 2006. Cryptosporidiosis: prevalence, genotype analysis, and symptoms associated with infections in children in Kenya. The American Journal of Tropical Medicine and Hygiene 75, 78-82.
Gestal, C., Azevedo, C., 2005. Ultrastructure of *Goussia cruciata* (Apicomplexa: Coccidia) infecting the liver of horse mackerel, *Trachurus trachurus* (L.), from Ibero- Atlantic waters. Journal of Fish Diseases 28, 125-132.

Gibson-Kueh, S., Yang, R., Thuy, N., Jones, J., Nicholls, P., Ryan, U., 2011. The molecular characterization of an Eimeria and *Cryptosporidium* detected in Asian seabass (*Lates calcarifer*) cultured in Vietnam. Veterinary Parasitology 181, 91-96.

Glazebrook, J., Campbell, R., 1987. Diseases of barramundi (*Lates calcarifer*) in Australia: a review. Management of wild and cultured sea bass/barramundi, 204-206.

Guyot, K., Follet-Dumoulin, A., Lelievre, E., Sarfati, C., Rabodonirina, M., Nevez, G., Cailliez, J., Camus, D., Dei-Cas, E., 2001. Molecular characterization of *Cryptosporidium* isolates obtained from humans in France. Journal of Clinical Microbiology 39, 3472-3480.

Hadfield, S.J., Chalmers, R.M., 2012. Detection and characterization of *Cryptosporidium cuniculus* by real-time PCR. Parasitology Research 111, 1385-1390.

Hammer, Ø., Harper, D.A., Ryan, P.D., 2001. PAST: paleontological statistics software package for education and data analysis. Palaeontologia Electronica 4, 9.

Hansen, H., Alarcon, M., 2019. First record of the Asian fish tapeworm *Schyzocotyle* (*Bothriocephalus*) *acheilognathi* (Yamaguti, 1934) in Scandinavia. BioInvasions Records 8, 437-441.

Hasajová, A., Valenčáková, A., Malčeková, B., Danišová, O., Halán, M., Goldova, M., Sak, B., Květoňová, D., Kváč, M., Halánová, M., 2014. Significantly higher occurrence of *Cryptosporidium* infection in Roma children compared with non-Roma children in Slovakia. European Journal of Clinical Microbiology & Infectious Diseases 33, 1401-1406.

Helmy, Y.A., Krücken, J., Nöckler, K., von Samson-Himmelstjerna, G., Zessin, K.-H., 2013. Molecular epidemiology of *Cryptosporidium* in livestock animals and humans in the Ismailia province of Egypt. Veterinary Parasitology 193, 15-24.

Hemmer, N., Steinhagen, D., Drommer, W., Körting, W., 1998. Changes of intestinal epithelial structure and cell turnover in carp *Cyprinus carpio* infected with *Goussia carpelli* (Protozoa: Apicomplexa). Diseases of Aquatic Organisms 34, 39-44.

Hijjawi, N., 2010. Cryptosporidium: New developments in cell culture. Experimental Parasitology 124, 54-60.

Hillman, A.E., Yang, R., Lymbery, A.J., Thompson, R.A., 2016. *Eimeria* spp. infecting quenda (*Isoodon obesulus*) in the greater Perth region, Western Australia. Experimental Parasitology 170, 148-155.

Hohweyer, J., Cazeaux, C., Travaillé, E., Languet, E., Dumètre, A., Aubert, D., Terryn, C., Dubey, J.P., Azas, N., Houssin, M., Loïc, F., Villena, I., La Carbona, S., 2016. Simultaneous detection of the protozoan parasites Toxoplasma, *Cryptosporidium* and *Giardia* in food matrices and their persistence on basil leaves. Food Microbiology 57, 36-44.

Holubová, N., Sak, B., Horčičková, M., Hlásková, L., Květoňová, D., Menchaca, S., McEvoy, J., Kváč, M., 2016. *Cryptosporidium avium* n. sp.(Apicomplexa: Cryptosporidiidae) in birds. Parasitology Research 115, 2243-2251.

Holubová, N., Zikmundová, V., Limpouchová, Z., Sak, B., Konečný, R., Hlásková, L., Rajský, D., Kopacz, Z., McEvoy, J., Kváč, M., 2019. *Cryptosporidium proventriculi* sp. n.(Apicomplexa: Cryptosporidiidae) in Psittaciformes birds. European Journal of Protistology 69, 70-87.

Hoover, D., Hoerr, F., Carlton, W., Hinsman, E., Ferguson, H., 1981. Enteric cryptosporidiosis in a naso tang, *Naso lituratus* Bloch and Schneider. Journal of Fish Diseases 4, 425-428.

Horčičková, M., Čondlová, Š., Holubová, N., Sak, B., Květoňová, D., Hlásková, L., Konečný, R., Sedláček, F., Clark, M., Giddings, C., 2019. Diversity of Cryptosporidium in common voles and description of *Cryptosporidium alticolis* sp. n. and Cryptosporidium microti sp. n.(Apicomplexa: Cryptosporidiidae). Parasitology 146, 220-233.

Hotchkiss, E.J., Gilray, J.A., Brennan, M.L., Christley, R.M., Morrison, L.J., Jonsson, N.N., Innes, E.A., Katzer, F., 2015. Development of a framework for genotyping bovine-derived *Cryptosporidium parvum*, using a multilocus fragment typing tool. Parasites & Vectors - Journal Article 8, 500.

Iseki, M., 1979. *Cryptosporidium felis* sp. n.(Protozoa Eimeriorina) from the domestic cat. Jpn. J. Parasitol. 28, 285.

Ježková, J., Horčičková, M., Hlásková, L., Sak, B., Květoňová, D., Novák, J., Hofmannová, L., McEvoy, J., Kváč, M., 2016. *Cryptosporidium testudinis* sp. n., *Cryptosporidium ducismarci* Traversa, 2010 and *Cryptosporidium* tortoise genotype III (Apicomplexa: Cryptosporidiidae) in tortoises. Folia Parasitol (Praha) 63, 10.14411.

Jiang, Y., Ren, J., Yuan, Z., Liu, A., Zhao, H., Liu, H., Chu, L., Pan, W., Cao, J., Lin, Y., 2014. *Cryptosporidium andersoni* as a novel predominant Cryptosporidium species in outpatients with diarrhea in Jiangsu Province, China. BMC Infectious Diseases 14, 555.

Jirků, M., Modrý, D., Šlapeta, J.R., Koudela, B., Lukeš, J., 2002. The phylogeny of *Goussia* and *Choleoeimeria* (Apicomplexa; Eimeriorina) and the evolution of excystation structures in coccidia. Protist 153, 379-390.

Jirku, M., Valigurová, A., Koudela, B., Krízek, J., Modrý, D., Slapeta, J., 2008. New species of *Cryptosporidium Tyzzer*, 1907 (Apicomplexa) from amphibian host: morphology, biology and phylogeny. Folia Parasitologica 55, 81.

Katoh, K., Toh, H., 2010. Parallelization of the MAFFT multiple sequence alignment program. Bioinformatics 26, 1899-1900.

Kawamoto, F., Mizuno, S., Fujioka, H., Kumada, N., Sugiyama, E., Takeuchi, T., Kobayashi, S., Iseki, M., Yamada, M., Matsumoto, Y., 1987. Simple and rapid staining for detection of Entamoeba cysts and other protozoans with fluorochromes. Japanese Journal of Medical Science & Biology 40, 35.

Kearse, M., Moir, R., Wilson, A., Stones-Havas, S., Cheung, M., Sturrock, S., Buxton, S., Cooper, A., Markowitz, S., Duran, C., 2012. Geneious Basic: an integrated and extendable desktop software platform for the organization and analysis of sequence data. Bioinformatics 28, 1647-1649.

Khan, S.M., Debnath, C., Pramanik, A.K., Xiao, L., Nozaki, T., Ganguly, S., 2010. Molecular characterization and assessment of zoonotic transmission of *Cryptosporidium* from dairy cattle in West Bengal, India. Veterinary Parasitology 171, 41-47.

Kim, T.K., 2015. T test as a parametric statistic. Korean Journal of Anesthesiology 68, 540.

Kirkpatrick, B.D., Daniels, M.M., Jean, S.S., Pape, J.W., Karp, C., Littenberg, B., Fitzgerald, D.W., Lederman, H.M., Nataro, J.P., Sears, C.L., 2002. Cryptosporidiosis Stimulates an Inflammatory Intestinal Response in Malnourished Haitian Children. The Journal of Infectious Diseases 186, 94-101.

Kissinger, J.C., 2019. Evolution of Cryptosporidium. Nature microbiology 4, 730.
Koehler, A.V., Whipp, M.J., Haydon, S.R., Gasser, R.B., 2014. *Cryptosporidium cuniculus*-new records in human and kangaroo in Australia. Parasites & Vectors 7, 492.
Koinari, M., Karl, S., Elliot, A., Ryan, U., Lymbery, A.J., 2013. Identification of *Anisakis* species (Nematoda: Anisakidae) in marine fish hosts from Papua New Guinea. Veterinary Parasitology 193, 126-133.
Körting, W., 1975. Larval development of *Bothriocephalus* sp. (Cestoda: Pseudophyllidea) from carp (*Cyprinm carpio* L.) in Germany*. Journal of Fish Biology 7, 727-733.
Kosek, M., Alcantara, C., Lima, A.A., Guerrant, R.L., 2001. Cryptosporidiosis: An update. Lancet Infectious Diseases 1, 262-269.
Košuthová, L., Šmiga, Ľ., Oros, M., Barčák, D., Košuth, P., 2015. The pathogenic Asian fish tapeworm, *Bothriocephalus acheilognathi* Yamaguti, 1934 (Cestoda) in the Red discus (*Symphysodon discus*). Helminthologia 52, 287-292.
Kotloff, K.L.D., Nataro, J.P.M.D., Blackwelder, W.C.P., Nasrin, D.P., Farag, T.H.P., Panchalingam, S.P., Wu, Y.P., Sow, S.O.M.D., Sur, D.M.D., Breiman, R.F.M.D., Faruque, A.S.G.M.D., Zaidi, A.K.M.M., Saha, D.M.S., Alonso, P.L.M.D., Tamboura, B.P., Sanogo, D.M.D., Onwuchekwa, U.M.S., Manna, B.P., Ramamurthy, T.P., Kanungo, S.M., Ochieng, J.B.M., Omore, R.M., Oundo, J.O.P., Hossain, A.M.D., Das, S.K.M., Ahmed, S.M., Qureshi, S.M., Quadri, F.M., Adegbola, R.A.P., Antonio, M.P., Hossain, M.J.M., Akinsola, A.M.D., Mandomando, I.B.S., Nhampossa, T.M.D., Acácio, S.M.D., Biswas, K.P., O'Reilly, C.E.P., Mintz, E.D.M.D., Berkeley, L.Y.P., Muhsen, K.P., Sommerfelt, H.P., Robins-Browne, R.M., Levine, M.M.M.D., 2013. Burden and aetiology of diarrhoeal disease in infants and young children in developing countries (the Global Enteric Multicenter Study, GEMS): a prospective, case-control study. Lancet, The 382, 209-222.
Kuczynska, E., Shelton, D.R., 1999. Method for detection and enumeration of *Cryptosporidium parvum* oocysts in feces, manures, and soils. Applied and Environmental Microbiology 65, 2820-2826.
Kváč, M., Hanzlíková, D., Sak, B., Květoňová, D., 2009a. Prevalence and age-related infection of *Cryptosporidium suis*, *C. muris* and *Cryptosporidium* pig genotype II in pigs on a farm complex in the Czech Republic. Veterinary Parasitology 160, 319-322.
Kváč, M., Havrdová, N., Hlásková, L., Daňková, T., Kanděra, J., Ježková, J., Vítovec, J., Sak, B., Ortega, Y., Xiao, L., 2016. *Cryptosporidium proliferans* n. sp.(Apicomplexa: Cryptosporidiidae): molecular and biological evidence of cryptic species within gastric *Cryptosporidium* of mammals. PloS one 11, e0147090.
Kváč, M., Hofmannová, L., Hlásková, L., Květoňová, D., Vítovec, J., McEvoy, J., Sak, B., 2014. *Cryptosporidium erinacei* n. sp.(Apicomplexa: Cryptosporidiidae) in hedgehogs. Veterinary Parasitology 201, 9-17.
Kváč, M., Kestřánová, M., Pinková, M., Květoňová, D., Kalinová, J., Wagnerová, P., Kotková, M., Vítovec, J., Ditrich, O., McEvoy, J., 2013. *Cryptosporidium scrofarum* n. sp.(Apicomplexa: Cryptosporidiidae) in domestic pigs (Sus scrofa). Veterinary Parasitology 191, 218-227.
Kváč, M., Květoňová, D., Sak, B., Ditrich, O., 2009b. *Cryptosporidium* pig genotype II in immunocompetent man. Emerging Infectious Diseases 15, 982.

Kváč, M., Vlnatá, G., Ježková, J., Horčičková, M., Konečný, R., Hlásková, L., McEvoy, J., Sak, B., 2018. *Cryptosporidium occultus* sp. n.(Apicomplexa: Cryptosporidiidae) in rats. European Journal of Protistology 63, 96-104.

Lafferty, K.D., Harvell, C.D., Conrad, J.M., Friedman, C.S., Kent, M.L., Kuris, A.M., Powell, E.N., Rondeau, D., Saksida, S.M., 2015. Infectious Diseases Affect Marine Fisheries and Aquaculture Economics. Annual Review of Marine Science 7, 471-496.

Landsberg, J.H., Paperna, I., 1986. Ultrastructural study of the coccidian *Cryptosporidium* sp. from stomachs of juvenile cichlid fish. Diseases of Aquatic Organisms 2, 13-20.

Lee, J.J., Leedale, G.F., Bradbury, P., 2000. An illustrated guide to the protozoa: organisms traditionally referred to as protozoa, or newly discovered groups.

Leoni, F., Amar, C., Nichols, G., Pedraza-Diaz, S., McLauchlin, J., 2006. Genetic analysis of *Cryptosporidium* from 2414 humans with diarrhoea in England between 1985 and 2000. Journal of Medical Microbiology 55, 703-707.

Levine, N.D., 1980. Some corrections of coccidian (Apicomplexa: Protozoa) nomenclature. The Journal of Parasitology 66, 830-834.

Levine, N.D., 1984. Taxonomy and review of the coccidian genus *Cryptosporidium* (protozoa, apicomplexa). The Journal of Protozoology 31, 94.

Li, L., Desser, S.S., 1985. The protozoan parasites of fish from two lakes in Algonquin Park, Ontario. Canadian Journal of Zoology 63, 1846-1858.

Li, N., Xiao, L., Alderisio, K., Elwin, K., Cebelinski, E., Chalmers, R., Santin, M., Fayer, R., Kvac, M., Ryan, U., 2014. Subtyping *Cryptosporidium ubiquitum*, a zoonotic pathogen emerging in humans. Emerging Infectious Diseases 20, 217.

Li, X., Pereira, M.d.G.C., Larsen, R., Xiao, C., Phillips, R., Striby, K., McCowan, B., Atwill, E.R., 2015. *Cryptosporidium rubeyi* n. sp.(Apicomplexa: Cryptosporidiidae) in multiple *Spermophilus* ground squirrel species. International Journal for Parasitology: Parasites and Wildlife 4, 343-350.

Lindsay, D.S., Upton, S.J., Owens, D.S., Morgan, U.M., Mead, J.R., Blagburn, B.L., 2000. *Cryptosporidium andersoni* n. sp.(Apicomplexa: Cryptosporiidae) from cattle, Bos taurus. Journal of Eukaryotic Microbiology 47, 91-95.

Liu, H., Shen, Y., Yin, J., Yuan, Z., Jiang, Y., Xu, Y., Pan, W., Hu, Y., Cao, J., 2014. Prevalence and genetic characterization of *Cryptosporidium*, Enterocytozoon, Giardia and Cyclospora in diarrheal outpatients in China. BMC Infectious Diseases 14, 25.

Lovy, J., Friend, S.E., 2015. Intestinal coccidiosis of anadromous and landlocked alewives, Alosa pseudoharengus, caused by *Goussia ameliae* n. sp. and G. alosii n. sp.(Apicomplexa: Eimeriidae). International Journal for Parasitology: Parasites and Wildlife 4, 159-170.

Lucio-Forster, A., Griffiths, J.K., Cama, V.A., Xiao, L., Bowman, D.D., 2010. Minimal zoonotic risk of cryptosporidiosis from pet dogs and cats. Trends in Parasitology 26, 174-179.

Lukeš, J., 1994. Morphology of life cycle stages of *Goussia bohemica* n. sp.(apicomplexa, eimeriidae), a parasite of the goblet and epithelial cells of the gudgeon (*Gobio gobio* L.). European Journal of Protistology 30, 68-74.

Marcial, M.A., Madara, J.L., 1986. *Cryptosporidium*: cellular localization, structural analysis of absorptive cell-parasite membrane-membrane interactions in guinea pigs, and suggestion of protozoan transport by M cells. Gastroenterology 90, 583.

Marcogliese, D.J., Gendron, A.D., Forest, J.J., Li, W., Boyce, K., El-Shehabi, F., Drake, D.A.R., Mandrak, N., Sherry, J., McLaughlin, J.D., 2016. Range expansion and molecular confirmation of the Asian fish tapeworm in the lower Great Lakes and St. Lawrence River with notes on infections in baitfish. Journal of Great Lakes Research 42, 819-828.

Matsche, M.A., Adams, C.R., Blazer, V.S., 2019a. Newly Described Coccidia *Goussia bayae* from White Perch Morone americana: Morphology and Phylogenetics Support Emerging Taxonomy of Goussia within Piscine Hosts. Journal of Parasitology 105, 1-10.

Matsche, M.A., Blazer, V.S., Mazik, P.M., 2019b. Seasonal development of the coccidian parasite *Goussia bayae* and hepatobiliary histopathology in white perch Morone americana from Chesapeake Bay. Diseases of Aquatic Organisms 134, 113-135.

Molloy, S.F., Smith, H.V., Kirwan, P., Nichols, R.A., Asaolu, S.O., Connelly, L., Holland, C.V., 2010. Identification of a high diversity of *Cryptosporidium* species genotypes and subtypes in a pediatric population in Nigeria. The American Journal of Tropical Medicine and Hygiene 82, 608-613.

Molnár, K., Avenant-Oldewage, A., Székely, C., 2004. A survey of coccidian infection of freshwater fishes in South Africa, with the description of *Goussia anopli* n. sp.(Apicomplexa: Eimeriidae). Systematic Parasitology 59, 75-80.

Morgan, D.L., Gill, H.S., 2000. Fish associations within the different inland habitats of lower south-western Australia. Records of the Western Australian Museum 20, 31-37.

Morgan, D.L., Gill, H.S., Maddern, M.G., Beatty, S.J., 2004. Distribution and impacts of introduced freshwater fishes in Western Australia. New Zealand Journal of Marine and Freshwater Research 38, 511-523.

Morgan, f.U., Pallant, L., Dwyer, B., Forbes, D., Rich, G., Thompson, R., 1998. Comparison of PCR and microscopy for detection of *Cryptosporidium parvum* in human fecal specimens: clinical trial. Journal of Clinical Microbiology 36, 995-998.

Morgan, J., 2015. Morphological and Molecular Characterisation of *Cryptosporidium* in Ornamental Fish. Veterinary and Life Sciences, Murdoch University . Honours Thesis. In Print.

Morgan, U.M., Xiao, L., Fayer, R., Lal, A.A., Thompson, R.C.A., 1999. Variation in *Cryptosporidium*: towards a taxonomic revision of the genus (Review).

Morgan- Ryan, U.M., Fall, A., Ward, L.A., Hijjawi, N., Sulaiman, I., Payer, R., Thompson, R.A., Olson, M., Lal, A., Xiao, L., 2002. *Cryptosporidium hominis* n. sp.(Apicomplexa: Cryptosporidiidae) from *Homo sapiens*. Journal of Eukaryotic Microbiology 49, 433-440.

Morine, M., Yang, R., Ng, J., Kueh, S., Lymbery, A.J., Ryan, U.M., 2012. Additional novel *Cryptosporidium* genotypes in ornamental fishes. Veterinary Parasitology 190, 578-582.

Morrison, C., Leger, J., Morrison, C., 1993. Light and electron microscopic study of the pathology and merogony of *Goussia gadi* (Apicomplexa: Coccidia) in the swimbladder wall of haddock, *Melanogrammus aeglefinus*. Diseases of Aquatic Organisms 17, 113-125.

Morrison, C., Marryatt, V., 2012. Coccidia found in some marine finfish off Nova Scotia. In: Pathology in Marine Science. Proceedings of the Third International Colloquium on Pathology in Marine Aquaculture, pp. 165-173.

Morse, T.D., Nichols, R., Grimason, A., Campbell, B., Tembo, K., Smith, H., 2007. Incidence of cryptosporidiosis species in paediatric patients in Malawi. Epidemiology & Infection 135, 1307-1315.

Muench, T.R., White, M.R., 1997. Cryptosporidiosis in a tropical freshwater catfish (*Plecostomus* spp.). Journal of Veterinary Diagnostic Investigation 9, 87-90.

Murphy, B.G., Bradway, D., Walsh, T., Sanders, G.E., Snekvik, K., 2009. Gastric Cryptosporidiosis in Freshwater Angelfish (Pterophyllum scalare). Journal of Veterinary Diagnostic Investigation 21, 722-727.

Muthusamy, D., Rao, S.S., Ramani, S., Monica, B., Banerjee, I., Abraham, O.C., Mathai, D.C., Primrose, B., Muliyil, J., Wanke, C.A., 2006. Multilocus genotyping of *Cryptosporidium* sp. isolates from human immunodeficiency virus-infected individuals in South India. Journal of Clinical Microbiology 44, 632-634.

Nader, J.L., Mathers, T.C., Ward, B.J., Pachebat, J.A., Swain, M.T., Robinson, G., Chalmers, R.M., Hunter, P.R., Van Oosterhout, C., Tyler, K.M., 2019. Evolutionary genomics of anthroponosis in *Cryptosporidium*. Nature Microbiology 4, 826.

Neira, P., Muñoz, N., Wilson, G., Barthel, M.M., Rosales, M.L., Henríquez, C., 2012. *Cryptosporidium* species in immunodeficient and immunocompetent patients of Valparaíso: a descriptive study. Revista Chilena de Infectologia: Organo Oficial de la Sociedad Chilena de Infectologia 29, 63-71.

Ng, J.S.Y., Eastwood, K., Walker, B., Durrheim, D.N., Massey, P.D., Porigneaux, P., Kemp, R., McKinnon, B., Laurie, K., Miller, D., 2012. Evidence of *Cryptosporidium* transmission between cattle and humans in northern New South Wales. Experimental Parasitology 130, 437-441.

Okhuysen, P.C., Rich, S.M., Chappell, C.L., Grimes, K.A., Widmer, G., Feng, X., Tzipori, S., 2002. Infectivity of a *Cryptosporidium parvum* Isolate of Cervine Origin for Healthy Adults and Interferon-γ Knockout Mice. The Journal of Infectious Diseases 185, 1320-1325.

Ong, C.S., Eisler, D.L., Alikhani, A., Fung, V.W., Tomblin, J., Bowie, W.R., Isaac-Renton, J.L., 2002. Novel *Cryptosporidium* genotypes in sporadic cryptosporidiosis cases: first report of human infections with a cervine genotype. Emerging Infectious Diseases 8, 263.

Osman, M., El Safadi, D., Benamrouz-Vanneste, S., Cian, A., Moriniere, R., Gantois, N., Delgado-Viscogliosi, P., Guyot, K., Bosc, S., Chabé, M., Petit, T., Viscogliosi, E., Certad, G., 2017. Prevalence, transmission, and host specificity of *Cryptosporidium* spp. in various animal groups from two French zoos. Parasitology Research 116, 3419-3422.

Painter, J.E., Hlavsa, M.C., Collier, S.A., Xiao, L.H., Yoder, J.S., 2015. Cryptosporidiosis Surveillance - United States, 2011-2012. Mmwr Surveillance Summaries 64, 1-13.

Palenzuela, O., Alvarez-Pellitero, P., Sitjà-Bobadilla, A., 2010. Molecular Characterization of *Cryptosporidium molnari* Reveals a Distinct Piscine Clade. Applied and Environmental Microbiology 76, 7646-7649.

Palermo, C.a., 2016. *Cryptosporidium* in fish: morphological and molecular characterisation, eBook.

Palmer, C.J., Xiao, L., Terashima, A., Guerra, H., Gotuzzo, E., Saldías, G., Bonilla, J.A., Zhou, L., Lindquist, A., Upton, S.J., 2003. *Cryptosporidium muris*, a rodent pathogen, recovered from a human in Peru. Emerging Infectious Diseases 9, 1174.

Paparini, A., Gofton, A., Yang, R., White, N., Bunce, M., Ryan, U.M., 2015. Comparison of Sanger and next generation sequencing performance for genotyping *Cryptosporidium* isolates at the 18S rRNA and actin loci. Experimental Parasitology 151-152, 21-27.

Paparini, A., Yang, R.C., Chen, L.D., Tong, K.S., Gibson-Kueh, S., Lymbery, A., Ryan, U.M., 2017. *Cryptosporidium* in fish: alternative sequencing approaches and analyses at multiple loci to resolve mixed infections. Parasitology 144, 1811-1820.

Paperna, I., 1987. Scanning electron microscopy of the coccidian parasite *Cryptosporidium* sp. from cichlid fishes. Diseases of Aquatic Organisms 3, 231-232.

Paperna, I., Vilenkin, M., 1996. Cryptosporidiosis in the gourami *Trichogaster leeri*: description of a new species and a proposal for a new genus, Piscicryptosporidium, for species infecting fish. Diseases of Aquatic Organisms 27, 95-101.

Pavlásek, I., 1983. *Cryptosporidium* sp. in *Cyprinus carpio* Linné, 1758 in Czechoslovakia. Folia Parasitologica 30.

Pavlásek, I., 1999. Cryptosporidia: biology, diagnosis, host spectrum, specificity, and the environment. Remedia Klin. Mikrobiol 3, 290-301.

Pavlasek, I., Lavickova, M., Horak, P., Kral, J., Kral, B., 1995. *Cryptosporidium varanii* n. sp. Apicomplexa: Cryptosporidiidae) in Emerald monitor, 99-108.

Percival, S.L., 2014. Microbiology of waterborne diseases: microbiological aspects and risks, Second;2; Edition. Elsevier, Academic Press, Amsterdam.

Petrincová, A., Valenčáková, A., Luptáková, L., Ondriska, F., Kalinová, J., Halánová, M., Danišová, O., Jarčuška, P., 2015. Molecular characterization and first report of *Cryptosporidium* genotypes in human population in the Slovak Republic. Electrophoresis 36, 2925-2930.

Power, M.L., Ryan, U.M., 2008. A new species of *Cryptosporidium* (Apicomplexa: Cryptosporidiidae) from eastern grey kangaroos (*Macropus giganteus*). Journal of Parasitology 94, 1114-1118.

Quail, M.A., Smith, M., Coupland, P., Otto, T.D., Harris, S.R., Connor, T.R., Bertoni, A., Swerdlow, H.P., Gu, Y., 2012. A tale of three next generation sequencing platforms: comparison of Ion Torrent, Pacific Biosciences and Illumina MiSeq Sequencers. BMC Genomics 13, 341.

Rahel, F.J., 2007. Biogeographic barriers, connectivity and homogenization of freshwater faunas: it's a small world after all. Freshwater Biology 52, 696-710.

Rašková, V., Květoňová, D., Sak, B., McEvoy, J., Edwinson, A., Stenger, B., Kváč, M., 2013. Human cryptosporidiosis caused by *Cryptosporidium tyzzeri* and *C. parvum* isolates presumably transmitted from wild mice. Journal of Clinical Microbiology 51, 360-362.

Reiczigel, J., Marozzi, M., Fábián, I., Rózsa, L., 2019. Biostatistics for parasitologists–a primer to Quantitative Parasitology. Trends in Parasitology 35, 277-281.

Reid, A., Lymbery, A., Ng, J., Tweedle, S., Ryan, U., 2010. Identification of novel and zoonotic *Cryptosporidium* species in marine fish. Veterinary Parasitology 168, 190-195.

Ren, X., Zhao, J., Zhang, L., Ning, C., Jian, F., Wang, R., Lv, C., Wang, Q., Arrowood, M.J., Xiao, L., 2012. *Cryptosporidium tyzzeri* n. sp.(Apicomplexa: Cryptosporidiidae) in domestic mice (*Mus musculus*). Experimental Parasitology 130, 274-281.

Rieux, A., Paraud, C., Pors, I., Chartier, C., 2013. Molecular characterization of *Cryptosporidium* spp. in pre-weaned kids in a dairy goat farm in western France. Veterinary Parasitology 192, 268-272.

Roberts, R.J., 2012. Fish pathology. John Wiley & Sons.

Robinson, G., Chalmers, R., 2010. The European rabbit (*Oryctolagus cuniculus*), a source of zoonotic cryptosporidiosis. Zoonoses and public health 57, e1-e13.

Roellig, D.M., Yoder, J.S., Madison-Antenucci, S., Robinson, T.J., Van, T.T., Collier, S.A., Boxrud, D., Monson, T., Bates, L.A., Blackstock, A.J., Shea, S., Larson, K., Xiao, L., Beach, M., 2017. Community Laboratory Testing for *Cryptosporidium*: Multicenter Study Retesting Public Health Surveillance Stool Samples Positive for *Cryptosporidium* by Rapid Cartridge Assay with Direct Fluorescent Antibody Testing. PLOS ONE 12, e0169915.

Rosenthal, B.M., Dunams-Morel, D., Ostoros, G., Molnár, K., 2016. Coccidian parasites of fish encompass profound phylogenetic diversity and gave rise to each of the major parasitic groups in terrestrial vertebrates. Infection, Genetics and Evolution 40, 219-227.

Rush, B., Chapman, P., Ineson, R., 1987. *Cryptosporidium* and drinking water. The Lancet 330, 632-633.

Ryan, U., Fayer, R., Xiao, L., 2014. *Cryptosporidium* species in humans and animals: current understanding and research needs. Parasitology 141, 1667-1685.

Ryan, U., Lawler, S., Reid, S., 2017a. Limiting swimming pool outbreaks of cryptosporidiosis-the roles of regulations, staff, patrons and research. Journal of Water and Health 15, 1-16.

Ryan, U., O'Hara, A., Xiao, L., 2004a. Molecular and Biological Characterization of a *Cryptosporidium molnari*-Like Isolate from a Guppy (*Poecilia reticulata*). Applied and Environmental Microbiology 70, 3761-3765.

Ryan, U., Paparini, A., Monis, P., Hijjawi, N., 2016. It's official - *Cryptosporidium* is a gregarine: What are the implications for the water industry? Water Research 105, 305-313.

Ryan, U., Paparini, A., Oskam, C., 2017b. New Technologies for Detection of Enteric Parasites. Trends in Parasitology.

Ryan, U., Paparini, A., Tong, K.S., Yang, R.C., Gibson-Kueh, S., O'Hara, A., Lymbery, A., Xiao, L.H., 2015. *Cryptosporidium huwi* n. sp (Apicomplexa: Eimeriidae) from the guppy (*Poecilia reticulata*). Experimental Parasitology 150, 31-35.

Ryan, U., Xiao, L., Read, C., Sulaiman, I., Monis, P., Lal, A., Fayer, R., Pavlasek, I., 2003a. A redescription of *Cryptosporidium galli* Pavlasek, 1999 (Apicomplexa: Cryptosporidiidae) from birds. The Journal of Parasitology, 809-813.

Ryan, U., Xiao, L., Read, C., Zhou, L., Lal, A.A., Pavlasek, I., 2003b. Identification of Novel *Cryptosporidium* Genotypes from the Czech Republic. Applied and Environmental Microbiology 69, 4302-4307.

Ryan, U.M., Monis, P., Enemark, H.L., Sulaiman, I., Samarasinghe, B., Read, C., Buddle, R., Robertson, I., Zhou, L., Thompson, R.C.A., Xiao, L., 2004b. *Cryptosporidium suis* n. sp. (apicomplexa: cryptosporidiidae) in pigs (*sus scrofa*). Journal of Parasitology 90, 769-773.

Ryan, U.M., Power, M., Xiao, L., 2008. *Cryptosporidium fayeri* n. sp.(Apicomplexa: Cryptosporidiidae) from the Red Kangaroo (*Macropus rufus*). Journal of Eukaryotic Microbiology 55, 22-26.

Santos, L., Ramos, F., 2018. Antimicrobial resistance in aquaculture: current knowledge and alternatives to tackle the problem. International Journal of Antimicrobial Agents.

Savioli, L., Smith, H., Thompson, A., 2006. *Giardia* and *Cryptosporidium* join the 'Neglected Diseases Initiative'.

Scholz, T., 1997. A revision of the species of Bothriocephalus Rudolphi, 1808 (Cestoda: Pseudophyllidea) parasitic in American freshwater fishes. Systematic Parasitology 36, 85-107.

Scholz, T., Drábek, R., Hanzelová, V., 1998. Scolex morphology of Proteocephalus tapeworms (Cestoda: Proteocephalidae), parasites of freshwater fish in the Palaearctic Region. Folia Parasitologica 45, 27-43.

Scholz, T., Šimková, A., Razanabolana, J.R., Kuchta, R., 2018. The first record of the invasive Asian fish tapeworm (*Schyzocotyle acheilognathi*) from an endemic cichlid fish in Madagascar. Helminthologia 55, 84-87.

Shields, J.M., Hill, V.R., Arrowood, M.J., Beach, M.J., 2008. Inactivation of *Cryptosporidium parvum* under chlorinated recreational water conditions. Journal of Water and Health 6, 513.

Silva, S.O.S., Richtzenhain, L.J., Barros, I.N., Gomes, A.M.M.C., Silva, A.V., Kozerski, N.D., de Araújo Ceranto, J.B., Keid, L.B., Soares, R.M., 2013. A new set of primers directed to 18S rRNA gene for molecular identification of *Cryptosporidium* spp. and their performance in the detection and differentiation of oocysts shed by synanthropic rodents. Experimental Parasitology 135, 551-557.

Sitja-Bobadilla, A., 2005. Epidemiology of *Cryptosporidium molnari* in Spanish Gilthead Sea Bream (*Sparus aurata* L.) and European Sea Bass (*Dicentrarchus labrax* L.) Cultures: from Hatchery to Market Size. Applied and Environmental Microbiology 71, 131-139.

Slavin, D., 1955. *Cryptosporidium meleagridis* (sp. nov.). Journal of Comparative Pathology and Therapeutics 65, 262-IN223.

Souza, G.A., Moresca, V.O., Teixeira, G.M., Jerep, F.C., Aguiar, A., 2018. First record of the invasive tapeworm, *Schyzocotyle acheilognathi* (Pseudophyllidea; Bothriocephalidae) in native freshwater fish, Brazil. Anais da Academia Brasileira de Ciências 90, 2845-2849.

Spanakos, G., Biba, A., Mavridou, A., Karanis, P., 2015. Occurrence of *Cryptosporidium* and *Giardia* in recycled waters used for irrigation and first description of *Cryptosporidium parvum* and *C. muris* in Greece. Parasitology Research 114, 1803-1810.

Sponseller, J.K., Griffiths, J.K., Tzipori, S., 2014. The evolution of respiratory Cryptosporidiosis: evidence for transmission by inhalation. Clinical Microbiology Reviews 27, 575-586.

Squire, S.A., Ryan, U., 2017. *Cryptosporidium* and *Giardia* in Africa: current and future challenges. Parasites & Vectors U6 -Journal Article 10.

Steinhagen, D., Oesterreich, B., Körting, W., 1997. Carp coccidiosis: clinical and hematological observations of carp infected with *Goussia carpelli*. Diseases of Aquatic Organisms 30, 137-143.

Striepen, B., 2013. Time to tackle cryptosporidiosis. Nature 503, 189-191.

Strong, W.B., Nelson, R.G., 2000. Preliminary profile of the *Cryptosporidium* parvum genome: an expressed sequence tag and genome survey sequence analysis. Molecular & Biochemical Parasitology 107, 1-32.

Sulaiman, I.M., 2002. Molecular phylogeny and evolutionary relationships of *Cryptosporidium* parasites at the actin locus. The Journal of Parasitology 88, 388-394.

Sunnotel, O., Lowery, C.J., Moore, J.E., Dooley, J.S.G., Xiao, L., Millar, B.C., Rooney, P.J., Snelling, W.J., 2006. *Cryptosporidium*. Letters in Applied Microbiology 43, 7-16.

Szekely, C., Molnar, K., 1992. *Goussia trichogasteri* n. sp.(Apicomplexa: Eimenidae) infecting the aquarium-cultured golden gourami *Trichogaster trichopterus*. Diseases of Aquatic Organisms 13, 79-81.

Tamura, K., Stecher, G., Peterson, D., Filipski, A., Kumar, S., 2013. Molecular evolutionary genetics analysis version 6.0. Mol Biol Evol 30, 2725-2729.

Thompson, R.C.A., Morgan, U., 1998. Molecular characterisation of *Cryptosporidium*. Parasitology International 47, 141-141.

Tiangtip, R., Jongwutiwes, S., 2002. Molecular analysis of *Cryptosporidium* species isolated from HIV‐infected patients in Thailand. Tropical Medicine & International Health 7, 357-364.

Traversa, D., Iorio, R., Otranto, D., Modrý, D., Šlapeta, J., 2008. *Cryptosporidium* from tortoises: Genetic characterisation, phylogeny and zoonotic implications. Molecular and Cellular Probes 22, 122-128.

Tyzzer, E., 1907. A sporozoan found in the peptic glands of the common mouse. Proceedings of the Society for Experimental Biology and Medicine 5, 12-13.

Tyzzer, E., 1912. *Cryptosporidium parvum* (sp. nov.), a coccidium found in the small intestine of the common mouse. Arch. Protistenkd. 26, 394-412.

Tyzzer, E.E., 1910. An extracellular coccidium, *Cryptosporidium muris* (gen. et sp. nov.), of the gastric glands of the common mouse. The Journal of medical research 23, 487.

Urrea-Quezada, A., González-Díaz, M., Villegas-Gómez, I., Durazo, M., Hernández, J., Xiao, L., Valenzuela, O., 2017. Clinical Manifestations of Cryptosporidiosis and Identification of a New *Cryptosporidium* Subtype in Patients From Sonora, Mexico. The Pediatric Infectious Disease Journal.

Valenzuela, O., González-Díaz, M., Garibay-Escobar, A., Burgara-Estrella, A., Cano, M., Durazo, M., Bernal, R.M., Hernandez, J., Xiao, L., 2014. Molecular characterization of *Cryptosporidium* spp. in children from Mexico. PloS One 9, e96128.

Van den Bossche, D., Cnops, L., Verschueren, J., Van Esbroeck, M., 2015. Comparison of four rapid diagnostic tests, ELISA, microscopy and PCR for the detection of Giardia lamblia, *Cryptosporidium* spp. and Entamoeba histolytica in feces. Journal of Microbiological Methods 110, 78-84.

Vetterling, J.M., Takeuchi, A., Madden, P.A., 1971. Ultrastructure of *Cryptosporidium wrairi* from the guinea pig. The Journal of protozoology 18, 248-260.

Waldron, L.S., Cheung-Kwok-Sang, C., Power, M.L., 2010. Wildlife-associated *Cryptosporidium fayeri* in human, Australia. Emerging Infectious Diseases 16, 2006.

Waldron, L.S., Dimeski, B., Beggs, P.J., Ferrari, B.C., Power, M.L., 2011. Molecular epidemiology, spatiotemporal analysis, and ecology of sporadic human cryptosporidiosis in Australia. Appl. Environ. Microbiol. 77, 7757-7765.

Wang, Y., Li, D., Song, L., Liu, Y., He, T., Liu, H., Wu, C., Schwarz, S., Shen, J., 2013. First report of the multiresistance gene cfr in *Streptococcus suis*. Antimicrobial Agents and Chemotherapy 57, 4061-4063.

Widerstrom, M., Schonning, C., Lilja, M., Lebbad, M., Ljung, T., Allestam, G., Ferm, M., Bjorkholm, B., Hansen, A., Hiltula, J.I., Langmark, J., Lofdahl, M., Omberg, M., Reutenwall, C., Samuelsson, E., Widgren, K., Wallensten, A., Lindh, J., Mittuniversitetet, Fakulteten för, h., Avdelningen för, h., 2014. Large Outbreak of *Cryptosporidium hominis* Infection Transmitted through the Public Water Supply, Sweden. Emerging Infectious Diseases 20, 581-589.

Xavier, R., Severino, R., Pérez-Losada, M., Gestal, C., Freitas, R., Harris, D.J., Veríssimo, A., Rosado, D., Cable, J., 2018. Phylogenetic analysis of apicomplexan parasites infecting commercially valuable species from the North-East Atlantic reveals high levels of diversity and insights into the evolution of the group. Parasites & Vectors 11, 63.

Xiao, L., 2010. Molecular epidemiology of cryptosporidiosis: An update. Experimental Parasitology 124, 80-89.

Xiao, L., Bern, C., Arrowood, M., Sulaiman, I., Zhou, L., Kawai, V., Vivar, A., Lal, A.A., Gilman, R.H., 2002. Identification of the *Cryptosporidium* pig genotype in a human patient. The Journal of Infectious Diseases 185, 1846-1847.

Xiao, L., Escalante, L., Yang, C., Sulaiman, I., Escalante, A.A., Montali, R.J., Fayer, R., Lal, A.A., 1999. Phylogenetic Analysis of & *Cryptosporidium* Parasites Based on the Small-Subunit rRNA Gene Locus. Applied and Environmental Microbiology 65, 1578.

Xiao, L., Fayer, R., Ryan, U., Upton, S.J., 2004. *Cryptosporidium* Taxonomy: Recent Advances and Implications for Public Health. Clinical Microbiology Reviews 17, 72-97.

Xiao, L., Feng, Y., 2017. Molecular epidemiologic tools for waterborne pathogens *Cryptosporidium* spp. and *Giardia duodenalis*. Food and Waterborne Parasitology 8-9, 14-32.

Xu, P., Widmer, G., Wang, Y., Ozaki, L.S., Alves, J.M., Serrano, M.G., Puiu, D., Manque, P., Akiyoshi, D., Mackey, A.J., 2004. The genome of *Cryptosporidium hominis*. Nature 431, 1107.

Yamaguti, S., 1934. Studies on the helminth fauna of Japan. Part 4. Cestodes of fishes. Japanese Journal of Zoology 6, 1-112.

Yang, R., Murphy, C., Song, Y., Ng-Hublin, J., Estcourt, A., Hijjawi, N., Chalmers, R., Hadfield, S., Bath, A., Gordon, C., Ryan, U., 2013. Specific and quantitative detection and identification of *Cryptosporidium hominis* andC. parvum in clinical and environmental samples. Experimental Parasitology 135, 142-147.

Yang, R.C., Dorrestein, G.M., Ryan, U., 2016. Molecular characterisation of a disseminated *Cryptosporidium* infection in a Koi carp (*Cyprinus carpio*). Veterinary Parasitology 226, 53-56.

Yang, R.C., Palermo, C., Chen, L.D., Edwards, A., Paparini, A., Tong, K.S., Gibson-Kueh, S., Lymbery, A., Ryan, U., 2015. Genetic diversity of *Cryptosporidium* in fish at the 18S and actin loci and high levels of mixed infections. Veterinary Parasitology 214, 255-263.

Zahedi, A., Durmic, Z., Gofton, A.W., Kueh, S., Austen, J., Lawson, M., Callahan, L., Jardine, J., Ryan, U., 2017a. *Cryptosporidium homai* n. sp.(Apicomplexa: Cryptosporidiiae) from the guinea pig (*Cavia porcellus*). Veterinary Parasitology 245, 92-101.

Zahedi, A., Gofton, A.W., Jian, F., Paparini, A., Oskam, C., Ball, A.J., Robertson, I.D., Ryan, U., 2017b. Next Generation Sequencing uncovers within-host differences in the genetic diversity of *Cryptosporidium* gp60 subtypes.

Zahedi, A., Monis, P., Aucote, S., King, B., Paparini, A., Jian, F.C., Yang, R.C., Oskam, C., Ball, A., Robertson, I., Ryan, U., 2016a. Zoonotic *Cryptosporidium* Species in Animals Inhabiting Sydney Water Catchments. PLoS One 11, e0168169.

Zahedi, A., Monis, P., Gofton, A.W., Oskam, C.L., Ball, A., Bath, A., Bartkow, M., Robertson, I., Ryan, U., 2018. *Cryptosporidium* species and subtypes in animals inhabiting drinking water catchments in three states across Australia.

Zahedi, A., Paparini, A., Jian, F., Robertson, I., Ryan, U., 2016b. Public health significance of zoonotic *Cryptosporidium* species in wildlife: Critical insights into better drinking water management. International Journal for Parasitology: Parasites and Wildlife 5, 88-109.

Zanguee, N., Lymbery, J.A., Lau, J., Suzuki, A., Yang, R., Ng, J., Ryan, U., 2010. Identification of novel *Cryptosporidium* species in aquarium fish. Veterinary Parasitology 174, 43-48.

Ziegler, P.E., Wade, S.E., Schaaf, S.L., Stern, D.A., Nadareski, C.A., Mohammed, H.O., 2007. Prevalence of *Cryptosporidium* species in wildlife populations within a watershed landscape in southeastern New York State. Veterinary Parasitology 147, 176-184.

Appendix

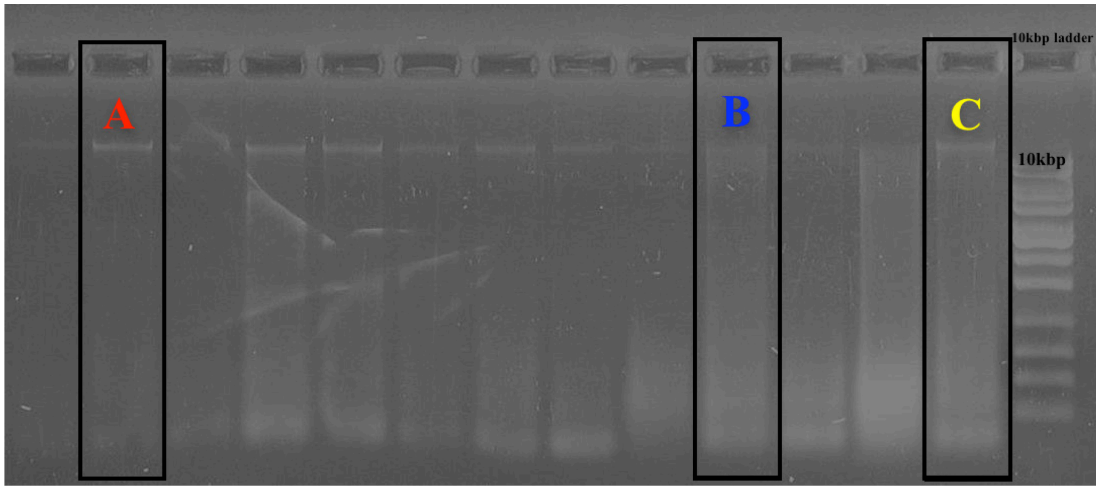

Figure A1.1. An example of Genomic DNA separated by gel electrophoresis on a 1% agarose gel. Sample A had a bright band above the 10kb ladder band as well as no smearing below indicating little to no RNA or degraded DNA contamination. Sample B did not have a bright band and exhibited smearing while sample C had too much smearing below the band. Therefore, if used for WGS sample A would have the best chance of a successful run for which a DNA concentration of ≥ 20 ng/L, 260/280 ratio close to 1.8 and a 260/230 ratio of 2 ≥ 2.2 would be ideal.

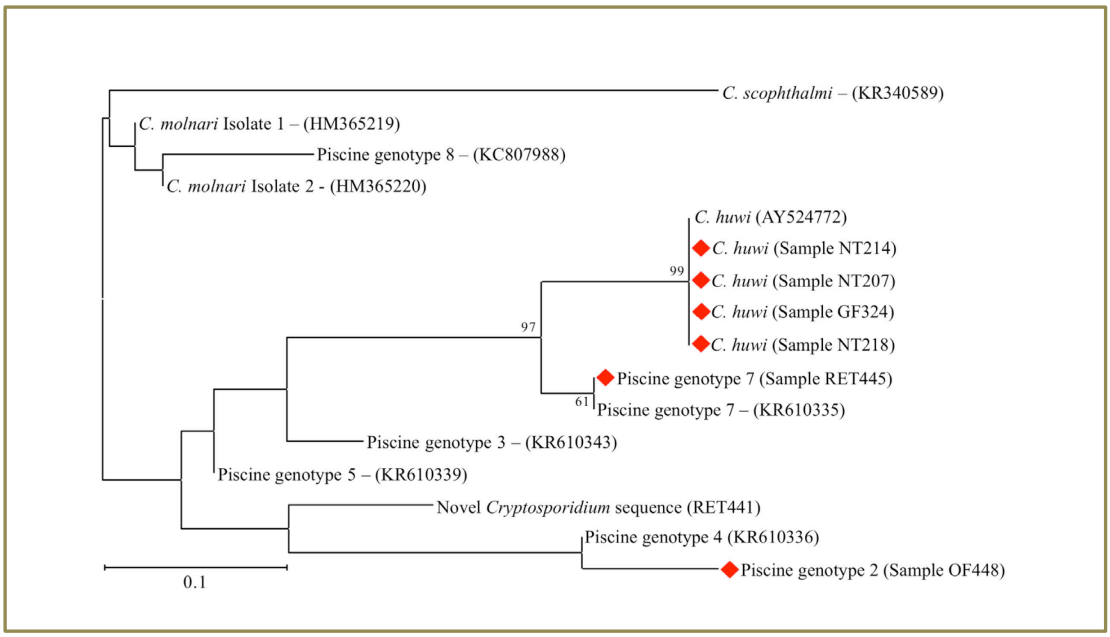

Figure A1.2. Phylogenetic tree of short (206bp) sequences from the actin locus. Diamonds indicate *Cryptosporidium* samples from the present study.

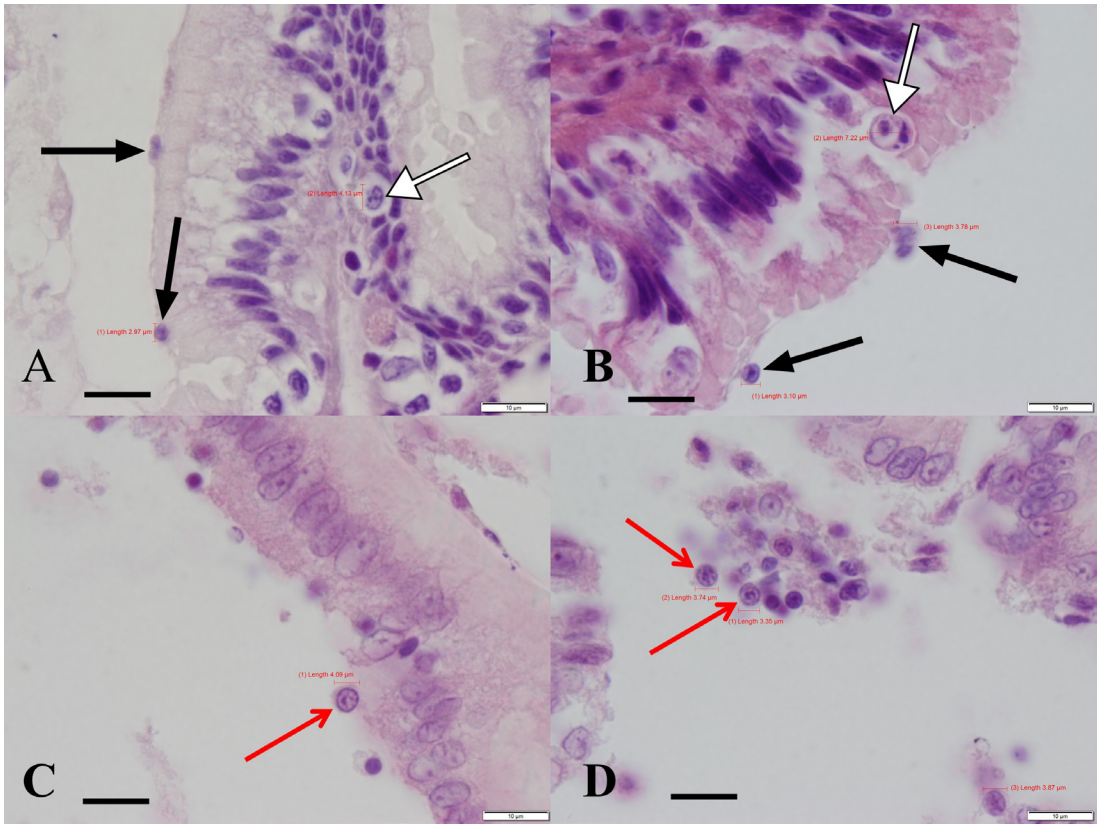

Figure A1.3. Histology images from a sample positive for a mixed infection. Sample RET438 produced a mixed sequence after nested PCR amplification at the 18S locus. *Cryptosporidium*-like organisms can be seen along the brush border of the gastric epithelium resembling oocyst life stages in size and shape (black arrows) (A and B). Spherical rganisms deeply embedded in gastric epithelium resemble oogonial and sporogonial stages of *Cryptosporidium* (white arrows) (A and B). Free spherical organisms found within GI tract lumen are the size and shape of *Cryptosporidium* oocysts (red arrows) (C and D). All scale bars = 10µm.